The Amundsen Sea Expedition 2013 – 2014 (ANA04B)

Chief Scientist: SangHoon Lee

IBRV Araon, 24 December 2013 – 25 January 2014
(Christchurch to Christchurch, NZ)

Prologue

The KOPRI Amundsen project turned into the second phase in 2013. The Amundsen team has conducted two field expeditions during the three-year block of the first phase, 2010 to 2012. The ultimate goal of the Amundsen project is to assess the warming trends and physical mechanisms of the temperature rise in the study area, as well as the chemical, biological, and biogeochemical consequences of the rapid warming in the western Antarctic. The phase one was designed to understand the basic physics, e.g., circulation patterns, of the study area, and the structure and functioning of the Amundsen Sea ecosystem. Science data and results that we produced from the first stage, and yet being published in research articles at this moment, in no doubt proved solid, unique, and valuable. Our effort to keep up with good science drew special attentions from broad professional societies, let alone the academic and scientific sectors. We will continue to reinforce the project with international components for further science collaboration.

As the Amundsen team fulfilled the phase one research goals, the phase two is directed toward more specific issues, such as, the balance of mass and heat, or features of specific biochemical processes in the study area, to name a few. Once three years' study on the specific issues is complete, this project will spin off again into the phase three. I personally do believe there are science issues that deserve lifetime research, however I have seen projects do better off when they evolve.

We knew this season's expedition would be short and intense, because the Araon ship time was allocated in the first place with priority to the logistics support for the construction of the 2nd Korean station at Terra Nova Bay. Impending on our departure, there came another 5-day cut on top of the already shrunken itinerary. KOPRI allowed no extension of the termination date of my cruise leg. Growing concerns landed on my shoulder, but what has to be done must be done in the given time frame, and we did it. During the 15-day stint, we have serviced 9 moorings, 6 in and 8 out; occupied more than 30 CTD stations, some were re-visited; carried out 5 sets of process study that was meticulously combined with trace metal study; however, got no property damage or lost, neither personal injuries. The work proceeded seamless and streamlined, and in addition, a great amount of time was saved; the credit should go to the Araon master and crew, who gladly worked around the clock, putting their mind in the job. The Amundsen team members should also be acknowledged for their dedication to the research. I always appreciate that I work with my Amundsen team.

This report is dedicated to my Amundsen team and the master and crew of Araon for their missions accomplished.

2014 Amundsen cruise ANA04B chief scientist, SangHoon Lee

Contents

Chapter 1

Physical Oceanography

H.K. Ha[1], T.W. Kim[1], H.J. Lee[1], C.Y. Kang[1], C.S. Hong[2], A.K. Wåhlin[3], J. Rolandsson[3], O. Karen[3], and T. Miles[4]
[1]Korea Polar Research Institute (KOPRI), Incheon 406-840, Korea
[2]Korea Institute of Ocean Science and Technology (KIOST), Ansan 425-600, Korea
[3]University of Gothenburg (UGOT), Gothenburg, Sweden
[4]Rutgers University (RU), New Brunswick, NJ 08901, USA

요약문

2013/14년 겨울, 쇄빙연구선 아라온호를 이용하여 남극 아문젠해에서 3번째 종합적인 해양탐사를 실시하였다. 해양물리 분야의 주된 연구주제는 남극순환 심층수(circumpolar deep water) 분포의 시공간적인 변동성을 규명하는 것이다. 총 35개의 CTD정점에서 수리적 자료와 해수샘플을 획득하였다. 2012년도에 설치된 3기의 계류시스템을 성공적으로 회수 및 재계류 하였고, 새롭게 도입된 3기의 계류시스템을 설치하였다. 특히, 닷슨빙붕(Dotson Ice Shelf) 전면에 설치된 3기의 계류시스템을 통해 빙붕하부로 유입되는 남극순환 심층수의 공급량과 열수지를 파악할 수 있을 것으로 기대된다. 국제공동연구의 일환으로, 스웨덴의 고덴버그대학과 미국의 럿거스대학과의 현장공동조사를 실시하였다. 고덴버그대학에서 기존에 설치한 3기의 계류시스템을 성공적으로 회수하였고, 새롭게 2기의 계류시스템을 설치하였다. 또한 럿거스대학에서 제공한 2기의 글라이더를 폴리냐 중심부근과 닷슨빙붕 부근에서 약 9일간 운영하였으며, 공간적인 해상도가 높은 자료를 획득하는 데 성공하였다.

Abstract

In order to monitor the circumpolar deep water (CDW) and associated rapid melting of glaciers in the Amundsen Shelf, three institutes (KOPRI, UGOT, and RU) from Korea, Sweden, and US have launched an international collaboration program. During the 2014 Amundsen Sea cruise (ANA04B) by IBRV Araon, a total of 35 CTD stations were visited, 6 moorings were successfully recovered and 8 moorings were newly deployed on the shelf troughs and near the ice shelf front as well as the polynya. In particular, the three moorings installed just in front of Dotson Ice Shelf will reveal the circulation pattern and pathways of

CDW and meltwater that are not addressed yet. The long-term time series from recovered moorings will be further investigated to reveal the spatial and temporal variability in CDW in the Amundsen Shelf. Two Teledyne-Webb Slocum gliders provided by RU were deployed in the polynya. A deep glider was configured to obtain high-resolution data of the Dotson Glacier inflow and outflow of CDW, while a shallow glider was tasked with sampling a cross-polynya gradient of the euphotic zone and station keep near the polynya center.

1.1 Hydrographic Survey

Purposes and aims

The Antarctic shelf regions are currently experiencing large changes coincident with seaward surging of the West Antarctic Ice Sheet (WAIS). An important reason for the decline is warm, salty ocean currents that access the floating glaciers through bathymetric troughs and melt the glacial ice from below. The most rapid melting is presently occurring in the Amundsen Sea. Due to limited in-situ data, in particular from the central part of this shelf, the main pathways of the warm deep water are poorly known. Budgets for ocean heat, salt and freshwater on the shelf and at the terminus of the ice sheet have not been quantified.

The purposes of physical oceanography are to

1. Quantify budgets for oceanic heat, salt and glacier melt water for the central Amundsen Shelf;
2. Quantify the variability of the oceanic heat transport on the shelf on time scales up to centennial;
3. Determine the importance of winds and large-scale ocean circulation as forcing factors for the inflow of warm water onto the shelf

These aims will be met by acquiring and analyzing data from autonomous subsurface moorings and hydrographic transects during two cruises with the IBRV Araon to the region. From these measurements, the oceanic heat loss and glacier meltwater production on the central Amundsen Shelf will be calculated and joined with existing estimates from other parts of the WAIS. The time series of the oceanic heat transport will be analyzed and correlated to atmospheric forcing and large-scale ocean circulation in order to determine their relative importance in forcing the warm water onto the shelf.

Materials and methods

With the international collaboration among KOPRI, UGOT and RU, an intensive oceanographic survey was conducted in the period of December 24, 2013 - January 25, 2014 using the IBRV Araon to understand the spatial and temporal variability of CDW on the Amundsen Shelf (Fig. 1.1). A total of 35 CTD stations were visited to collect the hydrographic data as well as the water samples. At each hydrographic station, at least one cast of CTD/Rosette system with additional probes (e.g., dissolved oxygen, fluorometer, transmissometer, PAR, and etc.) was conducted to measure the vertical profiles of temperature, salinity

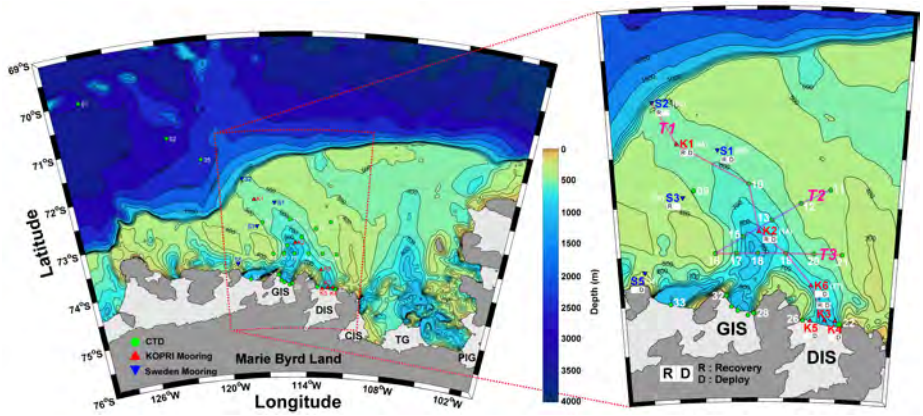

Figure 1.1: Map of study area. Green dots denote the CTD stations visited during the ANA04B expedition. Numbers indicate station numbers. Triangles are the mooring sites. Three transects (T-1, T-2 and T-3) were selected to reveal the spatial distribution of CDW along and cross the Dotson Trough (right panel).

and other related biochemical parameters. The serial numbers and calibration information of each sensor are given in Table 1.1. During the CTD upcasts, water samples were collected at several depths. A lowered acoustic Doppler current profiler (LADCP, RDI, 300 kHz) was attached to the CTD frame to measure the full profile of current velocities. The bin size was chosen as 5 m, and the number of bins was 20. Due to a serious malfunction, the vessel-mounted ADCP (RDI, 38 kHz) was not operated. After the troubleshooting by RDI, the 38 kHz ADCP will be mounted again on the vessel hull in 2014 summer.

Table 1.1: Configuration of CTD (SBE 911plus) sensors used during ANA04B cruise.

Sensor	S/N	Calibration date	Remarks
Temperature 1	2852	Feb. 21, 2013	UGOT
Temperature 2	4098	Feb. 21, 2013	
Conductivity 1	2401	Feb. 27, 2013	UGOT
Conductivity 2	2456	Feb. 21, 2013	
Pressure	0932	June 17, 2008	KOPRI
Oxygen	1928	Feb. 15, 2013	UGOT (St. 1, 2)
	1614	May 26, 2012	KOPRI (After St. 3)
Fluorometer	FLRTD-1400	May 22, 2012	KOPRI
Transmissometer	CST-1227DR	June 18, 2012	KOPRI
PAR	70228	April 17, 2009	KOPRI
Altimeter	51306	Nov. 15, 2010	KOPRI

Preliminary results

In January 2014, a total of 35 CTD stations were visited to investigate the spatial and temporal variability in CDW. The main along-trough transect (T-1) shows that the CDW seaward of the shelf break is warmer than 0.90°C, and has salinity about 34.72 psu. As the CDW flows onto the shelf it is cooled and freshened presumably by mixing with glacier meltwater. The layer of CDW (defined by 0°C isotherm) is much thinner than what was observed in 2012 (Fig. 1.2). This difference in thickness might be caused by inter-annual variability, by the fact that the survey was conducted earlier in the summer, or be a coincidental result of the large short-term variability that is observed by the moorings in the region. The survey of 2012 (ANA02C) was conducted in February-March, whereas that of 2014 was done in January. The main reason will be analyzed using the mooring time series combined with the hydrographic data collected during both years.

Two transects (T-2 and T-3) across the Dotson Trough show the intrusion of warm CDW, tilting toward the east side of trough (Figs. 1.3 and 1.4). This suggests that the trough bathymetry plays an important role for the inflow and outflow of CDW. The thickness of the layer of CDW in 2014 was thin compared to in 2012. In 2014, the isohaline of 34.3 psu was at about 600 m depth in the deepest part of the trough (St. 15), while in 2012, it was located around 500 m depth. A localized pool of cold water was present in St. 19, and might be associated with the interleaving of meltwater. Further analysis is needed to determine what caused this structure (e.g., chemical tracers such as noble gages).

1.2 Moorings

KOPRI moorings

Three mooring systems, located at the northern entrance (K1), the center of polynya (K2), and ice shelf front (K3), were successfully recovered and then re-deployed at the same location during ANA04B. Another three mooring systems (K4, K5, and K6) were newly installed just in front of Dotson ice shelf as well as southern part of polynya (for location, see Fig. 1.1). The setups for Micro-cats and ADCP were summarized in Table 1.2. The detail information on the recovery and deployment was given in Table 1.3 and 1.4. After the deployment, the triangulation was made to confirm the settlement status of moorings and record the exact GPS location for future recovery. The design diagrams and triangulation results for individual moorings are given in Appendix II and III.

UGOT moorings

Three recoveries and two deployments were carried through during the cruise. For mooring sites, see Fig. 1.1. For mooring design and triangulation, see Appendix II and III.

Mooring S1

The mooring with the highest priority was S1, which is situated in the center of the deep current that transports warm salty water towards the floating glaciers in the central shelf. It has been serviced and re-deployed since early

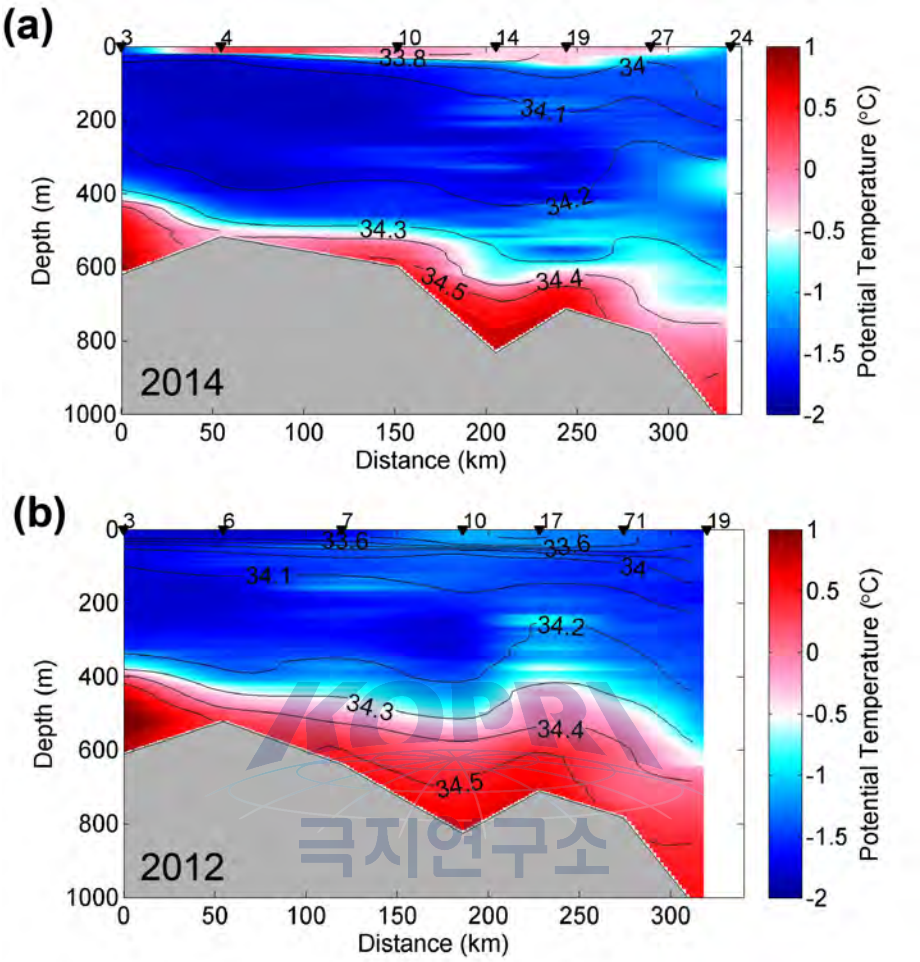

Figure 1.2: Vertical distribution of water mass properties along the Dotson Trough (T-1): (a) 2014 expedition, and (b) 2012 expedition. The color indicates the potential temperature, and the contour indicates the isohaline.

Table 1.2: Summary of setups for moored ADCP and MicroCat.

k:\My_Works\2013_KOPRI\01_Amundsen\Mooring\mooring_field_sampling_strategy.xlsx

		ADCP		
		150 kHz	300kHz	75kHz
Deployment Timing Setup	Duration(days)	730	450	450
	Ensemble interval	15 min	15 min	15 min
	Ping int.	2 sec	2 sec	2.5 sec
Porfiling Setup	Pings Per	25	20	40
	Number of Depth	44	37	60
	Depth Cell Size	8	4	8
Environmental Setup	Transducer Depth	450 m	560 m	450 m
	Salinity	35 ppt	35 ppt	35 ppt
	Magnetic Variation	0	0	0
	Temperature	-1	-1	-1
Deployment Consequences	First cell range	12.21 m	6.11 m	15.03 m
	Last cell range	356.21 m	150.11 m	487.03 m
	Max range	355.47 m	143.45 m	476.58 m
	Standard deviation	1.42 cm/s	1.66 cm/s	2.31 cm/s
	Ensemble size	1034 bytes	894 bytes	1354 bytes
	Storage required	69.11 MB	36.83 MB	55.78 MB
	Power usage	1788.53 Wh	446.84 Wh	1696.13 Wh
	Battery usage	4 of 4	1 of 1	3.8 of 4
	Processing Bandwidth (BW)	Narrow BW	Narrow BW	Narrow BW
	Power			Low

	MicroCat	
	37-SM	37-SMP
Interval	15 min	60 min
	Deployment Endurance Calculator 1.5 Model = SBE 37 SM RS-232 Firmware 3.0 and higher Pressure Sensor = Strain gauge Sample Interval = 900 Sampling Type = Autonomous Transmit Real Time Not Enabled Battery Type is: AA Lithium Battery Capacity = 8.8 Amp-Hours Battery Endurance is: 5670 Days Batteries are not expected to last longer than 2 years	Deployment Endurance Calculator 1.5 Model = SBE 37 SMP ODO RS-232 Firmware 1.0 and higher Pressure Sensor = Strain gauge Sample Interval = 3600 Pump on before sampling 110.2 seconds Sampling Type = Autonomous Transmit Real Time Not Enabled Deployment Temperature: -1.0 Deployment Pressure: 500.0 Oxygen Time Constant (Tau20): 5.5 Battery Type is: AA Lithium Battery Capacity = 257040 Joules

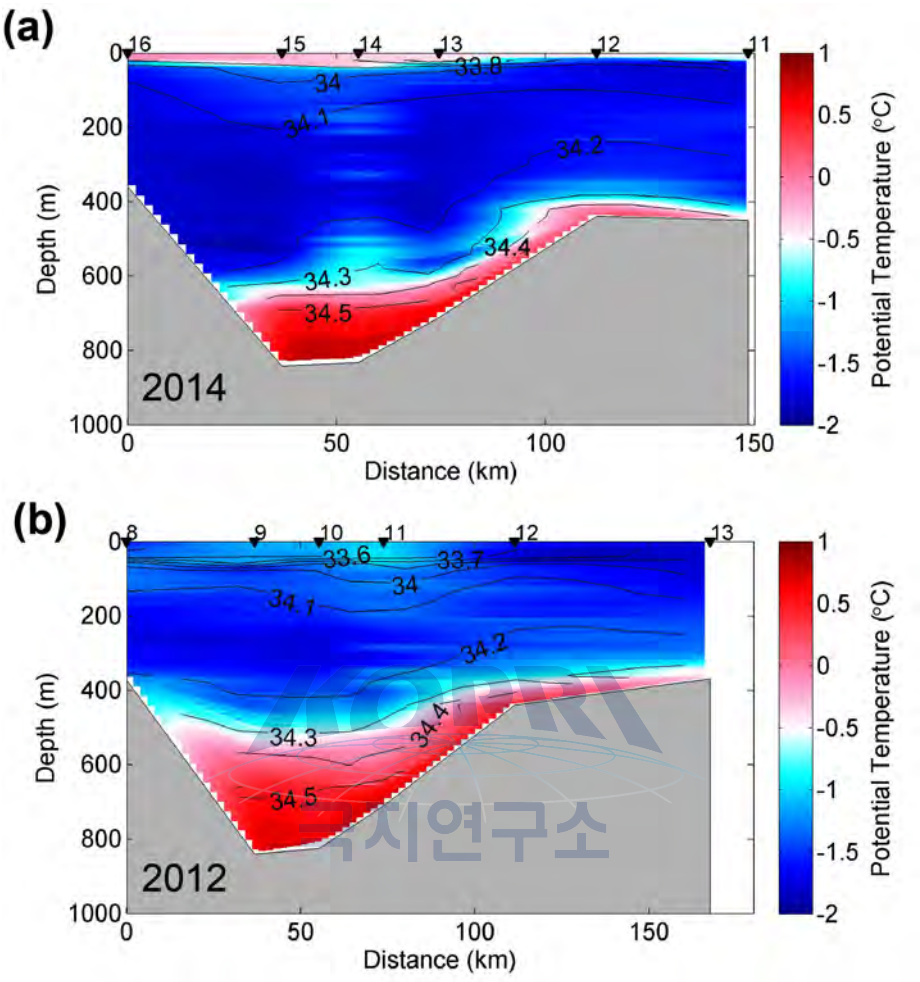

Figure 1.3: Vertical distribution of water mass properties across the Dotson Trough (T-2): (a) 2014 expedition, and (b) 2012 expedition. The color indicates the potential temperature, and the contour indicates the isohaline.

Table 1.3: Detail information on recovered KOPRI moorings. GPS location was determined by triangulation before releasing the acoustic release.

St.	Latitude (S)	Longitude (W)	Depth (m)	Recovery	
				(YYYY/MM/DD)	Time (UTC)
K1	72° 23.208′	117° 42.627′	530	2014/01/02	xx:xx
K2	73° 16.886′	114° 56.973′	830	2014/01/06	05:13
K3	74° 11.253′	112° 32.436′	1057	2014/01/09	02:51

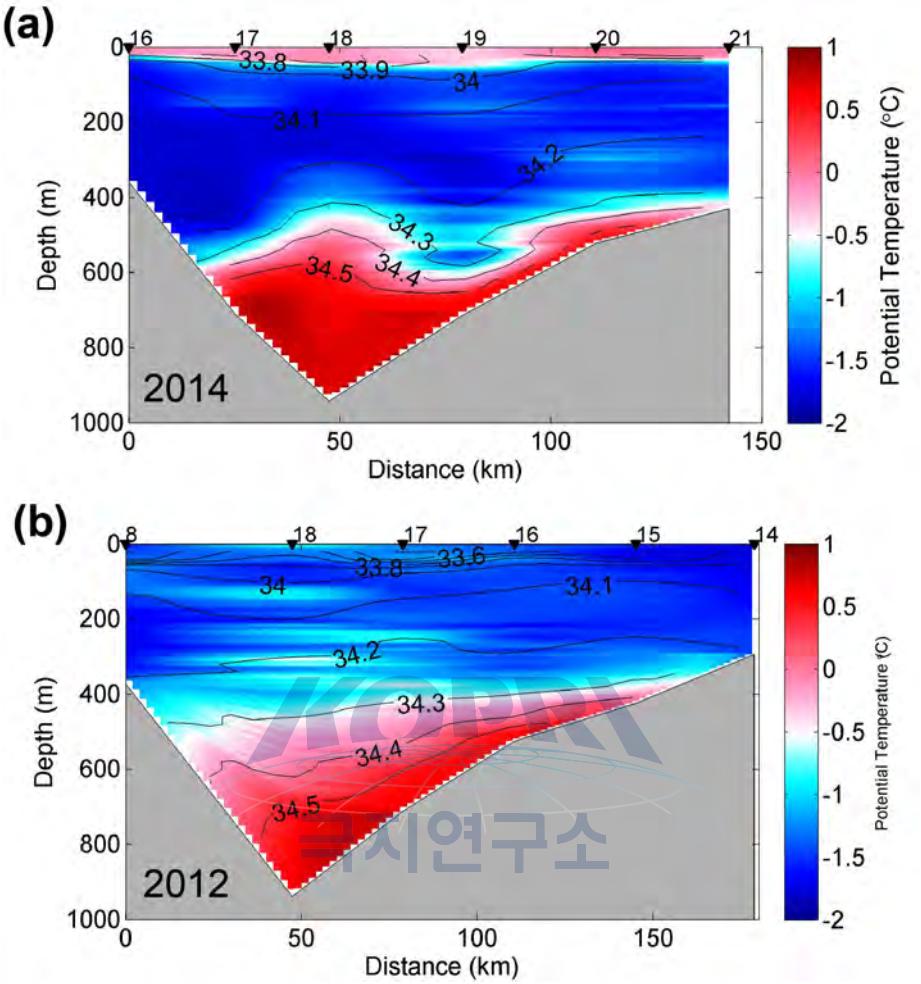

Figure 1.4: Vertical distribution of water mass properties across the Dotson Trough (T-2): (a) 2014 expedition, and (b) 2012 expedition. The color indicates the potential temperature, and the contour indicates the isohaline.

Table 1.4: Detail information on deployed KOPRI moorings. GPS location was determined by triangulation after finishing the deployment.

St.	Latitude (S)	Longitude (W)	Depth (m)	Date (YYYY/MM/DD)	Release Time (UTC)	No. deployment	CTD Station
K1	72° 23.188′	117° 42.757′	523	2014/01/03	12:45	3rd	4
K2	73° 16.790′	114° 57.024′	840	2014/01/06	13:50	3rd	14
K3	74° 10.292′	112° 31.699′	1028	2014/01/09	15:15	2nd	24
K4	74° 10.576′	112° 08.083′	785	2014/01/08	22:06	1st	23
K5	74° 10.946′	113° 03.823′	774	2014/01/09	21:10	1st	25
K6	73° 49.176′	113° 02.712′	~~782~~ 780	2014/01/10	12:20	1st	27

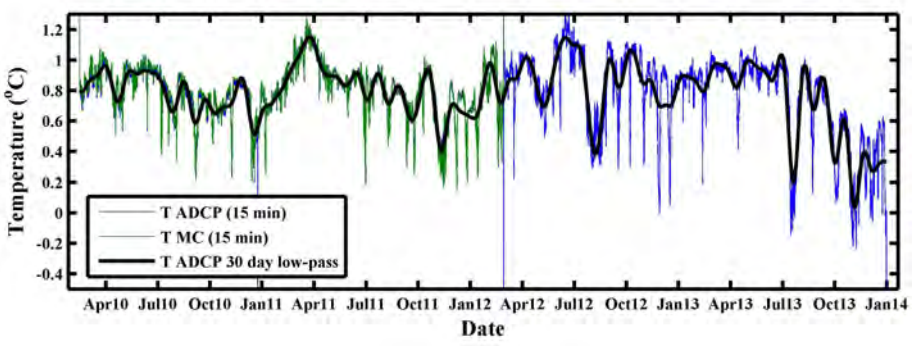

Figure 1.5: Four years of bottom temperature record at mooring site S1.

2010. The mooring was successfully recovered on 17:11 UTC of January 3, 2014 and a new mooring was deployed in the same site. The position now contains a 4-year unbroken time series of bottom temperature Fig. 1.5 and current velocity between the bottom and 300 m depth. This is the longest existing continuous record of velocity and bottom temperature from a 'warm' Antarctic shelf, i.e. one that is flooded with warm deep water. The 4-year time series will be used to study the external forcing of flow of warm deep water onto the shelf. It is noteworthy that the temperature dropped and had higher variability during 2013 compared to the previous 3 years. This is in accordance with the observations from the CTD that the layer of CDW was thinner and colder during the present cruise compared to the previous ones undertaken by the Araon and the Oden. Regrettably the Microcats measuring temperature and salinity higher in the water column ran out of power and stopped recording data in early 2013. The temperature- and salinity data from the water column can be used to further study the origin of water masses that flows onto the shelf.

Mooring S2

Mooring S2 was located at the shelf break with the purpose of studying the upstream source conditions for the inflow to Dotson Trough and to connect the shelf circulation with the currents on the shelf break. A light sea ice cover drifting at approximately 0.5-1 knots was present on the site which was reached on 03:58 UTC, January 2, 2014. A decision was made to attempt a recovery regardless of the sea ice, using the Araon as a shield from the ice. The Araon was put in hold position 200 m upstream of the mooring site, with heading 90 degrees angle to the sea ice drift, and the position and heading could be maintained impeccably using the DP system. The zodiac was launched in order to tow the mooring to the Araon after release. The release command was sent without any problems. The top buoy was reached by the zodiac relatively rapidly, but problems with the handling of the zodiac caused the recovery onto the aft deck to be significantly delayed. During that time the ADCP buoy got stuck in the sea ice. After re-deploying the zodiac (which was in the meantime mistakenly lifted back onto the Araon) the ADCP buoy could be salvaged by the zodiac.

Data from all instruments were recovered, but the Microcats had stopped recording in early 2013 due to power shortage. Fig. 1.6 shows the velocity at site S2. The velocity field is strongly dominated by tides, and the average velocity

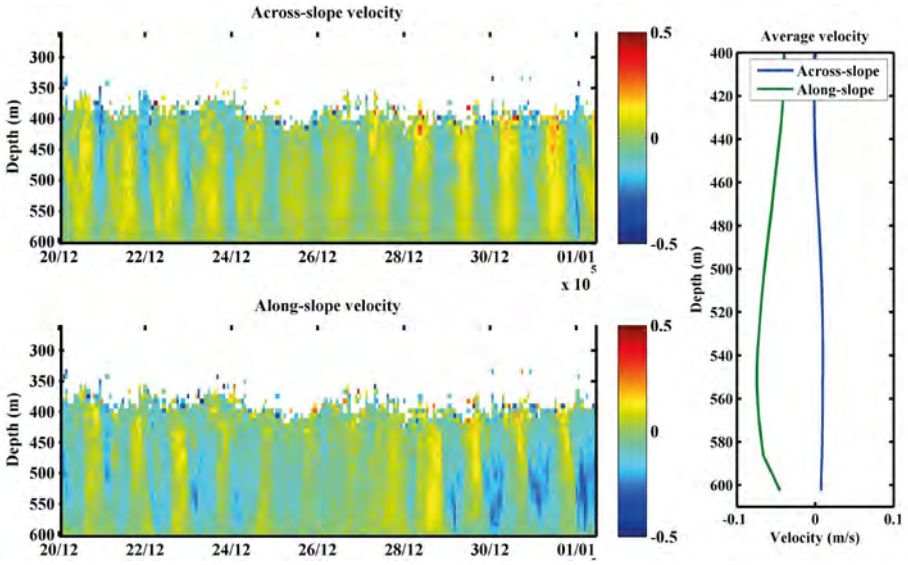

Figure 1.6: Velocity at site S2. Left panels show the recorded velocity during the days before recovery. Right panel shows the average velocity. Negative along-shelf velocities are towards the south-west, negative across-shelf velocities are toward the south-east.

is southwestward along the shelf break. A preliminary examination shows the existence of internal waves. These may be important for the mixing between water masses, and to transfer mechanical energy along the shelf break.

Mooring S3

Mooring site S3 was first visited on January 5, 2014. The first attempt to contact the acoustic releasers failed (possibly due to disturbance caused by sea ice). After moving the ship to a new position a successful wake-up call was sent, and the mooring was triangulated and found to have moved about 40 m towards the east since deployment. After several attempts a successful release command was sent, with confirmation from the releaser. However, the mooring did not move to the surface. An image of the mooring could be obtained by the scientific echo sounder (EK60), showing the top buoy in the expected position and the instruments lined up underneath it. The crew estimated that a dredging operation would take 6-8 hours, and a decision was made to abandon the mooring and if time allowed revisit the site after carrying through the other parts of the science program. The mooring would hence not be redeployed. Ten days later the site was revisited, and an attempt to dredge for the mooring was done. After the first contact between the dredging line and the mooring, the mooring floated to the surface by its own buoyancy. There were no traces of mud on the releasers and the anodes were covered by rust from the chain indicating that the releasers had been in the water column and not buried in mud. The wire had severe damage throughout its length, with the protective plastic torn in several places and bends and rust in the wire. It is possible that the wire got twisted during deployment, which would explain the damaged wire and might have caused the releasers to be entangled in the chain or in the wire. All four Microcats were recovered. Fig. 1.7 shows the temperature and pressure of the

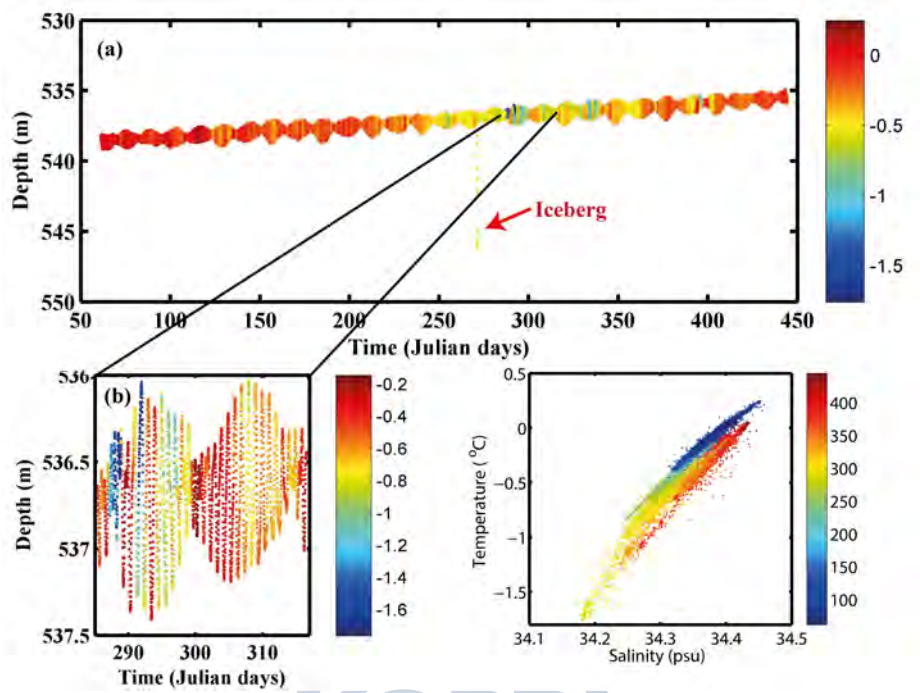

Figure 1.7: (a) Plot showing the pressure and temperature (according to color bar) as a function of time for the deepest sensor on mooring S3. The abrupt pressure drop at around 270 days is likely caused by an iceberg moving over the mooring and pushing the top buoy down by about 10 meters. The gradual decrease of pressure over the year may be caused by sensor drift which will be determined after recalibration. (b) The undulations are caused by tides, here an example of the neap- and spring tide cycles. (c) T-S diagram showing the mixture between warm deep water and glacier meltwater.

deepest Microcat at site S3, together with a TS- plot of the data. The TS data lines up on the 'Gade line', indicating it is a product of mixing between warm deep water and glacier melt water.

Mooring S5

The location for mooring S5 is on the southern part of the sill separating the Dotson-Getz shelf basin from the basins further west (Fig. 1.8). Before deploying the mooring at S5 a multibeam survey was conducted. Figure 1.8 shows the result of the multibeam survey with the final location of the mooring indicated. As expected, since very few bathymetric data exists from this region, the IBCSO data base turned out to be quite inaccurate. Among other features a new trench leading into the sill area was discovered. The sill depth was up to 100 meters deeper than in the IBCSO data. The deep trough North of the sill area appears to be about 150 m deeper than in the IBCSO data, and the walls significantly steeper. The multibeam data from the cruise will be reported to the International Bathymetric Chart of the Oceans on the return, so that the data can be incorporated into future gridded products such as the IBCSO.

Data

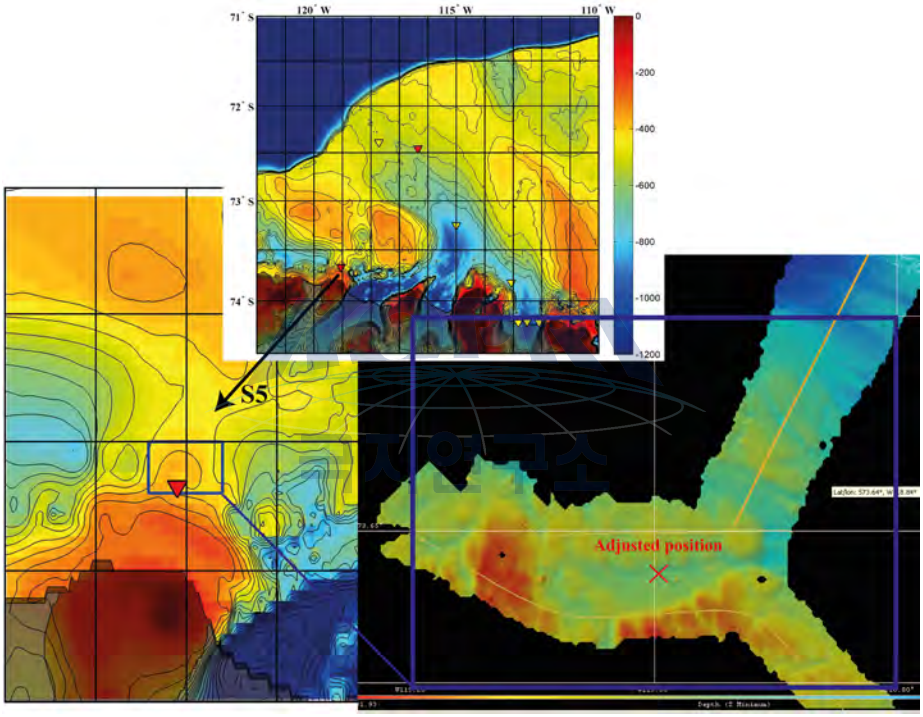

Figure 1.8: Bathymetry of the sill separating the Dotson-Getz basins from the basin further west.

Raw data from 11 of the UGOT Microcats and both ADCPs have been shared with KOPRI. 5 of the Microcats had minor or major problems with extracting data, and will be sent to Seabird for service, repair and support for extracting data. A final gridded and quality-checked product (including the salvaged data from the Microcats that will be sent to Seabird) will be developed by UGOT and shared with KOPRI before August 15, 2014. Joint publications using the data sets will be prepared similar to the joint work and publications that have already been undertaken. A draft plan for publications utilizing the data will be created during the SCAR guest professor visit by Dr. Wåhlin to KOPRI, scheduled to the end of May 2014.

1.3 Autonomous Glider Operation

Teledyne-Webb Slocum gliders are buoyancy-driven autonomous underwater vehicles. The gliders sample a 'sawtooth' upcast and downcast pattern underwater and surface at regular intervals to transmit data and mission information via an iridium satellite connection. These instrument platforms are ideally suited to compliment shipboard sampling by significantly increasing the temporal- and spatial- resolution of a field study that uses traditional rosette sampling systems. Past studies in the Antarctic include a single shallow glider deployment as part of the ASPIRE program, a deployment in the Ross Sea polynya, and numerous deployments along the Western Antarctic Peninsula (WAP). Two Teledyne-Webb Slocum gliders were deployed as part of the KOPRI 2014 Amundsen research cruise (ANA04B). RU25D, a deep glider, was configured to obtain high resolution data of the Dotson Glacier inflow and outflow of CDW, while RU24 was tasked with sampling a cross-polynya gradient of the euphotic zone and station keep near the polynya center (Fig. 1.9).

RU24 Shallow FiRE Glider

RU24 is a shallow glider rated to 100 meters depth that was equipped with a standard Seabird Electronics (SBE) un-pumped glider conductivity temperature and depth (CTD) sensor, an Aanderaa Optode for oxygen measurements and a FiRE sensor. We deployed RU24 at 73°58' 56.68" South and 112°59' 15.96" approximately 10 km from the western edge of the Dotson ice shelf on 13:00 UTC, January 4, 2014. The glider was programmed to sample due north into the polynya center. The glider surfaced approximately every hour and collected CTD and oxygen measurements on every down and upcast with a sample rate of approximately 0.5 Hz. To conserve power the FiRE sensor sampled at 0.1 Hz and alternated between sampling every down and upcast and only collecting 1 profile per hour long segment. RU24 was plagued by compass issues and could not maintain an accurate heading. Glider depth-averaged currents are suspect from this deployment and should not be used in analysis until further post-processing is performed.

During the northward transect between January 4th and January 7th two water masses were sampled. Surface water temperatures above 60 meters depth were warm (> 0°C) and temperatures below 60 meters were -1°C (Fig. 1.10a). Salinity was uniform throughout the water column near 34 psu (Fig. 1.10b). Toward the end of the cross-polynya transect and throughout the entire station

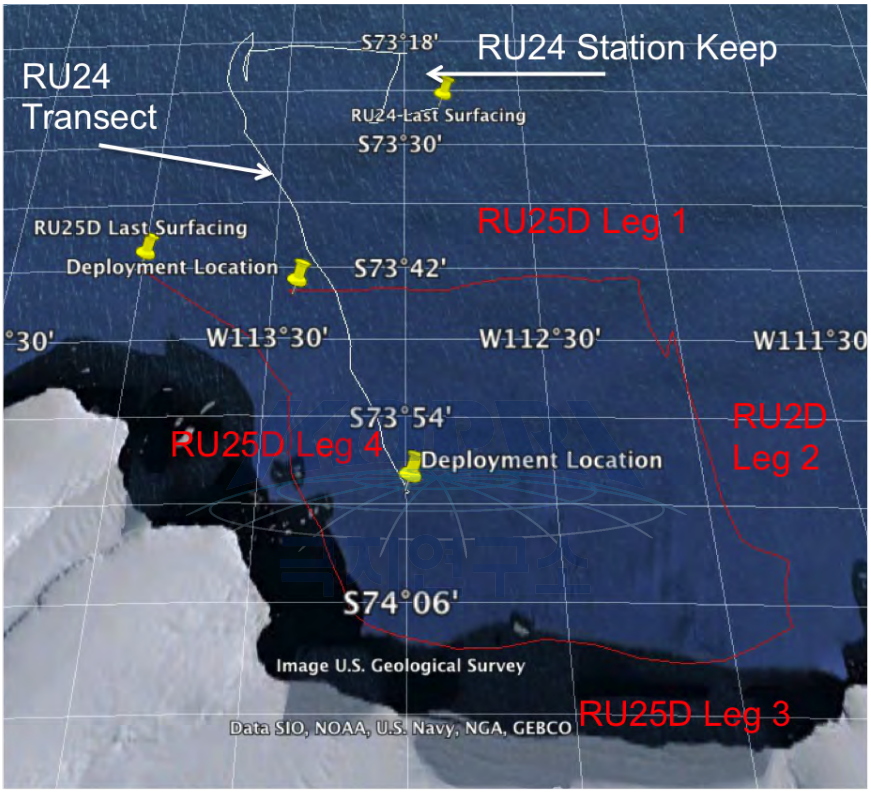

Figure 1.9: A map of the Glider deployment locations and sampling patterns. The track and Leg designations for RU25D are in red. The track and sampling segment for RU24 is in white.

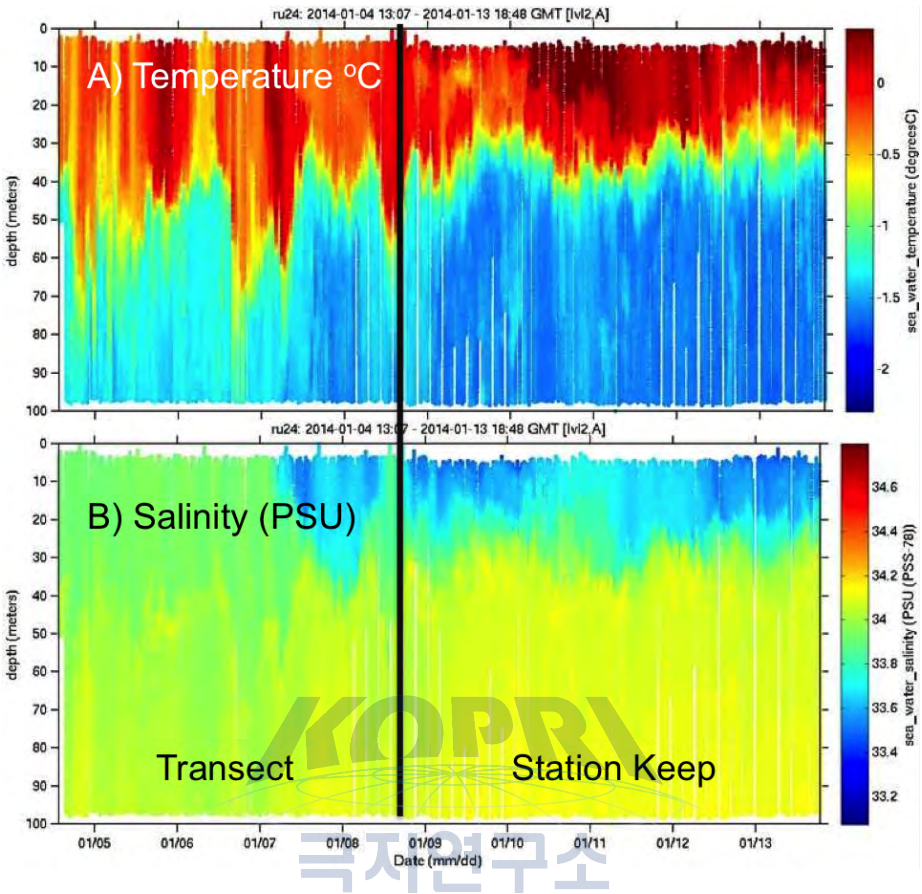

Figure 1.10: (A) RU24 Temperature (°C) and (B) Salinity (psu). Vertical lines indicate the transition from the cross polynya transect to station keeping locations.

keeping period, surface temperature increased and salinity decreased slightly. The source of this warmer and fresher surface water mass is currently unknown as there is no obvious source of freshwater input into the center of the polynya. This may be due to local sea-ice melt in the region but this needs to be confirmed via satellite imagery and compared with shipboard data. Oxygen saturation and concentration (Fig. 1.11) varied coincidently with temperature for the entire deployment and were elevated in the surface layer and depleted in the lower layer.

Initial Fv/Fm (Fig. 1.12) values were elevated at mid-depth near 0.3-0.4 between January 5th and January 7th during the cross-polynya transect. These values quickly dropped as RU24 moved northward. Further post-processing is necessary to obtain accurate Fv/Fm values. We collected an in lab blank to insure data quality. We used 0.7 micron filtered seawater and flooded the FiRE sensor once before cleaning and once after cleaning. There was little observed bio fouling so we do not expect cleaning to make a significant difference on blank values. Pre-cleaning average blank Fv/Fm values were 0.0215 and post-cleaning values were 0.04, with potential differences due to instrument noise.

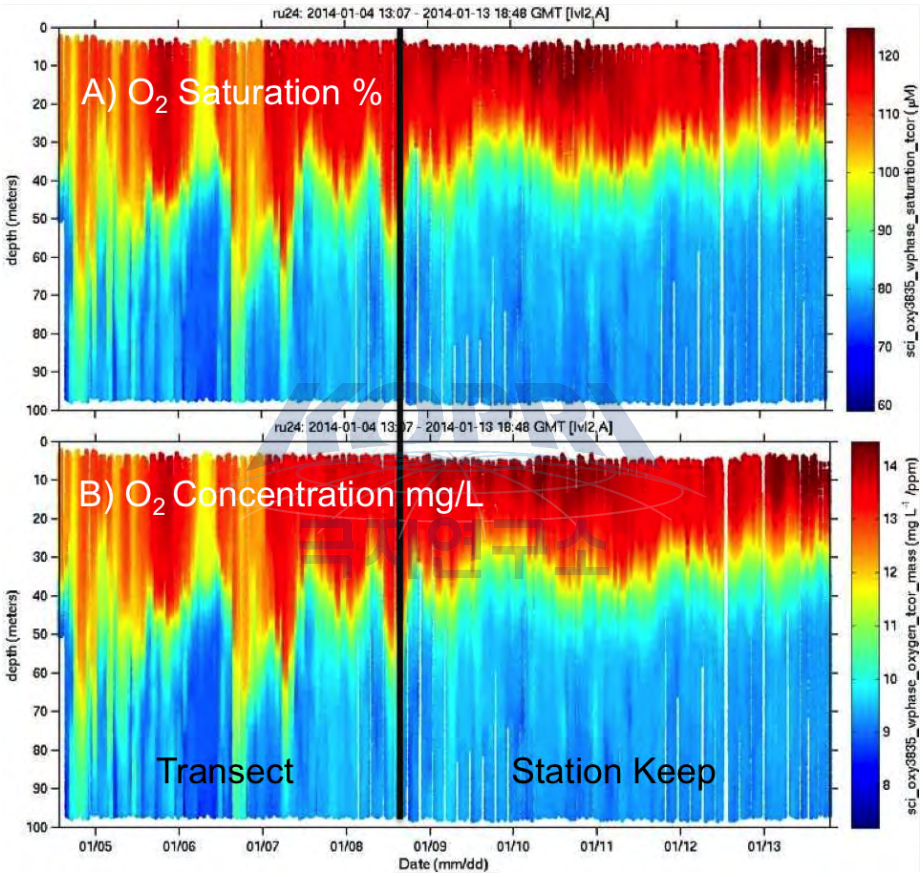

Figure 1.11: (A) RU24 Oxygen Saturation (%) and (B) Concentration (mg L-1). Vertical lines the same as in Fig. 1.10

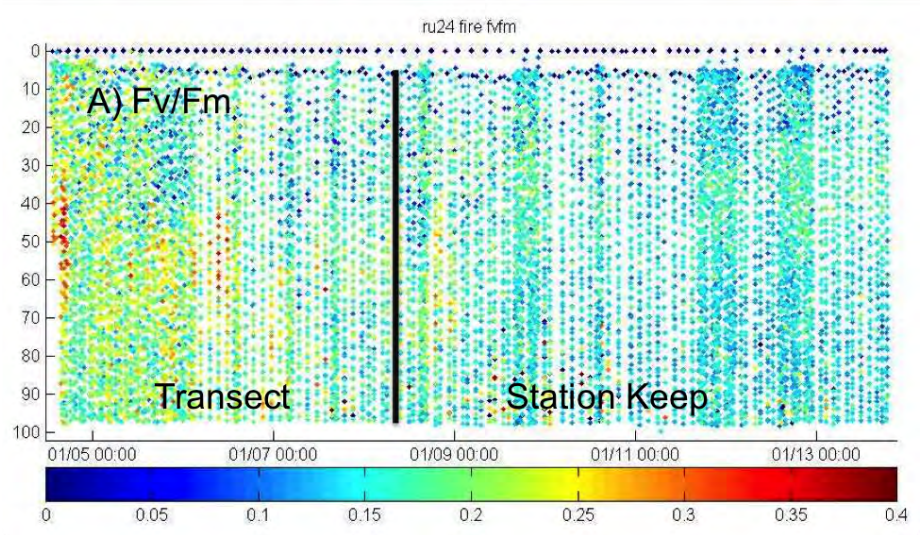

Figure 1.12: RU24 Fv/Fm from the FiRE sensor. Vertical lines the same as in Fig. 1.10

RU25D Deep Glider

RU25D is a deep glider rated to 1000 meters depth and was also equipped with a CTD, Aanderaa Optode and an additional Wetlabs Ecopuck. The Ecopuck measured Chlorophyll fluorescence, Colored Dissolved Organic Material (CDOM) and one channel of optical backscatter. This glider collected data with all sensors at a nominal 0.5 Hz on up- and down- casts continuously for the duration of the mission. Dive time is highly dependent on bathymetry, with 700 to 1000 meter dives taking approximately 3 to 4 hours.

RU25D was deployed at 73°43' 30.59" South and 113°25' 41.18" West at 17:05 UTC, January 4, 2014 and flew 4 distinct sections in front of the Dotson ice-shelf with a total deployment time of 8.87 days and 234.4 km sampled. The first section was cross channel toward the west (Fig. 1.9). The second leg was southward on the eastern flank of the channel, in a region previously identified by shipboard surveys and moorings as a pathway for CDW onshore and eventually beneath the ice-shelf. The third leg was a second cross-channel section westward approximately 10 km north of the Dotson Ice Shelf. The fourth leg was along isobath to the north and west in an effort to follow the outflow region along to the next ice shelf, The Getz. Throughout the deployment CDW (> 0°C) was associated with low oxygen, low chlorophyll, high salinity and high temperatures. Surface waters had high temperatures, low salinity, high oxygen and high chlorophyll (Fig. 1.13, 1.14, and 1.15).

We observed CDW up to a depth of 500 meters on the eastern side of the channel during both leg 1 and leg 3 with a downward slope to the west, where CDW reached only between 600 and 700 meters (Fig. 1.13). The depth of CDW along leg 2, i.e. the eastern flank of the channel remained relatively constant in temperature and depth at 500 meters. During leg 3 approximately 5 km north of the Dotson ice-shelf we identified a clear signature of basal melt water

between 200 and 100 meters. Relative to surface waters this water mass had cool temperatures ($\sim$ -1°C), salinities near 34 psu (Fig. 1.13a) and low oxygen ($\sim$ 70 % saturation). Below this water mass there was a signature of modified surface water with high oxygen ($>$ 90 % saturation) and low temperatures ($\sim$ -1°C) (Fig. 1.14). Chlorophyll was elevated in surface waters throughout the deployment, except for the region directly in front of the Dotson ice-shelf (Fig. 1.14a). Colored Dissolved Organic Matter (CDOM) was elevated in the CDW water masses and surface waters. The cause for this is unresolved, and will require further analysis and comparison with shipboard data.

During the 4th and final leg the glider was piloted northward and eventually westward toward the Getz ice-shelf along the outflow region. During this transit the glider sampled over a shallow ridge, where a clear CDW signal was identified from 400 to 100 meters depth (Fig. 1.13, 1.14, and 1.15). With no separation between CDW and surface water in this region there is potential for direct exchange between surface and deep waters after CDW has flowed out of the Dotson ice-shelf region. This would be an ideal location for future ship, mooring and glider based sampling, as this is a previously unknown feature of potential topographically steered upwelling.

1.4 Surface Drifter Deployment

A total of 30 drifters provided by NOAA (Dr. Shaun Dolk) were deployed in transit between Christchurch and Amundsen Sea. In particular, 4 drifters were deployed in the polynya of Amundsen Sea to investigate the surface circulation in the vicinity of Dotson Ice Shelf. The details on the drifters deployed during ANA04B were given in Table 1.5.

Acknowledgements

We are very grateful to the captain and crew of IBRV Araon for their professional support with all mooring works in making successful recoveries and deployments. The UGOT part of the project has been funded by the Swedish Research Council and the Swedish Polar Research Secretariats, for which we are grateful.

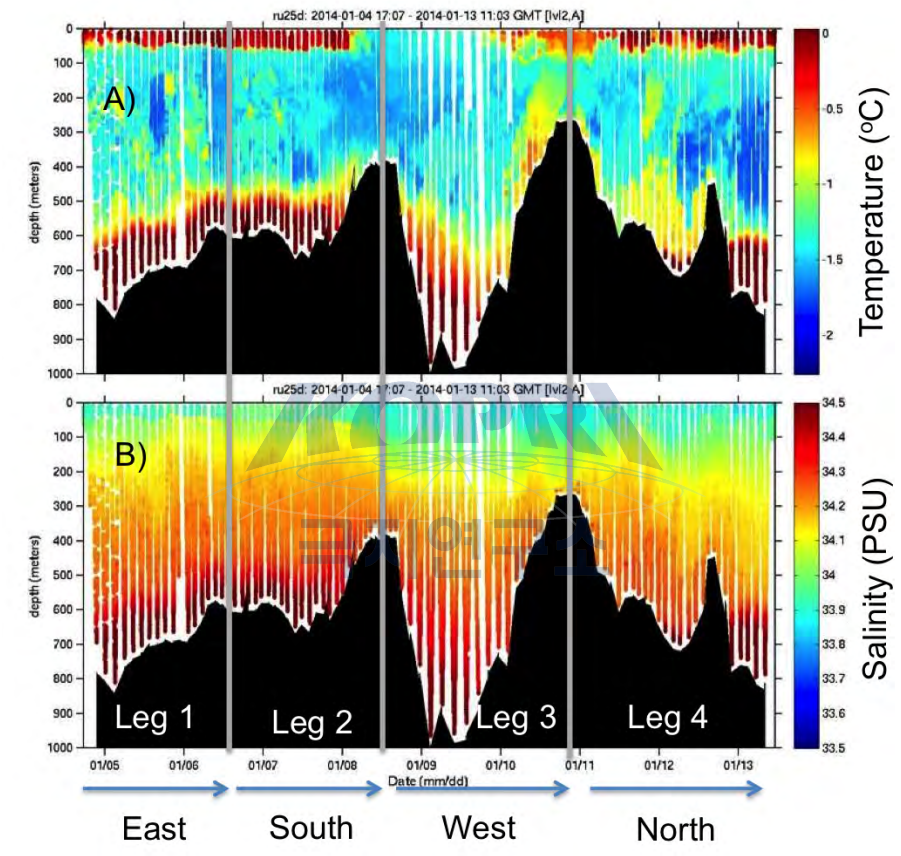

Figure 1.13: (A) RU25D Temperature (°C) and (B) Salinity (psu). Vertical lines separate Leg1, Leg2, Leg 3 and Leg 4, while arrows at bottom indicate direction of glider transit along that leg.

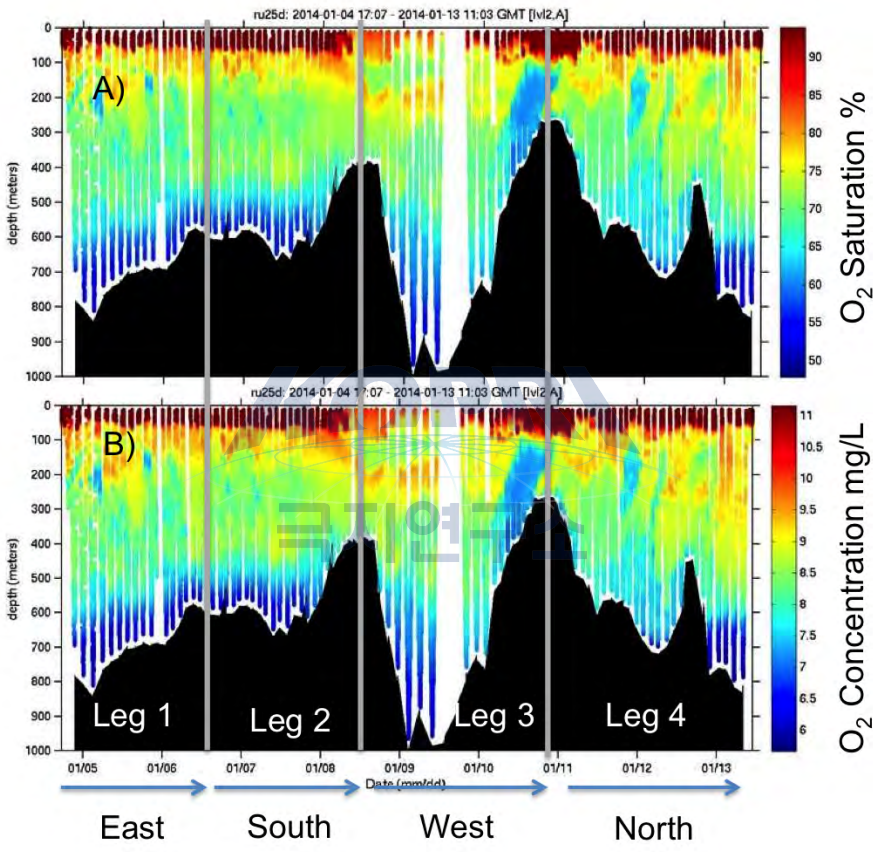

Figure 1.14: (A) RU25D Oxygen Saturation (%) and (B) Concentration (mg L-1) with line annotations the same as in Fig. 1.13

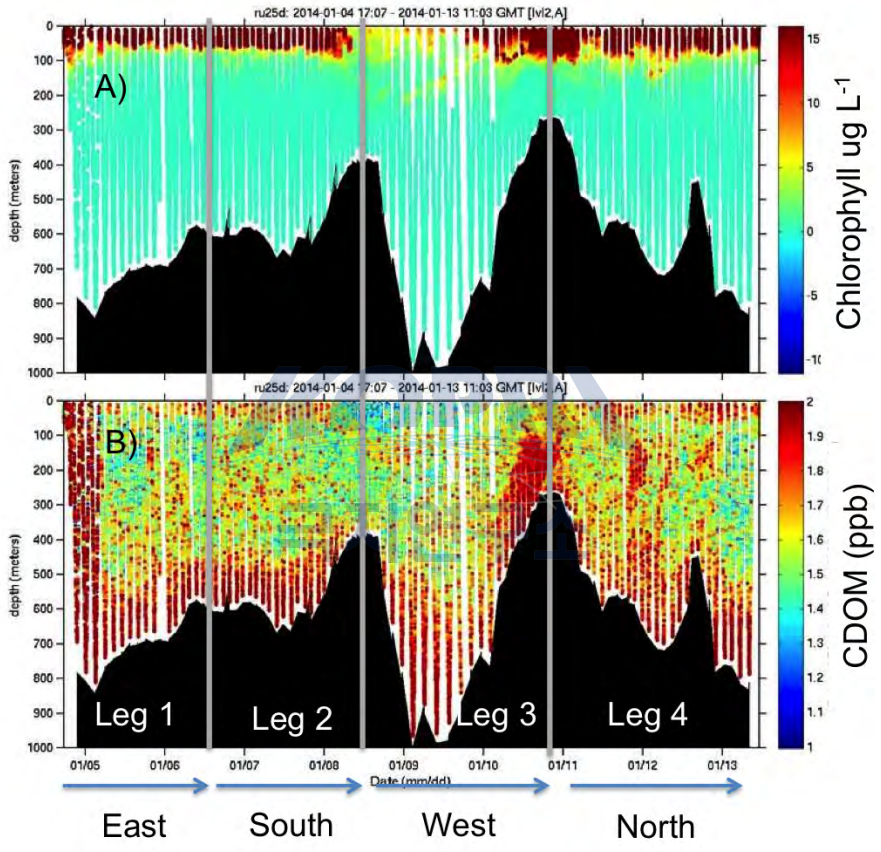

Figure 1.15: (A) RU25D Chlorophyll (μg L^{-1}) and (B) Colored Dissolved Organic Matter (ppb) with line annotations the same as in Fig. 1.13

Table 1.5: NOAA drifter deployed during the ANA04B.

N	ID	Date (mm/dd/yy)	Time (UTC)	Latitude (S)	Longitude (W)	Remark
1	**116429**	12/26/13	17:40	55° 00.2′	172° 57.2′	SPO, ACC
2	**116431**	12/26/13	20:44	55° 30.2′	172° 17.1′	
3	**116164**	12/26/13	23:22	56° 00.2′	171° 34.0′	
4	**116430**	12/27/13	02:07	56° 30.2′	170° 53.0′	
5	**116426**	12/27/13	03:34	56° 45.2′	170° 31.0′	
6	**116427**	12/27/13	04:56	57° 00.2′	170° 10.0′	
7	**116423**	12/27/13	06:19	57° 15.5′	169° 48.0′	
8	**116424**	12/27/13	07:40	57° 30.4′	169° 25.7′	
9	**116425**	12/27/13	10:24	58° 00.3′	168° 41.0′	
10	**116162**	12/27/13	13:13	58° 30.3′	167° 56.5′	
11	**116166**	12/27/13	16:02	59° 00.3′	167° 11.5′	
12	**116167**	12/27/13	18:53	59° 30.3′	166° 25.7′	
13	**116428**	12/27/13	20:20	59° 45.4′	166° 02.2′	
14	**116422**	12/27/13	21:45	60° 00.5′	165° 37.8′	
15	**116199**	12/27/13	23:06	60° 15.2′	165° 15.2′	
16	**116165**	12/28/13	00:31	60° 30.2′	164° 48.6′	
17	**116202**	12/28/13	03:41	61° 00.2′	163° 43.4′	
18	**116160**	12/28/13	06:51	61° 30.2′	162° 38.0′	
19	**116203**	12/28/13	09:59	62° 00.2′	161° 31.3′	
20	**116168**	12/28/13	13:05	62° 30.2′	160° 23.4′	
21	**116163**	12/28/13	16:17	63° 00.3′	159° 14.6′	
22	**116300**	12/28/13	19:27	63° 30.3′	158° 04.3′	
23	**116206**	12/28/13	23:03	64° 05.2′	156° 41.7′	
24	**116201**	01/08/14	00:15	73° 29.9′	112° 58.3′	AS, CTD/ST#20
25	**116161**	01/08/14	11:55	73° 51.4′	112° 02.3′	AS, WayPoint2 (EK60)
26	**116208**	01/09/14	16:05	74° 10.2′	112° 33.3′	AS, K3 (#24) (Dotson IS)
27	**116209**	01/10/14	13:10	73° 49.5′	113° 04.0′	AS, K6 (#27)
28	**116205**	01/18/14	11:12	66° 59.7′	153° 34.5′	SPO, ACC
29	**116207**	01/18/14	20:15	66° 00.0′	156° 50.5′	
30	**116204**	01/19/14	06:00	65° 00.0′	160° 00.0′	

Appendix I. ANA04B cruise log spreadsheet.

See the following pages.

Scientific Cruise Daily Log

Ship: R/V Araon | **Cruise:** ANA04 | **Leg:** B

Prepared by H. J. Lee (KOPRI) hyunjung@kopri.re.kr

STN No.	Gear	Cast No.	Date	Cast start	Bottom or at depth	Cast end	Latitude	Longitude	Water depth	Cast depth	Cable payout	No. of spl. depth Core length	Wind speed	Wind direction	Ship speed	Heading	Remarks	Device Driver
			(UTC)	(UTC)	(UTC)	(UTC)			(m)	(m)	(m)		knot	(°)	knot	(°)		
Amundsen Sea																		
CTD: CTD;PHY: Phytoplankton; BON: Bongo net; BOX: Box core; OBY: ocean buoy;DBY: Drifter buoy;FLM: Fluoremeter;;GOF: Go Flo;GLD:Glider;RTN:Rectangular net;ICE: work on sea-ice;																		
	DBY	1	12-26-2013	17:40			55°00.2'S	172°57.20'W							14.0		116429 : Depolyed Drifter (SPO,ACC)	CS Hong
	DBY	2	12-26-2013	20:44			55°30.2'S	172°17.10'W							14.0		116431 : Depolyed Drifter (SPO,ACC)	CS Hong
	DBY	3	12-26-2013	23:22			56°00.2'S	171°34.00'W							14.0		116164 : Depolyed Drifter (SPO,ACC)	CS Hong
	DBY	4	12-27-2013	2:07			56°30.2'S	170°53.00'W							14.0		116430 : Depolyed Drifter (SPO,ACC)	CS Hong
	DBY	5	12-27-2013	3:34			56°45.2'S	170°31.00'W							14.0		116426 : Depolyed Drifter (SPO,ACC)	CS Hong
	DBY	6	12-27-2013	4:56			57°00.2'S	170°10.00'W							14.0		116427 : Depolyed Drifter (SPO,ACC)	CS Hong
	DBY	7	12.27.2013	6:19			57°15.5'S	169°48.00'W							14.0		116423 : Depolyed Drifter (SPO,ACC)	CS Hong
	DBY	8	12-27-2013	7:40			57°30.4'S	169°25.70'W							14.0		116424 : Depolyed Drifter (SPO,ACC)	CS Hong
	DBY	9	12-27-2013	10:24			58°00.3'S	168°41.00'W							14.0		116425 : Depolyed Drifter (SPO,ACC)	CS Hong
	DBY	10	12-27-2013	13:13			58°30.3'S	167°56.50'W							14.0		116162 : Depolyed Drifter (SPO,ACC)	CS Hong
	DBY	11	12-27-2013	16:02			59°00.3'S	167°11.50'W							14.0		116166 : Depolyed Drifter (SPO,ACC)	CS Hong
	DBY	12	12-27-2013	18:53			59°30.3'S	166°25.70'W							14.0		116167 : Depolyed Drifter (SPO,ACC)	CS Hong
	DBY	13	12-27-2013	20:20			59°45.4'S	166°02.20'W							14.0		116428 : Depolyed Drifter (SPO,ACC)	CS Hong
	DBY	14	12-27-2013	21:45			60°00.5'S	165°37.80'W							14.0		116422 : Depolyed Drifter (SPO,ACC)	CS Hong
	DBY	15	12-27-2013	23:06			60°15.2'S	165°15.20'W							14.0		116199 : Depolyed Drifter (SPO,ACC)	CS Hong
	DBY	16	12-28-2013	0:31			60°30.2'S	164°48.60'W							14.0		116165 : Depolyed Drifter (SPO,ACC)	CS Hong
	DBY	17	12-28-2013	3:41			61°00.2'S	163°43.40'W							14.0		116202 : Depolyed Drifter (SPO,ACC)	CS Hong
	DBY	18	12-28-2013	6:51			61°30.2'S	162°38.00'W							14.0		116160 : Depolyed Drifter (SPO,ACC)	CS Hong
	DBY	19	12-28-2013	9:59			62°00.2'S	161°31.30'W							14.0		116203 : Depolyed Drifter (SPO,ACC)	CS Hong
	DBY	20	12-28-2013	13:05			62°30.2'S	160°23.40'W							14.0		116168 : Depolyed Drifter (SPO,ACC)	CS Hong
	DBY	21	12-28-2013	16:17			63°00.3'S	159°14.60'W							14.0		116163 : Depolyed Drifter (SPO,ACC)	CS Hong
	DBY	22	12-28-2013	19:27			63°30.3'S	158°04.30'W							14.0		116300 : Depolyed Drifter (SPO,ACC)	CS Hong
	DBY	23	12-28-2013	23:03			64°05.2'S	156°41.70'W							14.0		116206 : Depolyed Drifter (SPO,ACC)	CS Hong
1	CTD	Test	12-31-2013	11:46		13:40	69°59.9'S	127°54.49'W	3500								Failed due to CTD fuse problem	TW Kim
1	CTD	1	12-31-2013	13:50		16:21	70°00.0'S	127°54.63'W	3515	3490		24	5.9	111.0	0.0	101.0	First deep casting	TW Kim
1	PHY	1	12-31-2013	16:35		16:50				70							20 micron mesh	EJ Yang
1	BON	1	12-31-2013	17:00		17:35				200							Vertical towing	DB Lee
1	CTD	2	12-31-2013	18:00		18:15	70°00.1'S	127°54.64'W	3518	100		24	4.5	109.0	0.0	101.4	Second shallow casting	HJ Lee
1	FLM	1	12-31-2013	18:38		19:00				50							Fluorescence Induction & Relaxation system	JS Park
1	CTD	3	12-31-2013	19:12		19:25	70°00.1'S	127°54.66'W	3517	60		24	5.4	95.0	0.0	101.0	Third shallow casting	CY Kang
1	GOF	1	12-31-2013	20:06		20:35	70°00.4'S	127°56.30'W		15		12					Cancelled due to equipment trouble	EJ Yang
2	CTD	1	01-01-2014	8:05		10:48	71°00.4'S	123°00.76'W	3260	3200		24	5.7	95.8	0.0	95.8	during downcasting ctd problem, the second cast overwrite the first cast file	HJ Lee
2	PHY	1	01-01-2014	11:06		11:13				70							20 micron mesh	EJ Yang
2	BON	1	01-01-2014	11:18		11:46				200							Vertical towing	DB Lee
2	FLM	1	01-01-2014	11:50		12:10				50							Fluorescence Induction & Relaxation system	JS Park
2	CTD	2	01-01-2014	12:37		12:53	71°00.7'S	123°01.64'W	3282	100		24	3.9	86.0	0.0	4.6	Second shallow casting	HJ Lee
2	CTD	3	01-01-2014	13:33		13:39	71°02.0'S	123°00.87'W	3277	2		24	5.4	340.0	0.6	342.0	Third shallow casting	CY Kang
2	CTD	4	01-01-2014	14:17		14:34	71°02.2'S	123°00.55'W	3284	100		24	6.9	359.0	0.7	306.0	Fourth shallow casting	CY Kang
2	GOF	1	01-01-2014	15:35		15:45	71°02.3'S	122°59.90'W		15		0					Cancelled due to equipment trouble	EJ Yang
2	GOF	2	01-01-2014	16:10		16:15	71°02.6'S	122°57.83'W		15		0					Cancelled due to equipment trouble	EJ Yang
2	GOF	3	01-01-2014	17:00		17:00	71°02.7'S	122°56.81'W		15		0					Cancelled due to equipment trouble	EJ Yang
3	OBY	1	01-02-2014	4:10		8:05	71°56.8'S	118°26.92'W	620								US S2 buoy recovery	A Wahlin
3	CTD	1	01-02-2014	8:54		9:40	71°57.0'S	118°27.07'W	620	610		24	10.8	77.8	0.0	41.6	First deep casting	HJ Lee
3	PHY	1	01-02-2014	10:15		10:25				70							20 micron mesh	EJ Yang
3	BON	1	01-02-2014	10:30		11:00				200							Vertical towing	DB Lee
3	FLM	1	01-02-2014	12:00		12:30				50							Fluorescence Induction & Relaxation system	JS Park
3	CTD	2	01-02-2014	12:40		12:56	71°57.0'S	118°27.03'W	643	100		24	10.2	66.4	0.0	57.2	Second shallow casting	CY Kang
3	CTD	3	01-02-2014	13:43		13:55	71°57.0'S	118°27.03'W	643	60		24	10.4	65.9	0.0	62.9	Third shallow casting	CY Kang
3	GOF	1	01-02-2014	14:15		15:00				600							Go_Flo deep casting	DS Hahm
4	OBY	1	01-02-2014	18:08		20:20	72°23.2'S	117°42.63'W	525								KOPRI K1 recovery	HK Ha
4	CTD	1	01-02-2014	21:19		22:04	72°23.2'S	117°42.64'W	517	508		24	15.3	26.7	0.0	70.8	First deep casting	CY Kang
4	PHY	1	01-02-2014	23:20		23:30				70							20 micron mesh	EJ Yang
4	BON	1	01-02-2014	23:30		0:00				200							Vertical towing	DB Lee
4	FLM	1	01-03-2014	0:00		0:30				50							Fluorescence Induction & Relaxation system	JS Park
4	CTD	2	01-03-2014	0:35		0:51	72°23.2'S	117°42.64'W	517	100		24	12.5	27.0	0.0	58.0	Second shallow casting	HJ Lee
4	CTD	3	01-03-2014	1:30		1:44	72°23.2'S	117°42.64'W	514	60		24	12.2	23.6	0.0	57.5	Third shallow casting	HJ Lee
4	GOF	1	01-03-2014	2:15		2:30				15		12					Go_Flo shallow casting (1)	EJ Yang
4	GOF	2	01-03-2014	4:05		4:30				15		12					Go_Flo shallow casting (2)	EJ Yang
4	GOF	3	01-03-2014	6:15		6:42				15		12					Go_Flo shallow casting (3)	EJ Yang
4	GOF	4	01-03-2014	8:00		8:25				15		12					Go_Flo shallow casting (4)	EJ Yang
4	BOX	1	01-03-2014	9:00	9:35	10:10				514							Box Core	EJ Yang
4	OBY	1	01-03-2014	11:25		13:30	72°23.2'S	117°42.76'W	523								KOPRI K1 Deploy	HK Ha
5	OBY	1	01-03-2014	17:50		19:00											US S1 buoy recovery	A Wahlin
5	CTD	1	01-03-2014	20:19		20:56	72°28.0'S	116°17.09'W	536	527		24	14.4	72.3	0.1	86.8	First deep casting	CY Kang
5	PHY	1	01-03-2014	21:15		21:29				70							20 micron mesh	EJ Yang

Scientific Cruise Daily Log

Ship: R/V Araon | **Cruise:** ANA04 | **Leg:** B | Prepared by H. J. Lee (KOPRI) hyunjung@kopri.re.kr

STN No.	Gear	Cast No.	Date	Cast start (UTC)	Bottom or at depth (UTC)	Cast end (UTC)	Latitude	Longitude	Water depth (m)	Cast depth (m)	Cable payout (m)	No. of spl. depth Core length	Wind speed knot	Wind direction (°)	Ship speed knot	Heading (°)	Remarks	Device Driver
								Amundsen Sea										
CTD: CTD;PHY: Phytoplankton; BON: Bongo net; BOX: Box core; OBY: ocean buoy;DBY: Drifter buoy;FLM: Fluoremeter;;GOF: Go Flo;GLD:Glider;RTN:Rectangular net;ICE: work on sea-ice;																		
5	BON	1	01-03-2014	21:32		21:46				200							Vertical towing	DB Lee
5	FLM	1	01-03-2014	22:06		22:30				50							Fluorescence Induction & Relaxation system	JS Park
5	CTD	2	01-03-2014	23:12		23:28			536	100		24					Second shallow casting	CY Kang
5	OBY	1	01-04-2014	0:53		2:30	72°27.3'S	116°21.13'W	557								US S1 buoy deploy	A Waulin
6	GLD	1	01-04-2014	12:24		13:35	73°60.0'S	112°59.98'W	527								Shallow Glider deployment	T Mailse
6	CTD	1	01-04-2014	13:54		14:43	73°60.0'S	112°59.98'W	527	515		24	9.6	253.2	0.0	253.2	First deep casting	CY Kang
7	GLD	1	01-04-2014	16:28		17:20	73°45.0'S	113°25.00'W	750								Deep Gilder deployment	T Mailse
7	CTD	1	01-04-2014	17:28		18:20	73°45.0'S	113°25.00'W	750	740		24	7.6	131.1	0.1	244.0	First deep casting	CY Kang
8	CTD	1	01-05-2014	2:13		3:02	72°55.4'S	117°35.26'W	543	535		24	12.3	114.0	0.0	246.0	First deep casting	HJ Lee
8	OBY	1	01-05-2014	3:30		5:30											Faild US S3 buoy recovery	A Wahlin
9	CTD	1	01-05-2014	6:12		6:57	72°51.6'S	117°12.01'W	626	612		24	11.5	113.0	0.1	140.7	First deep casting	HJ Lee
10	CTD	1	01-05-2014	10:17		11:05	72°48.0'S	115°17.89'W	599	590		24	14.2	127.0	0.0	115.0	First deep casting	HJ Lee
10	PHY	1	01-05-2014	11:15		11:30				70							20 micron mesh	EJ Yang
10	BON	1	01-05-2014	11:30		12:00				200							Vertical towing	DB Lee
10	FLM	1	01-05-2014	12:00		12:30				50							Fluorescence Induction & Relaxation system	JS Park
10	CTD	2	01-05-2014	12:40		12:56	72°48.0'S	115°17.89'W	599	100		24	16.6	116.3	0.0	137.3	Second shallow casting	CY Kang
10	CTD	3	01-05-2014	13:40		13:55	72°48.0'S	115°17.89'W	599	60		24	15.2	117.0	0.1	136.9	Third shallow casting	CY Kang
11	CTD	1	01-05-2014	19:46		20:25	72°51.0'S	112°30.09'W	450	440		24	12.7	138.7	12.7	138.7	First deep casting	CY Kang
12	CTD	1	01-05-2014	22:25		23:00	72°59.6'S	113°29.99'W	439	428		24	13.3	114.2	0.1	152.7	First deep casting	CY Kang
13	CTD	1	01-06-2014	1:05		2:07	73°10.0'S	114°30.01'W	711	705		24	12.7	105.0	0.2	149.2	First deep casting	HJ Lee
13	CTD	2	01-06-2014	3:02		3:19	73°10.0'S	114°30.01'W	711	100		24	12	113.0	0.1	151.4	Second shallow casting	HJ Lee
14	OBY	1	01-06-2014	4:25		7:10	73°10.0'S	114°30.01'W									KOPRI K2 buoy recovery	HK Ha
14	CTD	1	01-06-2014	7:35		8:26	73°10.0'S	114°30.01'W	832	820		24	8.9	132.0	0.0	257.2	First deep casting	HJ Lee
14	PHY	1	01-06-2014	9:15		9:35				70							20 micron mesh	EJ Yang
14	BON	1	01-06-2014	9:35		10:15				200							Vertical towing	DB Lee
14	FLM	1	01-06-2014	10:18		10:44				50							Fluorescence Induction & Relaxation system	JS Park
14	CTD	2	01-06-2014	10:57		11:13	73°16.9'S	114°56.97'W	832	100		24	11.2	141.0	0.1	176.0	Second shallow casting	HJ Lee
14	CTD	3	01-06-2014	11:57		12:09	73°16.9'S	114°56.97'W	832	40		24	11.6	149.0	11.6	105.0	Third shallow casting	HJ Lee
14	GOF	1	01-06-2014	12:30		12:50				15		11					Go_Flo shallow casting (1)	EJ Yang
14	GOF	2	01-06-2014	13:15		14:30				15		11					Go_Flo shallow casting (2)	EJ Yang
14	GOF	3	01-06-2014	15:20		15:27				15		11					Go_Flo shallow casting (3)	EJ Yang
14	GOF	4	01-06-2014	16:45		16:57				15		11					Go_Flo shallow casting (4)	EJ Yang
14	GOF	5	01-06-2014	18:35		18:55				15		11					Go_Flo shallow casting (5)	EJ Yang
14	GOF	6	01-06-2014	20:20		21:13				800		11					Go_Flo deep casting	DS Hahm
14	BOX	1	01-06-2014	21:35	23:00	23:25				840							Box Core	EJ Yang
14	OBY	1	01-06-2014	0:05		1:49	73°16.8'S	114°57.02'W		840							KOPRI K2 buoy deploy	HK Ha
15	CTD	1	01-07-2014	4:17		5:16	73°20.0'S	115°29.96'W	842	830		24	11.9	160.0	0.0	177.4	First deep casting	HJ Lee
16	CTD	1	01-07-2014	7:43		8:15	73°30.0'S	116°29.99'W	360	355		24	7.0	160.0			First deep casting	HK Ha
17	CTD	1	01-07-2014	9:45		10:44	73°29.3'S	115°42.23'W	710	700		24	4.6	168.3	0.0	170.0	First deep casting	HJ Lee
18	CTD	1	01-07-2014	12:05		13:04	73°30.0'S	115°01.00'W	942	932		24	8.2	141.0	0.0	166.8	First deep casting	HJ Lee
19	CTD	1	01-07-2014	14:53		15:55	73°30.0'S	114°00.04'W	714	704		24	11.3	162.0	0.4	183.6	First deep casting	CY Kang
19	PHY	1	01-07-2014	16:05		16:20				70							20 micron mesh	EJ Yang
19	BON	1	01-07-2014	16:23		17:00				200							Vertical towing	DB Lee
19	FLM	1	01-07-2014	17:03		17:23				50							Fluorescence Induction & Relaxation system	JS Park
19	CTD	2	01-07-2014	17:44		17:59	73°30.0'S	114°00.04'W	714	100		24	6.3	163.1	0.3	161.1	Second shallow casting	CY Kang
19	CTD	3	01-07-2014	18:45		19:14	73°30.0'S	114°00.02'W	714	400		24	8.3	158.9	0.0	176.0	Third shallow casting	CY Kang
19	CTD	4	01-07-2014	20:04		20:17	73°30.0'S	114°00.02'W	714	60		24	8.2	178.7	0.2	176.7	Fourth shallow casting	CY Kang
19	GOF	1	01-07-2014	20:43		21:30				690							Go_Flo deep casting	DS Hahm
20	CTD	1	01-07-2014	23:22		0:06	73°30.0'S	112°52.97'W	522	521		24	3.8	115.0	0.0	141.7	First deep casting	CY Kang
	DBY	24	01-08-2014	0:25		0:27	73°29.9'S	112°59.00'W							6.0		116201 : Depolyed Drifter (AS,CTD/ST#20)	CS Hong
21	CTD	1	01-08-2014	1:54		2:30	73°30.0'S	112°00.01'W	430	420		24	5.1	231.8	0.1	238.0	First deep casting	HJ Lee
	RTN	1	01-08-2014	5:30		6:45					400				2.0		oblique sample	HS La
	RTN	2	01-08-2014	9:50		10:45					400				2.0		oblique sample	HS La
	DBY	25	01-08-2014	11:55		11:57	73°51.4'S	112°02.42'W									116161 : Depolyed Drifter (AS, Waypoint2)	CS Hong
	RTN	1	01-08-2014	13:15		14:05					400						oblique sample	HS La
22	CTD	1	01-08-2014	17:29		18:19	74°12.2'S	111°58.46'W	632	623		24	4.0	199.0			First deep casting	HK Ha
22	CTD	2	01-08-2014	19:30		19:43	74°12.2'S	111°58.46'W	633	100		24	4.1	237.0	0.0	150.0	Second shallow casting	HJ Lee
23	OBY	1	01-08-2014	21:15		22:46	74°10.6'S	112°08.08'W	785								KOPRI K4 buoy deploy	HK Ha
23	CTD	1	01-08-2014	23:30		0:34	74°10.4'S	112°09.18'W	945	932		24	1.7	209.3	0.0	119.3	First deep casting	CY Kang
	RTN	1	01-09-2014	1:00		1:43					400				2.6		oblique sample	HS La
24	OBY	1	01-09-2014	2:05		4:15	74°11.1'S	112°32.43'W									KOPRI K3 buoy recovery	HK Ha
24	BOX	1	01-09-2014	5:45		6:45			1058									EJ Yang
24	CTD	1	01-09-2014	7:26		8:26	74°11.2'S	112°32.36'W	1054	1040		24	3.7	198.0	0.0	141.5	First deep casting	HJ Lee
24	PHY	1	01-09-2014	8:35		8:48				70							20 micron mesh	EJ Yang
24	BON	1	01-09-2014	8:48		9:25				200							Vertical towing	DB Lee

Scientific Cruise Daily Log

Ship: R/V Araon | **Cruise:** ANA04 | **Leg:** B

Prepared by H. J. Lee (KOPRI) hyunjung@kopri.re.kr

STN No.	Gear	Cast No.	Date	Cast start	Bottom or at depth	Cast end	Latitude	Longitude	Water depth	Cast depth	Cable payout	No. of spl. depth Core length	Wind speed	Wind direction	Ship speed	Heading	Remarks	Device Driver
			(UTC)	(UTC)	(UTC)	(UTC)			(m)	(m)	(m)		knot	(°)	knot	(°)		
Amundsen Sea																		
CTD: CTD;PHY: Phytoplankton; BON: Bongo net; BOX: Box core; OBY: ocean buoy;DBY: Drifter buoy;FLM: Fluoremeter;;GOF: Go Flo;GLD:Glider;RTN:Rectangular net;ICE: work on sea-ice;																		
24	FLM	1	01-09-2014	9:30		9:50				50							Fluorescence Induction & Relaxation system	JS Park
24	CTD	2	01-09-2014	10:14		10:43	74°11.2'S	112°32.39'W	1054	400		24	6.7	172.0	0.1	251.3	Second shallow casting	HJ Lee
24	CTD	3	01-09-2014	11:29		11:38	74°11.2'S	112°32.39'W	1054	19		24	7.4	173.0	0.2	251.8	Third shallow casting	HJ Lee
24	GOF	1	01-09-2014	12:10		12:50				800							Go-FLO deep casting	DS Hahm
24	OBY	1	01-09-2014	13:20		15:57	74°10.3'S	112°31.70'W	1028								KOPRI K3 buoy deploy	HK Ha
	DBY	26	01-09-2014	14:04		14:07	74°10.2'S	112°33.02'W									116208 : Depolyed Drifter (AS,K3(#24) : Dotson Ice Shelf)	CS Hong
25	CTD	1	01-09-2014	17:07		18:05	74°12.5'S	112°49.22'W	806	780		24	7.0	190.0			First deep casting	HK Ha
25	OBY	1	01-09-2014	19:00		21:46	74°10.9'S	113°03.82'W	774								KOPRI K5 buoy deploy	HK Ha
26	CTD	1	01-09-2014	22:48		23:37	74°10.5'S	113°19.73'W	683	670		24	2.7	190.0	0.0	181.5	First deep casting	HJ Lee
26	CTD	2	01-10-2014	0:24		0:40	74°10.5'S	113°19.72'W	683	100		24	4.9	206.3	0.0	182.0	Second shallow casting	HJ Lee
27	CTD	1	01-10-2014	3:26		4:21	73°49.2'S	113°04.00'W	783	770		24	9.2	92.0	0.0	123.5	First deep casting	HJ Lee
27	PHY	1	01-10-2014	5:15		5:30				70							20 micron mesh	EJ Yang
27	BON	1	01-10-2014	5:35		6:10				200							Vertical towing	DB Lee
27	CTD	2	01-10-2014	6:24		6:38	73°49.2'S	113°04.01'W	783	100		24	10.1	100.7	0.0	127.8	Second shallow casting	HJ Lee
27	CTD	3	01-10-2014	7:14		7:25	73°49.2'S	113°04.01'W	783	11		24	9.7	94.8	0.0	127.1	Third shallow casting	HJ Lee
27	BOX	1	01-10-2014	7:30		8:50				738							Box Core	EJ Yang
27	GOF	1	01-10-2014	9:20		10:00				700							Go_Flo deep casting	DS Hahm
27	OBY	1	01-10-2014	10:30		12:56	73°49.2'S	113°02.71'W	780								KOPRI K6 buoy deploy	HK Ha
	DBY	27	01-10-2014	13:08		13:10	73°49.3'S	113°03.90'W									116209 : Depolyed Drifter (AS,K6)	CS Hong
26	GOF	1	01-10-2014	16:22		16:28	74°10.5'S	113°19.74'W				11					Go_Flo shallow casting (1)	EJ Yang
26	GOF	2	01-10-2014	17:50		18:02						11					Go_Flo shallow casting (2)	EJ Yang
26	GOF	3	01-10-2014	19:15		19:28						11					Go_Flo shallow casting (3)	EJ Yang
26	GOF	4	01-10-2014	20:22		0:00						11					Go_Flo shallow casting (4)	EJ Yang
28	CTD	1	01-11-2014	3:21		4:09	74°06.3'S	115°08.56'W	647	630		24	17.1	76.0	0.1	96.2	First deep casting	HJ Lee
29	CTD	1	01-11-2014	5:27		6:41	74°07.5'S	115°21.29'W	1125	1115		24	15.6	81.6	0.2	96.8	First deep casting	HJ Lee
30	CTD	1	01-11-2014	8:13		9:19	74°04.8'S	115°43.49'W	1058	1045		24	12.8	43.9	0.6	90.1	First deep casting	HJ Lee
30	GOF	1	01-11-2014	9:40		10:30				790		11					Go_Flo deep casting	DS Hahm
	RTN	1	01-11-2014	11:05		11:31				400					2.0		oblique sample	HS La
31	CTD	1	01-11-2014	12:28		13:24	74°02.2'S	115°57.40'W	1001	990		24	10.6	82.5	0.2	108.8	First deep casting	CY Kang
32	CTD	1	01-11-2014	15:16		16:01	73°55.5'S	116°08.17'W	636	626		24	12.0	81.1	0.3	105.2	First deep casting	CY Kang
32	PHY	1	01-11-2014	16:30		16:25				70							20 micron mesh	EJ Yang
32	BON	1	01-11-2014	16:30		17:05				200							Vertical towing	DB Lee
32	CTD	2	01-11-2014	17:22		17:39	73°55.5'S	116°08.18'W	636	150		24	10.3	79.9	0.2	81.7	Second shallow casting	CY Kang
32	CTD	3	01-11-2014	18:20		18:32	73°55.5'S	116°08.18'W	636	20		24	10.6	73.1	0.2	92.1	Third shallow casting	CY Kang
33	CTD	1	01-12-2014	2:17		3:10	74°00.0'S	118°10.90'W	765	755		24	9.1	58.0	0.0	86.5	First deep casting	HJ Lee
33	PHY	1	01-12-2014	3:20		3:35				70							20 micron mesh	EJ Yang
33	BON	1	01-12-2014	3:35		4:00				200							Vertical towing	DB Lee
	RTN	1	01-12-2014	4:15		5:00					400				2.0		oblique sample	HS La
34	OBY	1	01-12-2014	10:30		13:14	73°39.6'S	118°57.60'W									US S2 buoy deploy	A Wahlin
34	CTD	1	01-12-2014	13:30		14:06	73°39.7'S	118°57.71'W	444	434		24	1.7	33.7	0.0	76.7	First deep casting	CY Kang
8	OBY	1	01-12-2014	18:45		23:45	72°55.4'S	117°34.00'W									US S3 buoy recovery	A Wahlin
8	CTD	1	01-13-2014	0:05		0:30	72°55.1'S	117°34.70'W	546	535		5	2.4	17.0	0.0	141.7	First deep casting (revisit)	CY Kang
32			01-13-2014	5:40		10:45											Sea ice survey by Heli	SH Lee
32	GLD	1	01-13-2014	13:26		13:45	73°49.0'S	114°56.82'W									Deep Glider recovery	T Mailse
19	CTD	1	01-13-2014	16:26		16:43	73°30.0'S	113°60.00'W	734	100		24	9.6	147.3	0.0	168.2	First shallow casting (revisit)	CY Kang
19	MOC	1	01-13-2014	17:05		18:00				400								HS La
	GLD	1	01-13-2014	20:20		21:45	73°21.5'S	112°56.40'W									Shallow Glider recovery	T Mailse
14	CTD	1	01-14-2014	0:47		1:01	73°16.9'S	114°57.06'W	832	100		24	7.5	136.2	0.0	289.5	First shallow casting (revisit)	CY Kang
5	CTD	1	01-14-2014	6:10		6:26	72°27.3'S	116°20.92'W	563	100		24	4.6	169.3	0.0	96.2	First shallow casting (revisit)	HJ Lee
3	CTD	1	01-14-2014	11:22		11:38	71°57.0'S	118°27.20'W	639	100		24	7.1	215.4	0.0	243.4	First shallow casting (revisit)	CY Kang
35	CTD	1	01-14-2014	16:41		18:53	71°30.0'S	121°00.05'W	2805	1797		24	1.8	176.3	0.2	294.6	First deep casting	CY Kang
35	CTD	2	01-14-2014	19:59		20:17	71°30.0'S	120°59.98'W	2805	100		24	4.6	104.9	0.0	180.3	Second shallow casting	CY Kang
35	GOF	1	01-14-2014	20:35		20:50			2805	15		11					Go_Flo shallow casting(1)	EJ Yang
35	GOF	2	01-14-2014	22:05		22:15				15		11					Go_Flo shallow casting(2)	EJ Yang
35	GOF	3	01-15-2014	0:12		0:30				15		11					Go_Flo shallow casting(3)	EJ Yang
35	GOF	4	01-15-2014	1:45		2:25				770		11					Go_Flo deep casting(1)	DS Hahm
2	CTD	1	01-15-2014	9:21		11:34	70°60.0'S	123°00.02'W	3258	3249		24	4.8	286.0	0.0	16.0	First deep casting	HJ Lee
2	GOF	1	01-15-2014	12:00		12:35				770							Go_Flo deep casting	DS Hahm
	ICE	1	01-15-2014	18:00		3:00	71°09.0'S	124°29.30'W									KOPRI sea ice work	SH Lee
	DBY	28	01-18-2014	11:12			66°59.7'S	153°34.50'W									116205 : Depolyed Drifter (AS,K6)	CS Hong
	DBY	29	01-18-2014	20:15			66°00.0'S	156°50.50'W									116207 : Depolyed Drifter (AS,K6)	CS Hong
	DBY	30	01-19-2014	6:00			65°00.0'S	160°00.00'W									116204 : Depolyed Drifter (AS,K6)	CS Hong

Scientific Cruise Daily Log

Ship: R/V Araon | **Cruise:** ANA04 | **Leg:** B | Prepared by H. J. Lee (KOPRI) hyunjung@kopri.re.kr

STN No.	Gear	Cast No.	Date	Cast start	Bottom or at depth	Cast end	Latitude	Longitude	Water depth	Cast depth	Cable payout	No. of spl. depth Core length	Wind speed	Wind direction	Ship speed	Heading	Remarks	Device Driver
			(UTC)	(UTC)	(UTC)	(UTC)			(m)	(m)	(m)		knot	(°)	knot	(°)		

Amundsen Sea

CTD: CTD;PHY: Phytoplankton; BON: Bongo net; BOX: Box core; OBY: ocean buoy;DBY: Drifter buoy;FLM: Fluoremeter;;GOF: Go Flo;GLD:Glider;RTN:Rectangular net;ICE: work on sea-ice;

Appendix II. All layout diagrams of moorings serviced by KOPRI, BAS, MBL and UGOT.

See the following pages.

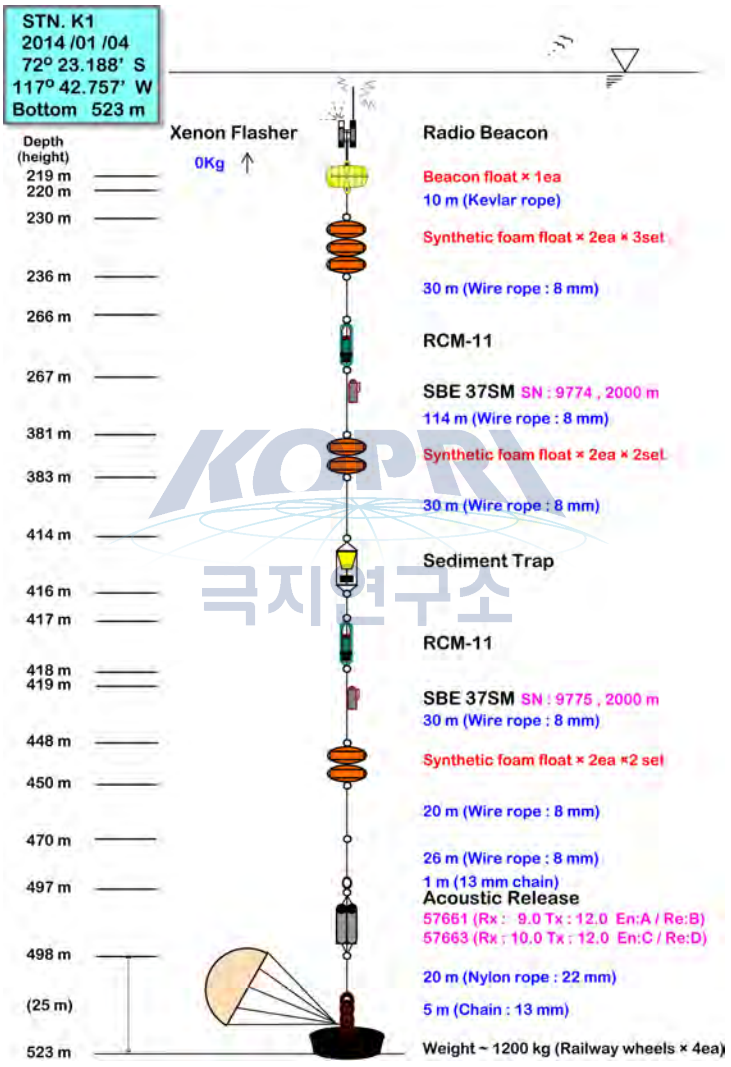
STN. K1
2014 /01 /04
72° 23.188' S
117° 42.757' W
Bottom 523 m
Depth (height)
219 m
220 m
230 m
236 m
266 m
267 m
381 m
383 m
414 m
416 m
417 m
418 m
419 m
448 m
450 m
470 m
497 m
498 m
(25 m)
523 m
Xenon Flasher
0Kg
Radio Beacon
Beacon float × 1ea
10 m (Kevlar rope)
Synthetic foam float × 2ea × 3set
30 m (Wire rope : 8 mm)
RCM-11
SBE 37SM SN : 9774 , 2000 m
114 m (Wire rope : 8 mm)
Synthetic foam float × 2ea × 2set
30 m (Wire rope : 8 mm)
Sediment Trap
RCM-11
SBE 37SM SN : 9775 , 2000 m
30 m (Wire rope : 8 mm)
Synthetic foam float × 2ea ×2 set
20 m (Wire rope : 8 mm)
26 m (Wire rope : 8 mm)
1 m (13 mm chain)
Acoustic Release
57661 (Rx : 9.0 Tx : 12.0 En:A / Re:B)
57663 (Rx : 10.0 Tx : 12.0 En:C / Re:D)
20 m (Nylon rope : 22 mm)
5 m (Chain : 13 mm)
Weight ~ 1200 kg (Railway wheels × 4ea)

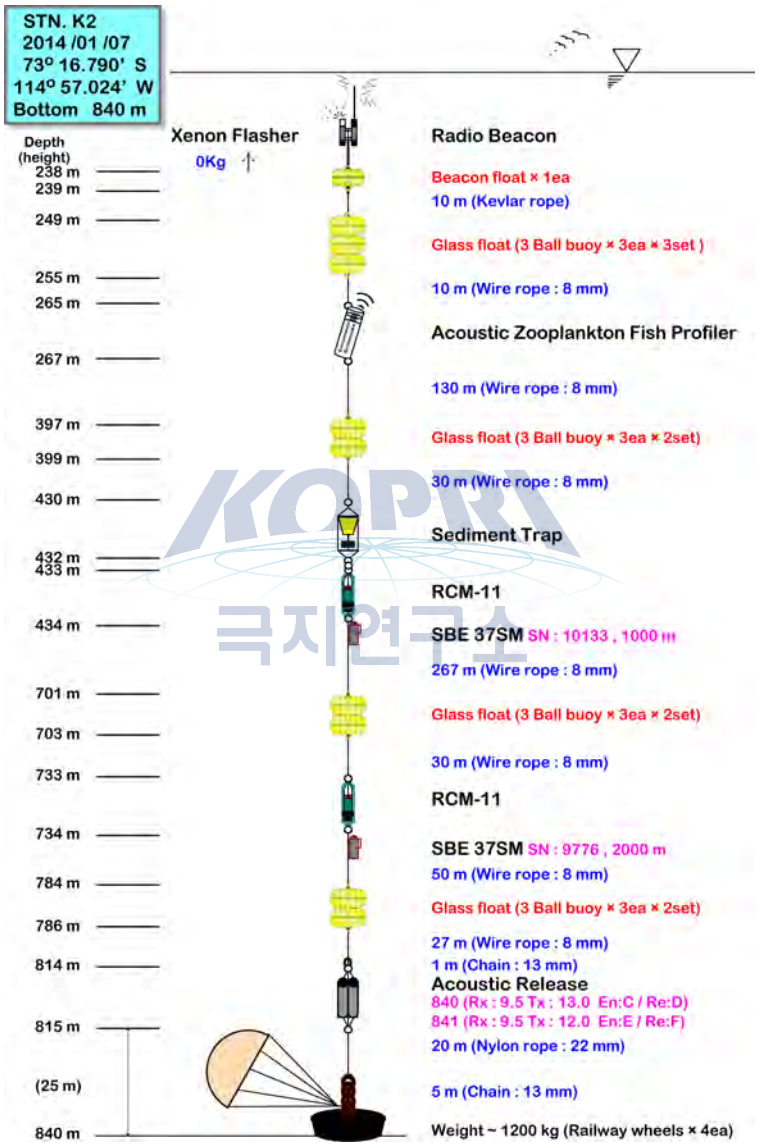
STN. K2
2014 /01 /07
73º 16.790' S
114º 57.024' W
Bottom 840 m
Depth (height)
238 m
239 m
249 m
255 m
265 m
267 m
397 m
399 m
430 m
432 m
433 m
434 m
701 m
703 m
733 m
734 m
784 m
786 m
814 m
815 m
(25 m)
840 m
Xenon Flasher
0Kg
Radio Beacon
Beacon float × 1ea
10 m (Kevlar rope)
Glass float (3 Ball buoy × 3ea × 3set)
10 m (Wire rope : 8 mm)
Acoustic Zooplankton Fish Profiler
130 m (Wire rope : 8 mm)
Glass float (3 Ball buoy × 3ea × 2set)
30 m (Wire rope : 8 mm)
Sediment Trap
RCM-11
SBE 37SM SN : 10133 , 1000 m
267 m (Wire rope : 8 mm)
Glass float (3 Ball buoy × 3ea × 2set)
30 m (Wire rope : 8 mm)
RCM-11
SBE 37SM SN : 9776 , 2000 m
50 m (Wire rope : 8 mm)
Glass float (3 Ball buoy × 3ea × 2set)
27 m (Wire rope : 8 mm)
1 m (Chain : 13 mm)
Acoustic Release
840 (Rx : 9.5 Tx : 13.0 En:C / Re:D)
841 (Rx : 9.5 Tx : 12.0 En:E / Re:F)
20 m (Nylon rope : 22 mm)
5 m (Chain : 13 mm)
Weight ~ 1200 kg (Railway wheels × 4ea)

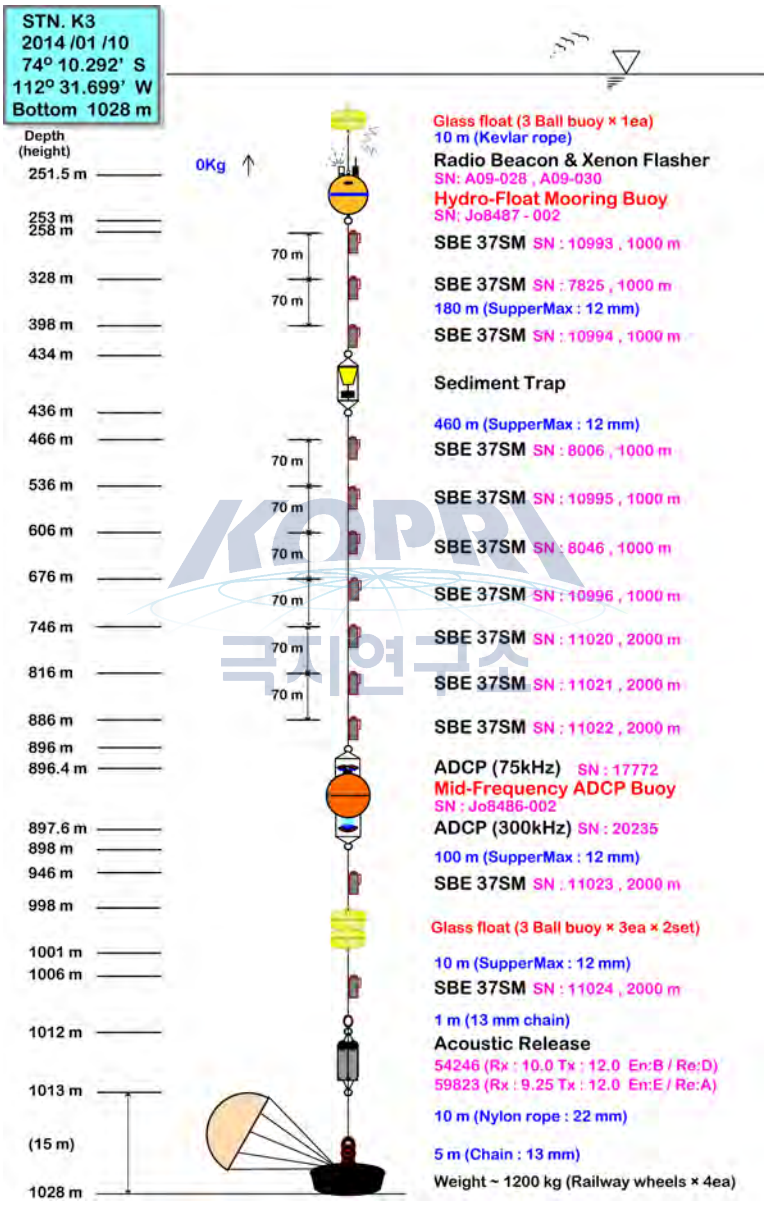
STN. K3
2014 /01 /10
74º 10.292' S
112º 31.699' W
Bottom 1028 m
Depth (height)
251.5 m
253 m
258 m
328 m
398 m
434 m
436 m
466 m
536 m
606 m
676 m
746 m
816 m
886 m
896 m
896.4 m
897.6 m
898 m
946 m
998 m
1001 m
1006 m
1012 m
1013 m
(15 m)
1028 m
0Kg
70 m
Glass float (3 Ball buoy × 1ea)
10 m (Kevlar rope)
Radio Beacon & Xenon Flasher
SN: A09-028 , A09-030
Hydro-Float Mooring Buoy
SN: Jo8487 - 002
SBE 37SM SN : 10993 , 1000 m
SBE 37SM SN : 7825 , 1000 m
180 m (SupperMax : 12 mm)
SBE 37SM SN : 10994 , 1000 m
Sediment Trap
460 m (SupperMax : 12 mm)
SBE 37SM SN : 8006 , 1000 m
SBE 37SM SN : 10995 , 1000 m
SBE 37SM SN : 8046 , 1000 m
SBE 37SM SN : 10996 , 1000 m
SBE 37SM SN : 11020 , 2000 m
SBE 37SM SN : 11021 , 2000 m
SBE 37SM SN : 11022 , 2000 m
ADCP (75kHz) SN : 17772
Mid-Frequency ADCP Buoy
SN : Jo8486-002
ADCP (300kHz) SN : 20235
100 m (SupperMax : 12 mm)
SBE 37SM SN : 11023 , 2000 m
Glass float (3 Ball buoy × 3ea × 2set)
10 m (SupperMax : 12 mm)
SBE 37SM SN : 11024 , 2000 m
1 m (13 mm chain)
Acoustic Release
54246 (Rx : 10.0 Tx : 12.0 En:B / Re:D)
59823 (Rx : 9.25 Tx : 12.0 En:E / Re:A)
10 m (Nylon rope : 22 mm)
5 m (Chain : 13 mm)
Weight ~ 1200 kg (Railway wheels × 4ea)

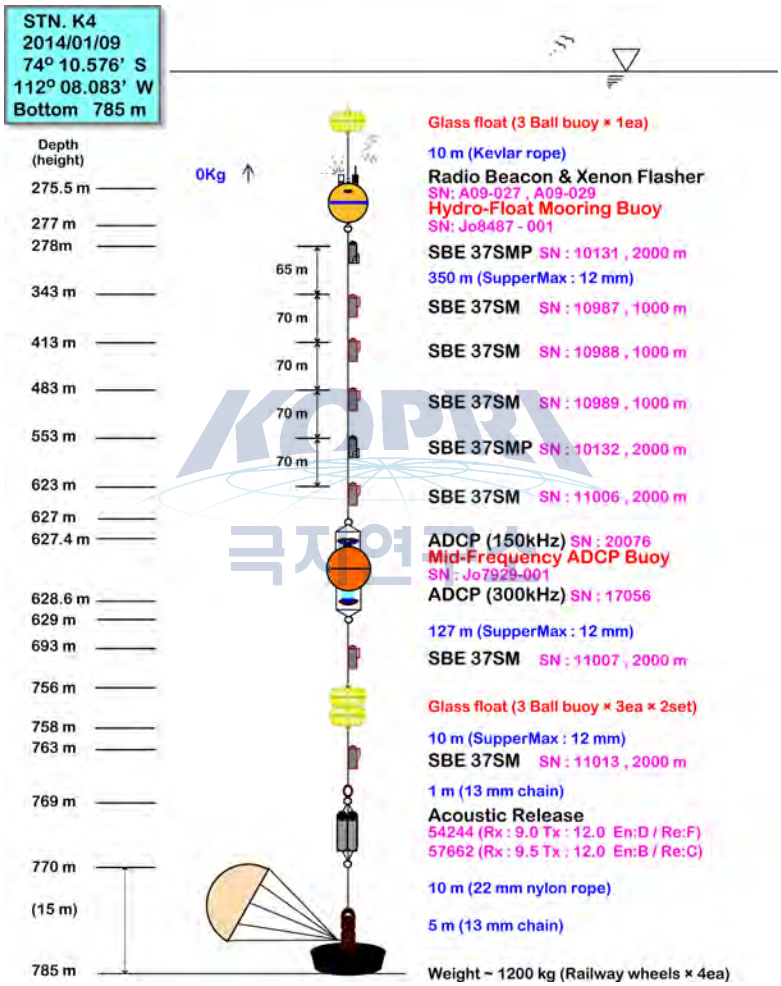
STN. K4
2014/01/09
74° 10.576' S
112° 08.083' W
Bottom 785 m
Depth (height)
275.5 m
277 m
278m
343 m
413 m
483 m
553 m
623 m
627 m
627.4 m
628.6 m
629 m
693 m
756 m
758 m
763 m
769 m
770 m
(15 m)
785 m
0Kg
65 m
70 m
70 m
70 m
70 m
Glass float (3 Ball buoy × 1ea)
10 m (Kevlar rope)
Radio Beacon & Xenon Flasher
SN: A09-027 , A09-029
Hydro-Float Mooring Buoy
SN: Jo8487 - 001
SBE 37SMP SN : 10131 , 2000 m
350 m (SupperMax : 12 mm)
SBE 37SM SN : 10987 , 1000 m
SBE 37SM SN : 10988 , 1000 m
SBE 37SM SN : 10989 , 1000 m
SBE 37SMP SN : 10132 , 2000 m
SBE 37SM SN : 11006 , 2000 m
ADCP (150kHz) SN : 20076
Mid-Frequency ADCP Buoy
SN : Jo7929-001
ADCP (300kHz) SN : 17056
127 m (SupperMax : 12 mm)
SBE 37SM SN : 11007 , 2000 m
Glass float (3 Ball buoy × 3ea × 2set)
10 m (SupperMax : 12 mm)
SBE 37SM SN : 11013 , 2000 m
1 m (13 mm chain)
Acoustic Release
54244 (Rx : 9.0 Tx : 12.0 En:D / Re:F)
57662 (Rx : 9.5 Tx : 12.0 En:B / Re:C)
10 m (22 mm nylon rope)
5 m (13 mm chain)
Weight ~ 1200 kg (Railway wheels × 4ea)

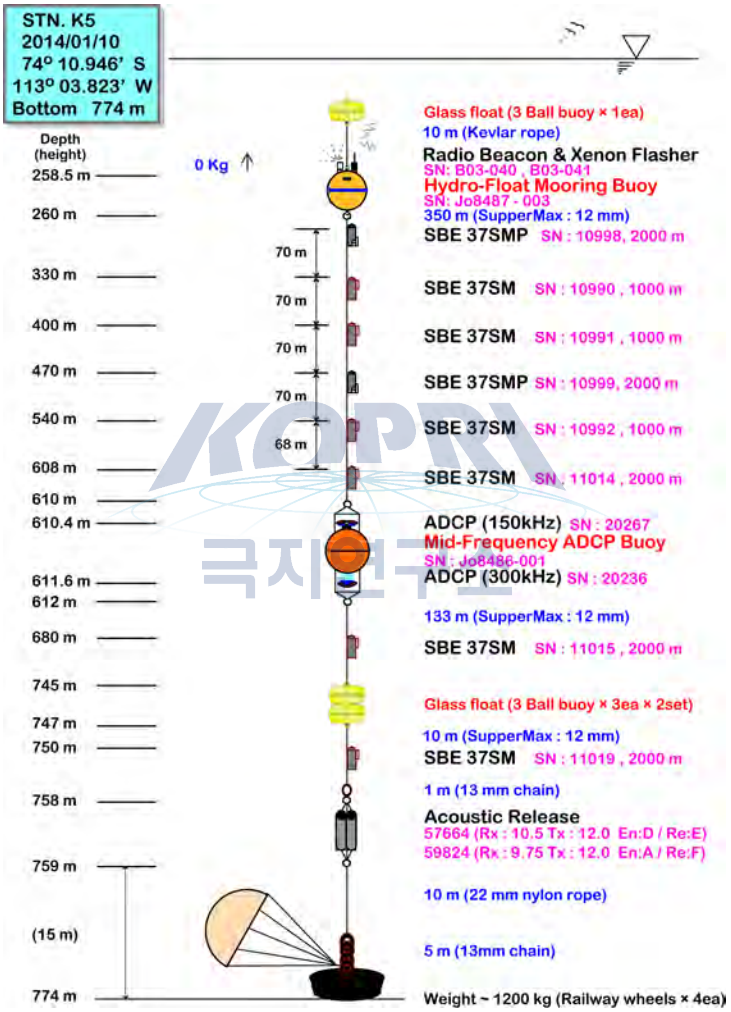
STN. K5
2014/01/10
74º 10.946' S
113º 03.823' W
Bottom 774 m
Depth
(height)
258.5 m
260 m
330 m
400 m
470 m
540 m
608 m
610 m
610.4 m
611.6 m
612 m
680 m
745 m
747 m
750 m
758 m
759 m
(15 m)
774 m
0 Kg
70 m
70 m
70 m
70 m
68 m
Glass float (3 Ball buoy × 1ea)
10 m (Kevlar rope)
Radio Beacon & Xenon Flasher
SN: B03-040 , B03-041
Hydro-Float Mooring Buoy
SN: Jo8487 - 003
350 m (SupperMax : 12 mm)
SBE 37SMP SN : 10998, 2000 m
SBE 37SM SN : 10990 , 1000 m
SBE 37SM SN : 10991 , 1000 m
SBE 37SMP SN : 10999, 2000 m
SBE 37SM SN : 10992 , 1000 m
SBE 37SM SN : 11014 , 2000 m
ADCP (150kHz) SN : 20267
Mid-Frequency ADCP Buoy
SN : Jo8486-001
ADCP (300kHz) SN : 20236
133 m (SupperMax : 12 mm)
SBE 37SM SN : 11015 , 2000 m
Glass float (3 Ball buoy × 3ea × 2set)
10 m (SupperMax : 12 mm)
SBE 37SM SN : 11019 , 2000 m
1 m (13 mm chain)
Acoustic Release
57664 (Rx : 10.5 Tx : 12.0 En:D / Re:E)
59824 (Rx : 9.75 Tx : 12.0 En:A / Re:F)
10 m (22 mm nylon rope)
5 m (13mm chain)
Weight ~ 1200 kg (Railway wheels × 4ea)

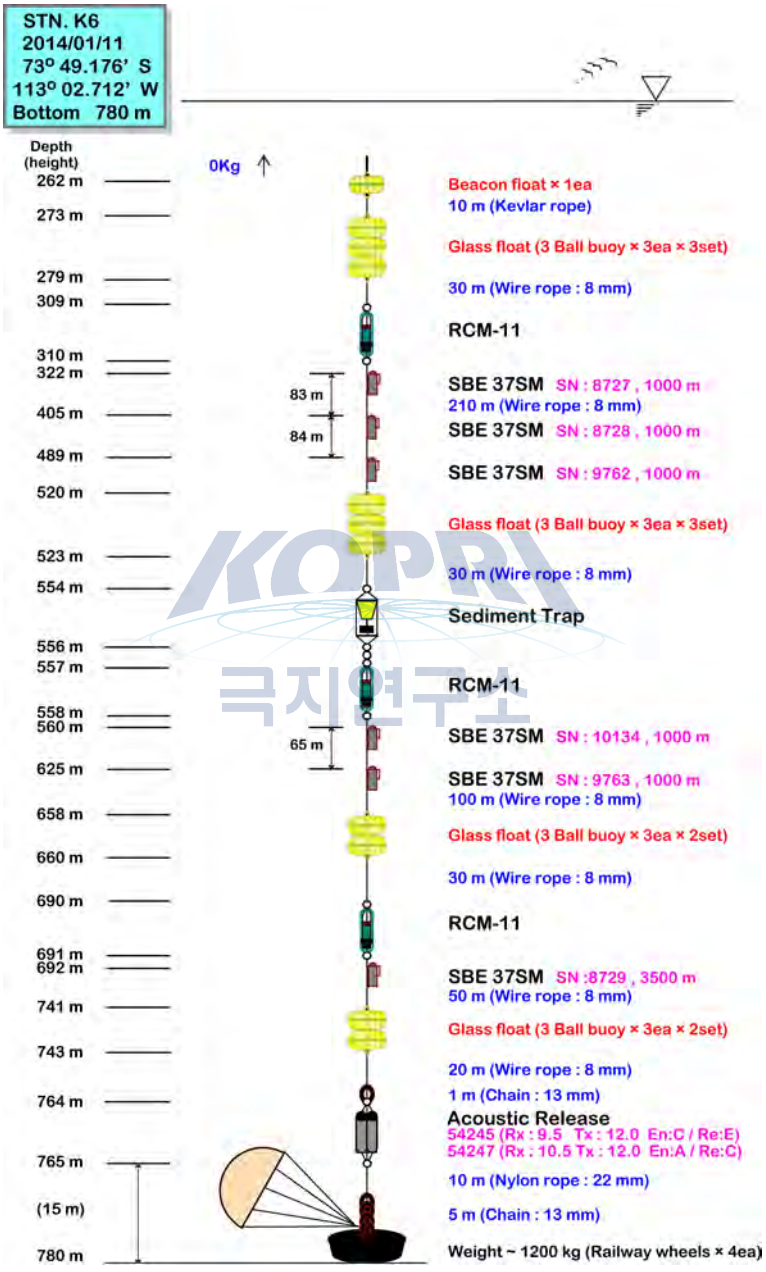
STN. K6
2014/01/11
73º 49.176' S
113º 02.712' W
Bottom 780 m
Depth (height)
0Kg
262 m
273 m
279 m
309 m
310 m
322 m
405 m
489 m
520 m
523 m
554 m
556 m
557 m
558 m
560 m
625 m
658 m
660 m
690 m
691 m
692 m
741 m
743 m
764 m
765 m
(15 m)
780 m
83 m
84 m
65 m
Beacon float × 1ea
10 m (Kevlar rope)
Glass float (3 Ball buoy × 3ea × 3set)
30 m (Wire rope : 8 mm)
RCM-11
SBE 37SM SN : 8727 , 1000 m
210 m (Wire rope : 8 mm)
SBE 37SM SN : 8728 , 1000 m
SBE 37SM SN : 9762 , 1000 m
Glass float (3 Ball buoy × 3ea × 3set)
30 m (Wire rope : 8 mm)
Sediment Trap
RCM-11
SBE 37SM SN : 10134 , 1000 m
SBE 37SM SN : 9763 , 1000 m
100 m (Wire rope : 8 mm)
Glass float (3 Ball buoy × 3ea × 2set)
30 m (Wire rope : 8 mm)
RCM-11
SBE 37SM SN :8729 , 3500 m
50 m (Wire rope : 8 mm)
Glass float (3 Ball buoy × 3ea × 2set)
20 m (Wire rope : 8 mm)
1 m (Chain : 13 mm)
Acoustic Release
54245 (Rx : 9.5 Tx : 12.0 En:C / Re:E)
54247 (Rx : 10.5 Tx : 12.0 En:A / Re:C)
10 m (Nylon rope : 22 mm)
5 m (Chain : 13 mm)
Weight ~ 1200 kg (Railway wheels × 4ea)

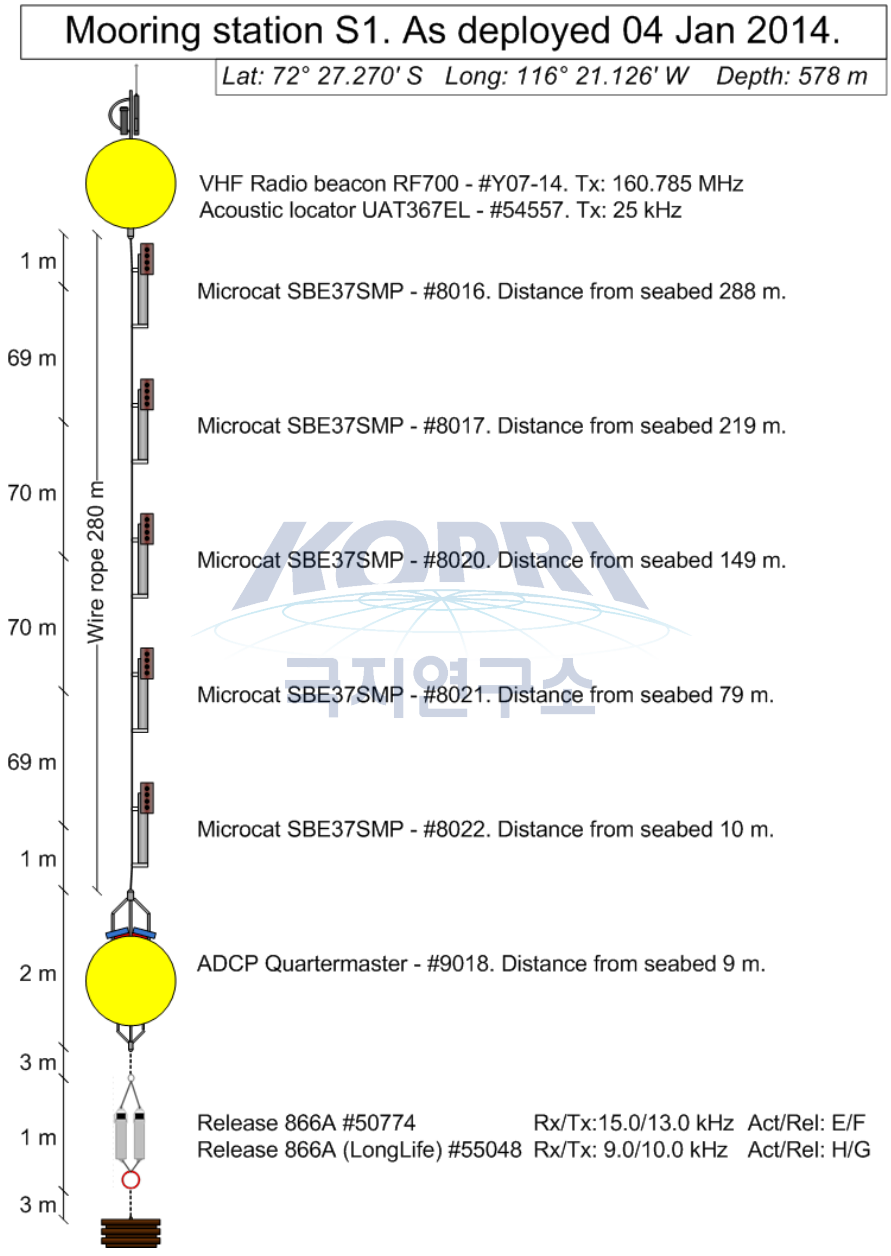
Mooring station S1. As deployed 04 Jan 2014.
Lat: 72° 27.270' S Long: 116° 21.126' W Depth: 578 m
VHF Radio beacon RF700 - #Y07-14. Tx: 160.785 MHz
Acoustic locator UAT367EL - #54557. Tx: 25 kHz
1 m
Microcat SBE37SMP - #8016. Distance from seabed 288 m.
69 m
Microcat SBE37SMP - #8017. Distance from seabed 219 m.
70 m
Wire rope 280 m
Microcat SBE37SMP - #8020. Distance from seabed 149 m.
70 m
Microcat SBE37SMP - #8021. Distance from seabed 79 m.
69 m
Microcat SBE37SMP - #8022. Distance from seabed 10 m.
1 m
2 m
ADCP Quartermaster - #9018. Distance from seabed 9 m.
3 m
1 m
Release 866A #50774 Rx/Tx:15.0/13.0 kHz Act/Rel: E/F
Release 866A (LongLife) #55048 Rx/Tx: 9.0/10.0 kHz Act/Rel: H/G
3 m

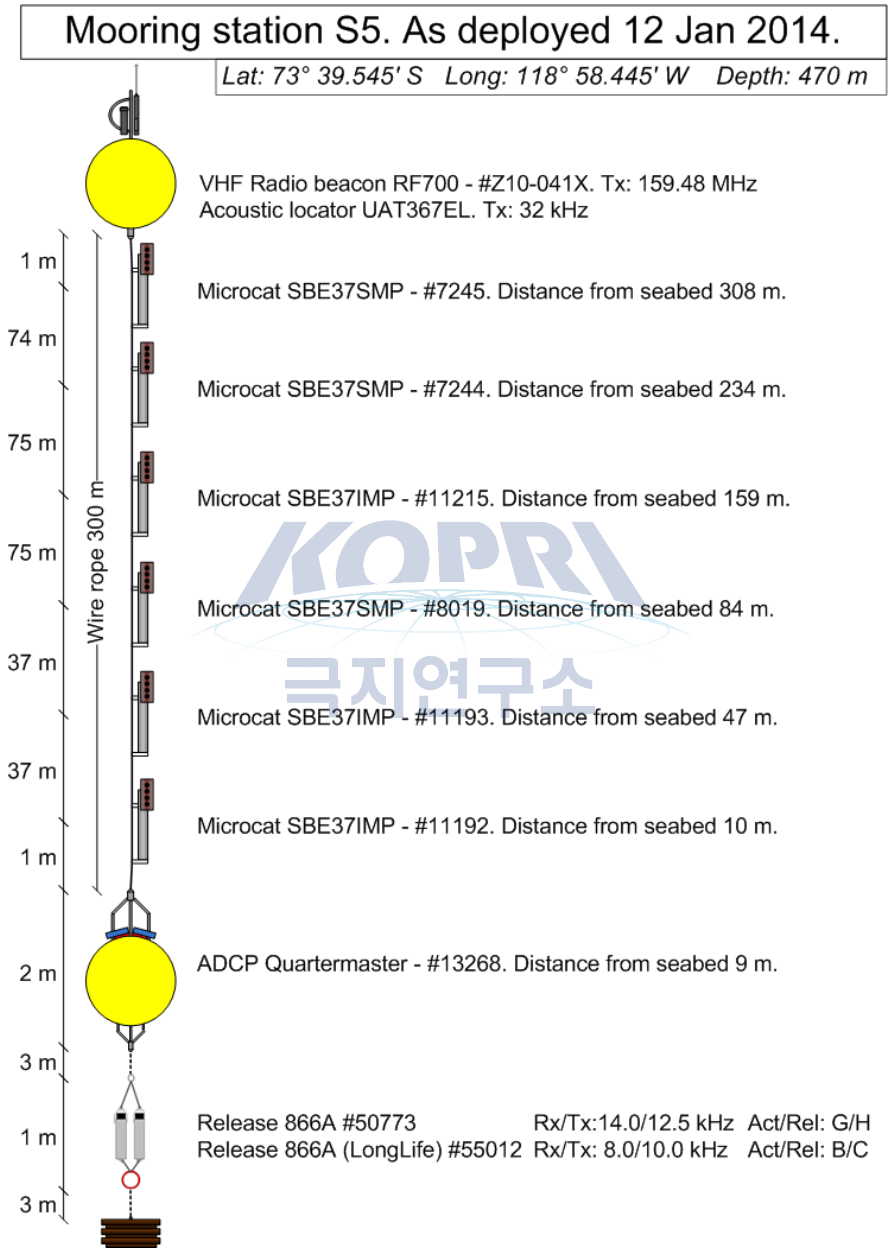
Mooring station S5. As deployed 12 Jan 2014.
Lat: 73° 39.545' S Long: 118° 58.445' W Depth: 470 m
VHF Radio beacon RF700 - #Z10-041X. Tx: 159.48 MHz
Acoustic locator UAT367EL. Tx: 32 kHz
1 m
Microcat SBE37SMP - #7245. Distance from seabed 308 m.
74 m
Microcat SBE37SMP - #7244. Distance from seabed 234 m.
75 m
Microcat SBE37IMP - #11215. Distance from seabed 159 m.
75 m
Microcat SBE37SMP - #8019. Distance from seabed 84 m.
37 m
Microcat SBE37IMP - #11193. Distance from seabed 47 m.
37 m
Microcat SBE37IMP - #11192. Distance from seabed 10 m.
1 m
Wire rope 300 m
2 m
ADCP Quartermaster - #13268. Distance from seabed 9 m.
3 m
1 m
Release 866A #50773 Rx/Tx:14.0/12.5 kHz Act/Rel: G/H
Release 866A (LongLife) #55012 Rx/Tx: 8.0/10.0 kHz Act/Rel: B/C
3 m

Appendix III. Triangulation results of K1, K2, K3, K4, K5, K6, S1 and S5.

See the following pages.

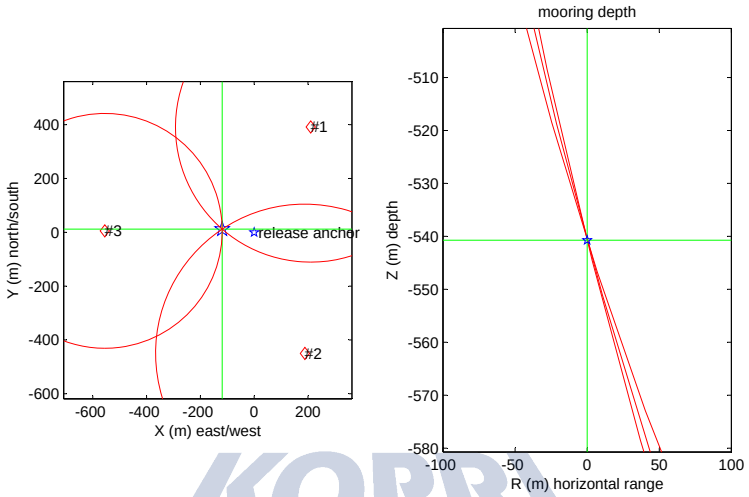

anchor release position: 72°S 23.195' 117°W 42.540'; depth: 523 m
3D mooring position: 72°S 23.189' 117°W 42.753'
drift: 119 m; direction: 276°
mooring depth: 541 m; slant error: 0 m
2D mooring position: 72°S 23.188' 117°W 42.757'
drift: 122 m; direction: 276°
horizontal error: 12 m
sound speed at site: 1500 m/s

#1 pos: 72°S 22.984' 117°W 42.165' range: 713 m range soundspeed 1500
#2 pos: 72°S 23.439' 117°W 42.204' range: 751 m range soundspeed 1500
#3 pos: 72°S 23.193' 117°W 43.531' range: 668 m range soundspeed 1500

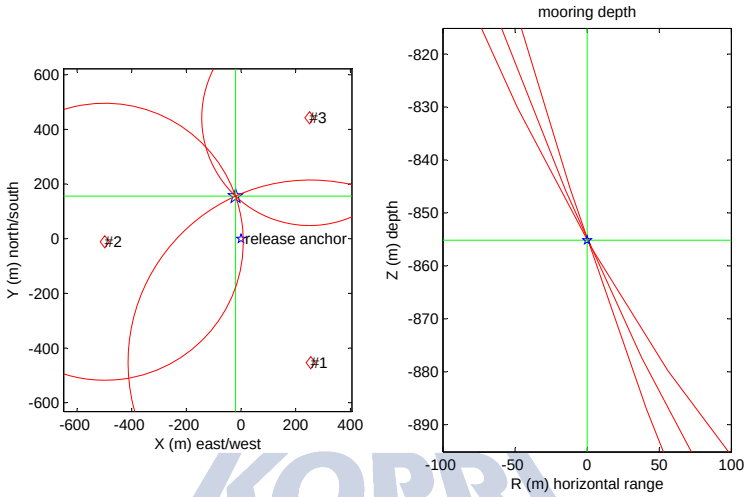

anchor release position: 73°S 16.880' 114°W 56.981'; depth: 840 m
3D mooring position: 73°S 16.796' 114°W 57.018'
drift: 157 m; direction: 353°
mooring depth: 855 m; slant error: 0 m
2D mooring position: 73°S 16.790' 114°W 57.024'
drift: 168 m; direction: 352°
horizontal error: 11 m
sound speed at site: 1500 m/s

#1 pos: 73°S 17.125' 114°W 56.502' range: 1058 m range soundspeed 1500
#2 pos: 73°S 16.886' 114°W 57.916' range: 964 m range soundspeed 1500
#3 pos: 73°S 16.641' 114°W 56.510' range: 910 m range soundspeed 1500

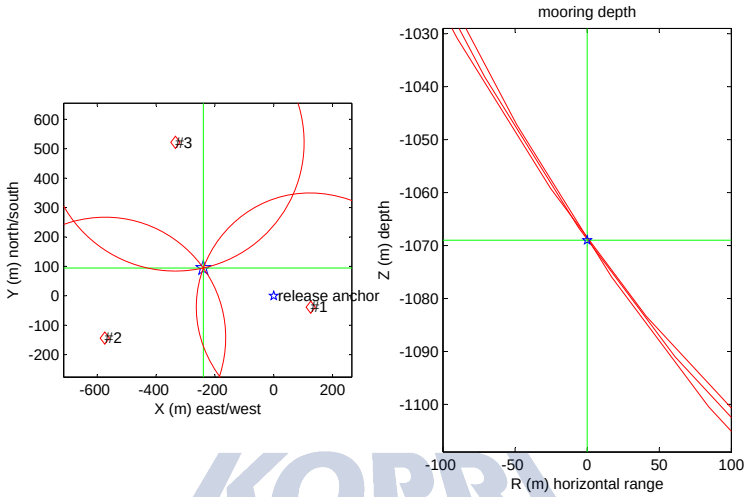

anchor release position: 74°S 10.337' 112°W 31.256'; depth: 1028 m
3D mooring position: 74°S 10.286' 112°W 31.730'
drift: 257 m; direction: 292°
mooring depth: 1069 m; slant error: 0 m
2D mooring position: 74°S 10.292' 112°W 31.699'
drift: 239 m; direction: 290°
horizontal error: 37 m
sound speed at site: 1500 m/s

#1 pos: 74°S 10.358' 112°W 31.007' range: 1114 m range soundspeed 1500
#2 pos: 74°S 10.414' 112°W 32.393' range: 1122 m range soundspeed 1500
#3 pos: 74°S 10.055' 112°W 31.918' range: 1132 m range soundspeed 1500

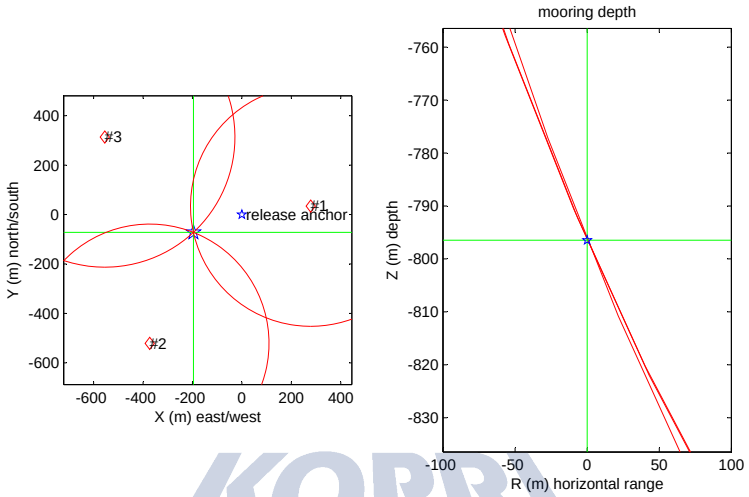

anchor release position: 74°S 10.536' 112°W 7.697', depth: 785 m
3D mooring position: 74°S 10.575' 112°W 8.085'
drift: 209 m; direction: 250°
mooring depth: 796 m; slant error: 0 m
2D mooring position: 74°S 10.576' 112°W 8.083'
drift: 208 m; direction: 250°
horizontal error: 10 m
sound speed at site: 1500 m/s

#1 pos: 74°S 10.518' 112°W 7.145' range: 912 m range soundspeed 1500
#2 pos: 74°S 10.818' 112°W 8.435' range: 910 m range soundspeed 1500
#3 pos: 74°S 10.367' 112°W 8.795' range: 934 m range soundspeed 1500

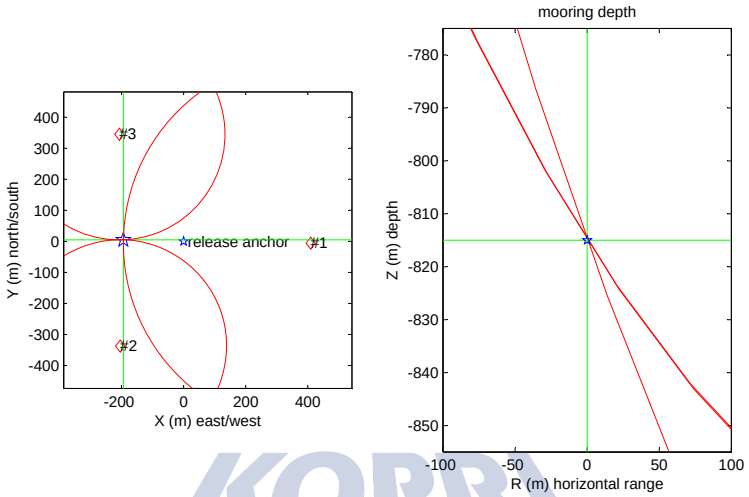

anchor release position: 74°S 10.948' 113°W 3.320'; depth: 774 m
3D mooring position: 74°S 10.945' 113°W 3.704'
drift: 194 m; direction: 271°
mooring depth: 815 m; slant error: 0 m
2D mooring position: 74°S 10.946' 113°W 3.823'
drift: 254 m; direction: 271°
horizontal error: 26 m
sound speed at site: 1500 m/s

#1 pos: 74°S 10.951' 113°W 2.509' range: 994 m range soundspeed 1500
#2 pos: 74°S 11.130' 113°W 3.724' range: 861 m range soundspeed 1500
#3 pos: 74°S 10.762' 113°W 3.729' range: 860 m range soundspeed 1500

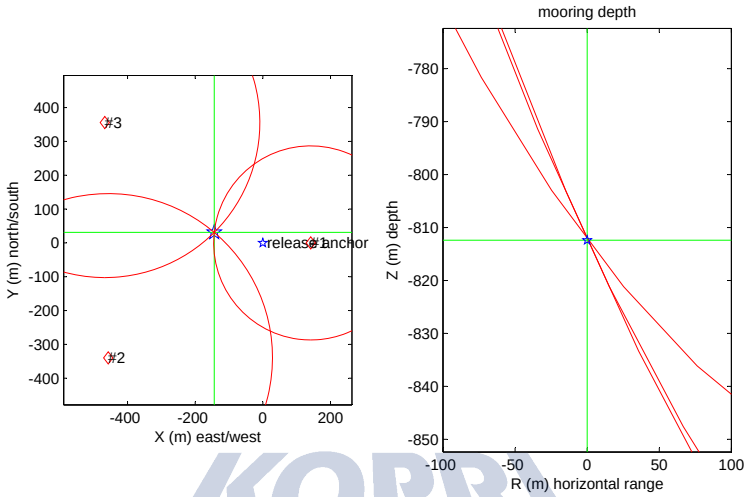

anchor release position: 73°S 49.199' 113°W 2.491'; depth: 780 m
3D mooring position: 73°S 49.182' 113°W 2.769'
drift: 147 m; direction: 282°
mooring depth: 812 m; slant error: 0 m
2D mooring position: 73°S 49.176' 113°W 2.712'
drift: 122 m; direction: 290°
horizontal error: 24 m
sound speed at site: 1500 m/s

#1 pos: 73°S 49.199' 113°W 2.216' range: 838 m range soundspeed 1500
#2 pos: 73°S 49.383' 113°W 3.376' range: 925 m range soundspeed 1500
#3 pos: 73°S 49.007' 113°W 3.396' range: 911 m range soundspeed 1500

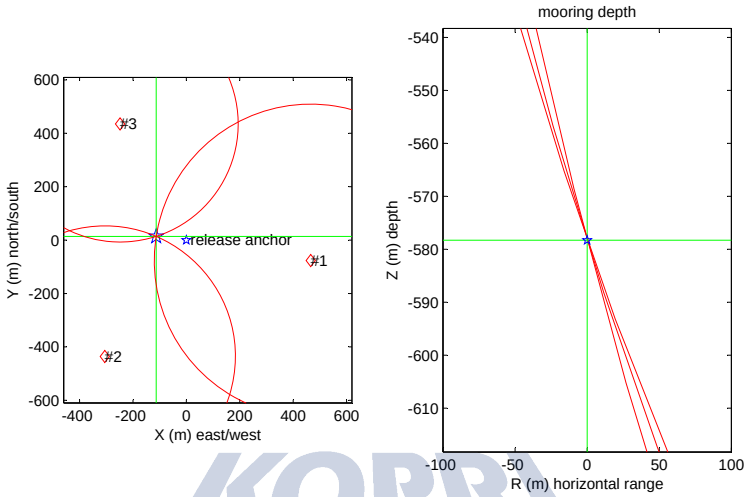

anchor release position: 72°S 27.278' 116°W 20.914'; depth: 557 m
3D mooring position: 72°S 27.271' 116°W 21.117'
drift: 114 m; direction: 277°
mooring depth: 578 m; slant error: 0 m
2D mooring position: 72°S 27.270' 116°W 21.126'
drift: 119 m; direction: 278°
horizontal error: 15 m
sound speed at site: 1500 m/s

#1 pos: 72°S 27.320' 116°W 20.080' range: 810 m range soundspeed 1500
#2 pos: 72°S 27.513' 116°W 21.461' range: 743 m range soundspeed 1500
#3 pos: 72°S 27.043' 116°W 21.359' range: 713 m range soundspeed 1500

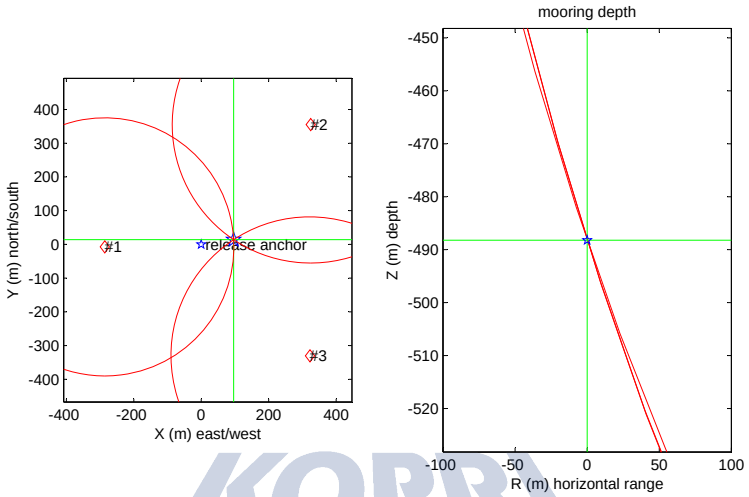

anchor release position: 73°S 39.545' 118°W 58.441'; depth: 471 m
3D mooring position: 73°S 39.537' 118°W 58.256'
drift: 97 m; direction: 82°
mooring depth: 488 m; slant error: 0 m
2D mooring position: 73°S 39.537' 118°W 58.259'
drift: 96 m; direction: 81°
horizontal error: 13 m
sound speed at site: 1500 m/s

#1 pos: 73°S 39.549' 118°W 58.990' range: 607 m range soundspeed 1500
#2 pos: 73°S 39.353' 118°W 57.818' range: 625 m range soundspeed 1500
#3 pos: 73°S 39.723' 118°W 57.822' range: 626 m range soundspeed 1500

Chapter 2

Chemical Oceanography

2.1 Nutrient measurements

Jinyoung Jung
Korea Polar Research Institute, Incheon 406-840, South Korea

요약문

해양생물의 생장에 있어서 없어서는 안 될 필수 영양원소인 탄소, 질소, 인은 서로 밀접한 연관이 있기 때문에 생물학적 탄소 펌프(생물학적 활동에 의한 대기 중 이산화탄소의 해양으로의 흡수)에 대한 이해를 증진시키기 위해서는 탄소뿐만 아니라 질소, 인 성분의 동시관측이 필수적이다. 아문젠해 탐사기간 동안 40개의 정점에서 영양염(아질산염+질산염, 인산염, 암모늄, 규산염)시료를 채취하여 선상에서 분석하였다. 외양에서의 영양염 농도는 높았고, 폴리냐에서의 농도는 급격히 감소하는 경향을 보여 활발한 해양생물활동의 영향으로 영양염의 소비가 증가하는 것을 알 수 있었으며, 암모늄의 농도 관측을 통해 아문젠해 폴리냐 내에서 유기물질의 분해가 활발히 일어나고 있음이 시사되었다.

Introduction

The oceanic cycles of life's essential elements—carbon (C), nitrogen (N) and phosphorus (P)—are closely coupled through the metabolic requirements of phytoplankton, whose average proportions of these elements, C/N/P = 106:16:1, are known as the Redfield ratios. The similarity between the average N/P ratio of plankton biomass and spatial variations of dissolved nitrate (NO_3^-) and phosphate (PO_4^{3-}) has long been taken to imply that a relatively constant number of N atoms per atom of P are assimilated by phytoplankton throughout the surface ocean and released by the respiration of organic matter at depth. The Redfield N/P ratio is therefore viewed as a critical threshold between the N-limitation and P-limitation of marine photosynthesis and the carbon it sequesters (Weber and Deutsch, 2010). The operation of the biological carbon pump in the sea is inextricably linked to the biogeochemical cycling of other nutrient elements. Limitation by macronutrients, such as N or micronutrients, such as iron (Fe), diminishes phytoplankton growth and ultimately the export of organic carbon to the deep sea. Carbon export is also governed by the relative use of new and recycled nutrients by the phytoplankton, which sets an upper limit on the

fraction of primary production that can be exported to depth (Brzezinski et al., 2003). To improve our understanding of roles of nutrients in biological processes such as variations of N/P ratio in water column and N and P uptake ratio by different phytoplankton species, we investigated spatial and temporal variations of nutrients (PO_4^{3-}, $NO_3^- + NO_2^-$, NH_4^+, and SiO_2) in seawater collected over the Amundsen Sea. The results for nutrients would be valuable for filling the data gap, and useful to understand biogeochemical cycles of C, N, and P as well as carbon sequestration by biological carbon pump in the Amundsen Sea.

Work at sea and preliminary results

Seawater sampling for nutrients was carried out at 40 stations (35 stations + 5 revisit stations) over the Amundsen Sea using a CTD/rosette sampler holding 24-10L Niskin bottles (OceanTest Equipment Inc., FL, USA) during Korea research ice breaker R/V Araon cruise (ANA04B, December 31, 2013 – January 15, 2014) (Fig. 2.1). Samples for nutrients were collected from the Niskin rosette into 50 ml conical tubes and immediately stored in a refrigerator at 2°C prior to chemical analyses. All nutrients samples were analyzed within 3 days. Concentrations of nutrients were measured using standard colorimetric methods adapted for use on a 4-channel continuous Auto-Analyzer (QuAAtro, Seal Analytical). The channel configurations and reagents were prepared according to the 'QuAAtro Applications'. Standard curves were run with each batch of samples using freshly prepared standards that spanned the range of concentrations in the samples. The r2 values of all the standard curves were greater than or equal to 0.99. In addition, reference materials for nutrients in seawater (RMNS) provided by 'KANSO Technos' (Lot. No. 'BF') were used along with standards at every batch of run in order to ensure accurate and inter-comparable measurements. Surface $NO_2^- + NO_3^-$ and PO_4^{3-} concentrations in the open ocean station (i.e., station 1 and 2) were higher than those observed in the polynya owing to low biological activity in these two stations. The surface $NO_2^- + NO_3^-$ and PO_4^{3-} concentrations gradually decreased with increasing fluorescence, indicating that $NO_2^- + NO_3^-$ and PO_4^{3-} were utilized by phytoplankton.

References

Brzezinski, M.A., Dickson, M.-L., Nelsonc, D.M., Sambrotto, R., (2003) Ratios of Si, C and N uptake by microplankton in the Southern Ocean. Deep-Sea Research II, 50, 619–633.

Weber, T.S., Deutsch, C., (2010) Ocean nutrient ratios governed by plankton biogeography. Nature, 467, 550-554.

2.2 Determination of dissolved oxygen by spectrophotometric Winkler method

Doshik Hahm
Korea Polar Research Institute, Korea

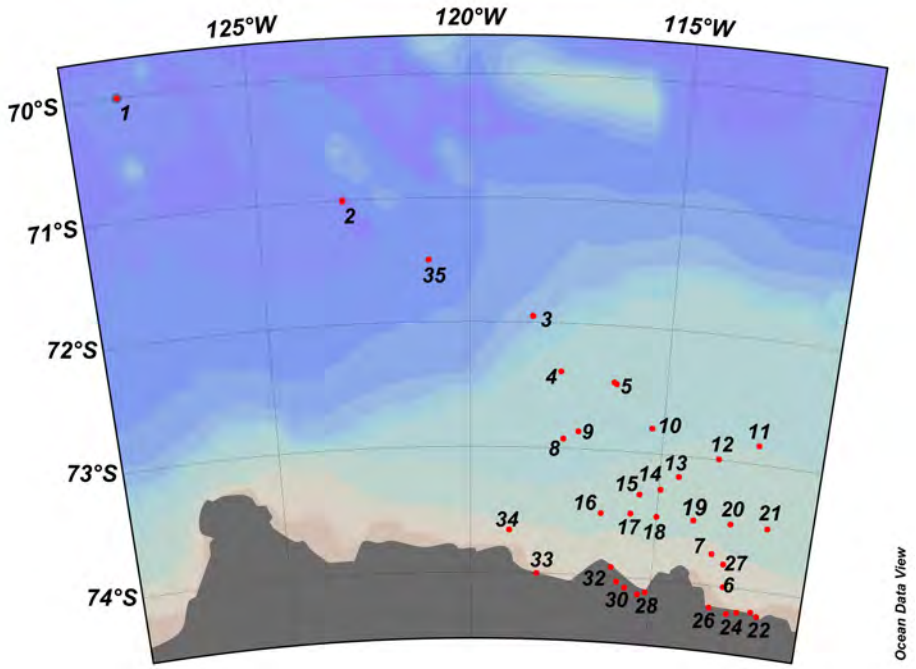

Figure 2.1: Map of study area. Red dots show the CTD stations during the expedition. The numbers indicate the station numbers.

Objectives

Due to its central role in biological redox reactions and the availability of reliable sensors, oxygen is one of the most common parameters in a sea-going observation. In the cruise, along with the oxygen sensor (SBE-43) attached to the CTD-rosette system, we determined oxygen concentration by spectrophotometric method (Labasque et al., 2004). The bottle oxygen measurements will be used to calibrate SBE-43 oxygen sensor, Aanderaa oxygen optode (No. 3835, part of O_2/Ar measurement system) and be paired with other chemical measurements such as nutrients, CH_4, N_2O and noble gases.

Work at sea

Our spectrophotometric measurement is a replication of Labasque et al. (2004) with the reagents prepared according to the WHP Reference Manual (Dickson, 1995). We measured samples in duplicate collected at the 14 CTD stations out of 35 (Fig. 2.4). The repeat measurement of the samples taken at the same water depth suggest that the overall precision of the measurement within the same batch (typically 2 to 3 hours) is less than 0.3%.

The difference between CTD sensor (SBE43) and flask measurements are shown Fig. 2.2. A newly calibrated oxygen sensor brought by Anna Wahlin along with temperature and salinity sensors was used in the beginning. However, it was soon noticed that the sensor exhibited significantly noisier signal than the old sensor. The old oxygen sensor was attached to the CTD again after the first two casts (red dots).

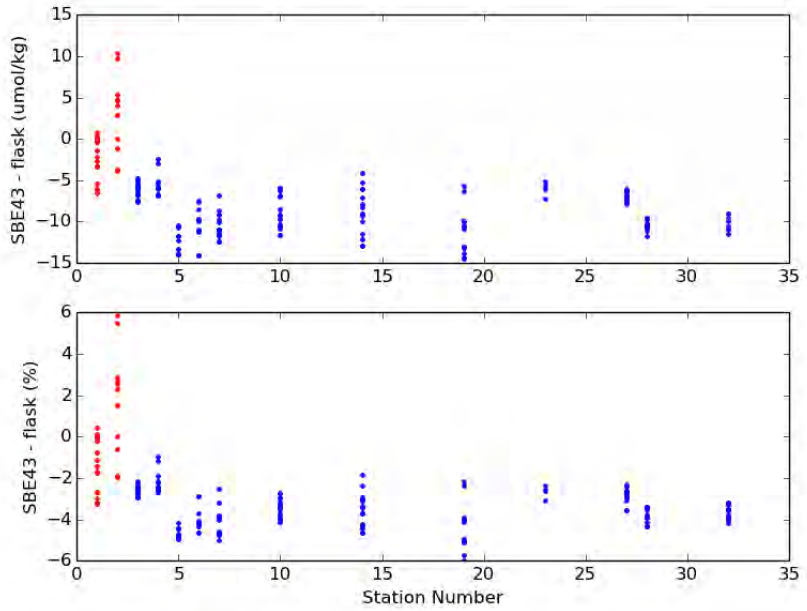

Figure 2.2: Comparison between CTD DO sensor (SBE43) and flask measurement. The most recently calibrated SBE43 sensor (red dots) was used for the first two stations only since it exhibited significantly noisier signal. The old sensor (blue dots) appeared to underestimate oxygen concentrations by 4.2 μmol/kg for waters deeper than 600 m.

The difference between the old SBE43 oxygen sensor and flask measurements at relatively stable depths (>600 m, mean of flask measurements: 195±9 μmol/kg) were 4.2 μmol/kg.

References

Dickson, A. G. (1995) Determination of dissolved oxygen in seawater by Winkler titration. WOCE Operations Manual. WHP Office Report WHPO 91-1, 1995.

Hydes, D. J., M. Aoyama, A. Aminot, K. Bakker, S. Becker, S. Coverly, A. Daniel, A. G. Dickson, O. Grosso, R. Kerouel, J. van Ooijen, K. Sato, T. Tanhua, E. M. S. Woodward, J. Z. Zhang (2010) Determination of dissolved nutrients (N, P, Si) in seawater with high precision and inter-comparability using gas-segmented continuous flow analysers. GO-SHIP Repeat Hydrography Manual. IOCCP Report No. 14, ICPO Publication Series No. 134.

Labasque, T., Chaumery, C., Aminot, A. and Kergoat, G. (2004). Spectrophotometric Winkler determination of dissolved oxygen: re-examination of critical factors and reliability. Marine Chemistry, 88, 53– 60.

Langdon, C. (2010) Determination of dissolved oxygen in seawater by Winkler titration using the amperometric technique. GO-SHIP Repeat Hydrography

Manual. IOCCP Report No. 14, ICPO Publication Series No. 134.

2.3 Inorganic carbon system observation

Rhee, Tae Siek; Jeon, Hyun-Duck
Korea Polar Research Institute, Korea,

요약문

아문젠해 수층 내부의 무기탄소 시스템 관측을 위해 쇄빙 연구선 아라온호를 이용하여 2013년 12월 24일부터 2014년 1월 25일까지 수리학적 관측이 수행되었다. 무기탄소계 인자인 총용존무기탄소 (Dissolved Inorganic Carbon; DIC), 총알칼리도 (Total Alkalinity; TA), pH에 대해서 40개 정점의 수층에서 채수한 400여개 시료가 선상에서 즉시 분석되었다. DIC는 인산을 이용하여 모두 이산화탄소로 산화시킨 후 이들 이산화탄소를 적정하는 쿨로메트릭 방법을 이용하였으며 TA는 알고 있는 농도의 염산을 해수에 적정하여 적정점을 찾아 농도를 계산하였다. pH는 전위법을 이용하여 분석하였다. 이와 함께 표층 해수 중 이산화탄소의 시공간적 변동에 대한 이해를 위해 해수 중 이산화탄소의 정량분석이 실시되었다. 아문젠해에서 이제까지 이들 네 개의 무기탄소 인자를 동일한 시기에 연속적으로 분석하여 보고 된 바는 없으며, 이들 자료를 이용하여 아문젠해 폴리냐와 해빙역, 외양을 중심으로한 무기탄소 시스템의 차이를 알아보고자 한다.

Objective

The Amundsen Sea is renowned as one of the biologically productive region in the entire Southern Ocean (Arrigo and van Dijken, 2003). Although many researcher have already focused on other Antarctic polynyas to understand the factors driving influx of carbon and cycles of inorganic carbon species, few studies on their biogeochemical characteristics have been carried out in the Amundsen Sea. The Amundsen Sea also has been reported about rapid melting of the ice sheets owing to inflow of the circumpolar deep water to the shelf (Rignot et al., 2008). The rapid melting of ice sheets will influence ecosystem in the Amundsen Sea, which will change in the inorganic and organic carbon storage. In order to study the impact by rapid climate changes on the carbon flux in the water column of the Amundsen Sea, we investigated a complete set of inorganic carbon system in the polynyas of Dotson and Getz ice sheets, sea-ice zone, and the open ocean.

Work at sea

Hydrographic research in the Amundsen Sea was carried out from December 24, 2013 to January 25, 2014 at 40 stations (Table 2.1). The area mainly covers Amundsen polynya, including Dotson and Getz polynyas, sea-ice zone, and the open ocean. At each hydrographic site, a total of 411 water samples were collected by casting CTD/Rosette system to investigate inorganic carbon system by measuring dissolved inorganic carbon (DIC), total alkalinity (TA), and pH. In addition to vertical profiling of DIC, TA, and pH, real time monitoring of dissolved CO_2 (pCO_2) with sea surface temperature (SST), sea surface

salinity (SSS), and fluorescence was conducted along the ship track. pCO_2 was measured using a non-dispersive infrared (NDIR, Licor 7000) detecting system with a two-stage equilibrator. Every 6 hours the system is calibrated by three different standard gases (262.65 ppmv, 368.21 ppmv, 439.33 ppmv). To make DIC and TA underway measurements, uncontaminated seawater samples were collected every 1.5 - 2 hours interval along the ship track. DIC and TA were analyzed on board using a Versatile Instrument for Determination of Titration Alkalinity (VINDTA 3C) equipped with a coulometric for DIC and a potentiometric titration in open cell for TA. pH was determined by potentiometry using a glass/reference electrode. This pH measurement system consists of thermostatic water bath, voltage follower, glass/reference electrode, and voltmeter with high impedance (DOE, 1994). The analytical systems for DIC, TA, and pH were calibrated using a certified reference material (CRM) provided by Andrew Dickson (Scripps Institution of Oceanography). The inventory of samples collected and analysed at the hydro-casting stations is listed in Table 2.1.

Preliminary results

Fig. 2.3 shows the preliminary results obtained along the ship track. During the expedition, pCO_{2sw} over the Amundsen Sea ranged from 115 to 450 μatm. Unlike the pattern that was observed in 2010, pCO_2 in the sea-ice zone (low sea surface temperature (< 0℃) and salinity (< 33psu) was similar to pCO_{2air} or somewhat supersaturated. This result likely due to exposure of the remnant of the mixed layer in the preceding late winter as sea ice begin to melt. pCO_2 concentration in the polynya was undersaturated with respect to the atmospheric CO_2. This pattern is similar to that observed in 2010, but the degree of saturation appears to be larger this year. In the Amundsen polynya, surface water gas distributions are strongly influenced by physical processes, including surface warming, localized upwelling, and sea ice melt (Tortell et al., 2012). Compared with ANA01C expedition in 2010, the extent and volume of sea ice in the Amundsen polynya has dwindled. Thus, more exposure of the mixed layer by sunlight likely resulted in enhanced phytoplankton growth and pCO_2 drawdown. Like 2011, seawater in Dotson and Getz ice sheets were divided in view of not only pCO_2 but also of other chemical items.

References

Arrigo, K.R., van Dijken, G.L., 2003, Phytoplankton dynamics within 37 Antarctic coastal polynya systems. J. Geophy. Res.-Oceans, 108 (C8)

Johnson, K. M., Wills, K. D., Butler, D. B., Johnson, W. K., Wong, C. S., 1993, Coulometric total carbon dioxide analysis for marine studies: maximizing the performance of an automated continuous gas extraction system and coulometric detector, Mar. Chem. 44, 167-187.

Rignot, E., Bamber, J.L., Van den Broeke, M.R., Davis, C., Li, Y., Van de Berg, W.J., and Van Meijgaard, E., 2008, Recent Antarctic ice mass loss from radar interferometery and regional climate modeling, Nature Geosci. 1, 106-110.

Tortell, P.D., Long, M.C., Payne, C.D., Alderkamp, A.-C, Dutrieux, P., Arrigo, K.R., 2012, Spatial distribution of pCO_2, $\Delta O_2/Ar$ and dimethylsulfide (DMS)

Table 2.1: Number of samples collected at the station for inorganic carbon system parameters.

Station No.	Cast No.	Sampling Date (GMT)	Latitude (°S)	Longitude (°W)	DIC & TA	pH
1	1	2013-12-31 13:50	70.00	127.91	9	9
2	1	2014-01-01 9:22	71.01	123.01	10	10
3	1	2014-01-02 8:54	71.95	118.45	12	12
4	1	2014-01-02 21:21	72.39	117.71	11	11
5	1	2014-01-03 20:19	72.47	116.29	10	10
6	1	2014-01-04 13:58	74.00	113.00	9	9
7	1	2014-01-04 17:27	73.75	113.42	12	12
9	1	2014-01-05 6:12	72.86	117.2	11	11
10	1	2014-01-05 10:17	72.80	115.3	12	12
11	1	2014-01-05 19:47	72.85	112.5	10	10
12	1	2014-01-05 22:25	73.00	113.5	10	10
13	1	2014-01-06 1:04	73.17	114.5	11	11
14	1	2014-01-06 7:35	73.28	114.95	10	10
15	1	2014-01-07 4:17	73.33	115.5	12	12
16	1	2014-01-07 7:43	73.5	116.5	8	8
17	1	2014-01-07 9:45	73.49	115.7	12	12
18	1	2014-01-07 12:05	73.5	115.00	10	10
19	1	2014-01-07 14:53	73.5	114.00	11	11
20	1	2014-01-07 23:22	73.5	113.00	12	12
21	1	2014-01-08 1:54	73.5	112.00	9	9
22	1	2014-01-08 17:30	74.20	111.97	12	12
23	1	2014-01-08 23:30	74.17	112.15	12	12
24	1	2014-01-09 7:26	74.19	112.54	10	10
25	1	2014-01-09 17:07	74.21	112.82	10	10
26	1	2014-01-09 22:48	74.17	113.33	11	11
27	1	2014-01-10 3:26	73.82	113.07	12	12
28	1	2014-01-11 3:21	74.11	115.14	12	12
29	1	2014-01-11 5:27	74.13	115.36	10	10
30	1	2014-01-11 8:13	74.08	115.72	14	14
31	1	2014-01-11 12:29	74.04	115.96	11	11
32	1	2014-01-11 15:16	73.93	116.14	12	12
33	1	2014-01-12 2:17	74.00	118.18	12	12
34	1	2014-01-12 13:31	73.66	118.95	9	9
19	2	2014-01-13 16:26	73.5	114	6	6
14	2	2014-01-14 0:47	73.28	114.95	6	6
5	2	2014-01-14 6:09	72.45	116.35	6	6
3	2	2014-01-14 11:22	71.95	118.45	6	6
35	1	2014-01-14 16:41	71.5	121.00	17	17
2	2	2014-01-15 9:22	71.00	123.00	14	14

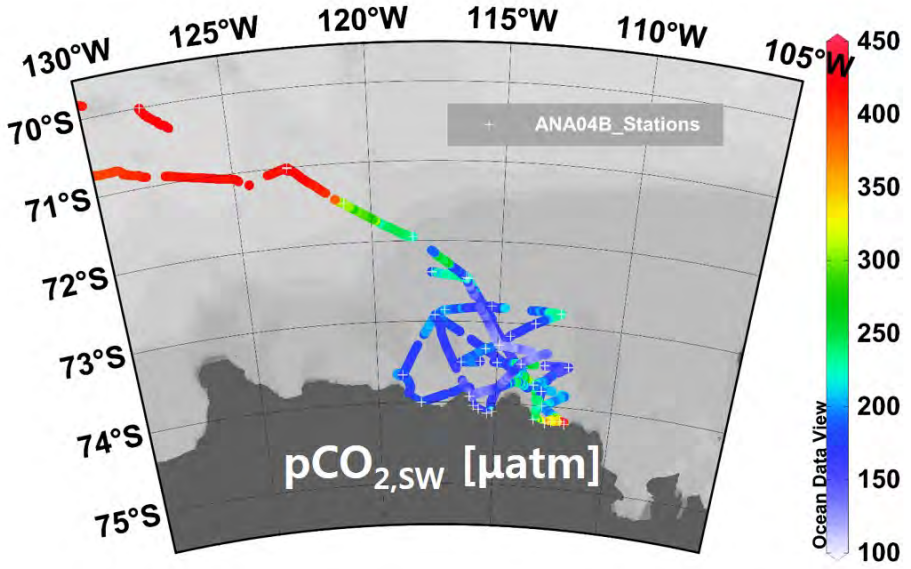

Figure 2.3: Dissolved pCO_2 at the surface waters along ship track.

in polynya waters and the sea ice zone of the Amundsen Sea, Antarctica, Deep-Sea Res. II, 71-76, 77-93.

2.4 Observations of dissolved and particulate matters

Jinyoung Jung, and Sun Yong Ha
Korea Polar Research Institute, Incheon 406-840, South Korea

요약문

해양표층에서의 일차생산은 지구규모의 탄소순환과 대기 중 이산화탄소의 해양으로의 흡수를 조절하는 중요한 역할을 한다. 식물플랑크톤의 광합성에 의해 생성되는 입자상 유기물질과 용존 유기물질은 생지화학적, 생태학적으로 뚜렷한 다른 특징을 가지고 있기 때문에 해양 생물학적 탄소펌프를 이해하기 위해 이 물질들의 이해가 요구된다. 하지만 현재까지 아문젠해에서 입자상, 용존 유기물질들을 연구한 예는 전무한 실정이다. 그러므로 이번 아문젠해 탐사를 통하여 입자상, 용존 유기물질의 거동을 이해하고자 한다.

Introduction

Primary production in the ocean surface plays a key role in the global carbon cycle and regulates the uptake of atmospheric CO_2 into the ocean. A great deal of effort has therefore been devoted to the precise estimation of primary production throughout the entire ocean. Photosynthesis by the planktonic community produces particulate organic carbon (POC) and dissolved organic carbon (DOC) at the surface; these 2 types of organic carbon materials have markedly

different biogeochemical and ecological characteristics (Karl et al., 1998). POC is available as a source of carbon and energy for many heterotrophs, whereas most cannot utilize DOC, which is mainly utilized by bacteria. Therefore, the partitioning of organic carbon production between POC and DOC is a primary constraint on marine carbon cycles. More than 99% of the organic nitrogen in the ocean exists in the form of dissolved organic nitrogen (DON). Particulate organic nitrogen (PON) represents only about 0.5% of the total organic nitrogen pool, but since some of the PON is heavy enough to sink, it represents a crucial component of the marine biological pump (Gruber, 2008). Until now, no study has been carried out to investigate the distribution and dynamics of dissolved and particulate organic matter in the Amundsen Sea. Our objective of this study therefore is to examine the dynamics of dissolved organic matter (DOM) and particulate organic matter (POM) and their C:N ratios during the expedition.

Work at sea and preliminary results

Seawater sampling for dissolved organic matter was carried out at 18 stations over the Amundsen Sea using a CTD/rosette sampler holding 24-10L Niskin bottles (Table 2.2). For dissolved organic matter measurements, a pre-cleaned (soaked in 10% HCl and rinsed with ultrapure water) Teflon tube was used to connect between spigot and pre-cleaned 47 mm filtration holder made of PP (PP-47, ADVANTEC). About 200 ml of seawater was filtered through a pre-combusted (at 550°C for 6 hours) Whatman GF/F filter (47 mm in diameter) under gravity. The filtered samples were collected directly into pre-cleaned glass bottles. The filtrate was distributed into three pre-combusted 20 ml glass ampoules with a sterilized serological pipette. Each ampoule was sealed with a torch, quick-frozen, and preserved at approximately -24°C until the analysis in our land laboratory. Simultaneous dissolved organic carbon/total dissolved nitrogen analyses will be basically made with an HTCO system consisting of a commercial unit, the Shimadzu TOC-V system (Shimadzu Co.), fitted with a chemiluminescence (CLS) detector that was incorporated into the total nitrogen micro analyzer. The concentration of DON will be obtained by the difference between total dissolved nitrogen and dissolved inorganic nitrogen (i.e., NO2 +NO3 and NH4+) concentrations.

A 1 L of seawater for analysis of POC was drained from the Niskin bottles into a pre-cleaned amber polyethylene bottle, as was the PON sample. POC and PON samples were filtered with pre-combusted (at 550°C for 6 hours) GF/F filters (25 mm in diameter) using a nitrogen gas purging system under low (<1.0 atm) pressure. The GF/F filters for POC and PON analyses were stored at -24°C in hinged-lid and airtight PP containers. Prior to analysis of POC sample, particulate inorganic carbon should be removed using acid. The filters for POC and PON measurements will be analyzed using a CHN analyzer in our land laboratory.

References

Karl, D.M., Hebel, D.V., Björkman, K., Letelier, R.M., (1998) The role of dissolved organic matter release in the productivity of the oligotrophic North Pacific Ocean. Limnology and Oceanography, 43,1270–1286.

Table 2.2: Dissolved and particulate organic matters sampling locations and sampling depths collected over the Amundsen Sea during the expedition

Station	Latitude	Longitude	Depth (m)
1	69° 59.89'S	127° 54.50'W	0, 20, 40, 60, 75, 100
2	71° 10.44'S	123° 00.76'W	0, 40, 100, 300, 500, 1000, 1500, 2000, 3200
3	71° 57.03'S	118° 27.06'W	0, 10, 25, 40, 60, 100, 150, 300, 450, 610
4	72° 23.20'S	117° 42.64'W	0, 10, 20, 40, 60, 100, 200, 300, 400, 450, 508
5	72° 28.02'S	116° 17.09'W	0, 17, 25, 40, 60, 100, 200, 300, 400, 450, 527
10	72° 48.02'S	115° 17.88'W	0, 10, 25, 40, 60, 100, 200, 300, 400, 500, 550, 590
14	73° 16.88'S	114° 56.96'W	0, 10, 20, 40, 60, 100, 240, 330, 400, 630, 700, 820
19	73° 29.98'S	114° 00.00'W	0, 15, 25, 40, 60, 100, 200, 300, 400, 500, 600, 703
22	74° 12.15'S	111° 58.45'W	0, 10, 20, 40, 60, 100, 210, 300, 400, 500, 623
26	74° 10.45'S	113° 19.72'W	0, 10, 20, 40, 60, 100, 200, 280, 400, 510, 600, 670
27	73° 49.24'S	113° 04.00'W	0, 10, 20, 40, 60, 100, 200, 300, 400, 500, 600, 770
28	74° 06.31'S	115° 08.55'W	0, 20, 40, 60, 80, 100, 150, 250, 350, 450, 550, 630
32	73° 55.45'S	116° 08.17'W	0, 20, 40, 60, 80, 100, 200, 300, 400, 500, 626
19(revisit)	73° 29.99'S	114° 00.00'W	0, 10, 20, 40, 60, 100
14(revisit)	73° 16.88'S	114° 57.06'W	0, 20, 40, 60, 100
5 (revisit)	72° 27.26'S	116° 20.91'W	0, 25, 40, 60, 100
3 (revisit)	71° 57.06'S	118° 27.09'W	0, 25, 40, 60, 100
35	71° 30.00'S	121° 00.08'W	0, 25, 40, 60, 100

Gruber, N., (2008) The Marine Nitrogen Cycle: Overview and Challenges. In "Nitrogen in the Marine environment 2nd edition: Academic Press, Elsevier, Chapter 1, pp. 1–43.

2.5 Observation of Nitrous oxide (N_2O)

Jinyoung Jung, and Tae Siek Rhee
Korea Polar Research Institute, Incheon 406-840, South Korea

요약문

아산화질소는 온실기체 중 하나로 이산화탄소보다 200배 강력한 온실효과를 나타낼 수 있다. 대기 중 존재하는 아산화질소의 상당부분이 해양에서 배출된 아산화질소로 구성되어 있기 때문에, 아산화질소는 해양질소순환 및 지구기후변화와 직접적으로 연결되어 있다. 해양에서 아산화질소는 질산화과정과 탈질과정에서 발생된다고 알려져 있다. 아문젠해 탐사에서는 질산화와 탈질과정에 대한 이해증진 및 해양내부 아산화질소의 수직구조를 관측하기 위해 7개 정점에서 아산화질소 시료채취를 하였다. 채취한 시료의 분석은 탐사 후 연구소에서 수행할 계획이다.

Objective

Nitrous oxide (N2O) acts as a greenhouse gas that is more than 200 times more potent than CO_2 (Ramaswamy et al., 2001). Therefore variations of N2O gas in the atmosphere can lead to changes in Earth's temperature and climate. Since the oceanic emission of N2O constitutes a substantial fraction to the total emission of N2O into the atmosphere, N2O provides for a direct potential link between the ocean nitrogen cycle and Earth's climate. In the case of aerobic remineralization, the formation of N2O is associated with the oxidation of NH4+ during nitrification. N2O is also formed during denitrification, as it

Table 2.3: N_2O sampling locations and sample numbers collected over the Amundsen Sea during the expedition

Station	Sample number	Latitude	Longitude
1	8	70°00.01'S	127°54.62'W
3	7	71°57.02'S	118°27.06'W
10	11	72°48.02'S	115°17.88'W
19	10	73°29.98'S	114°00.04'W
22	12	74°12.15'S	111°58.46'W
27	12	73°49.24'S	113°04.00'W
28	11	74°06.31'S	115°08.55'W

represents an intermediary product during the reduction of NO3 to N2. Oceanic source strength of N2O to the atmospheric budget is not well quantified due to the lack of observations for N2O in the ocean. In particular, sea-ice region and continental shelf of the Amundsen Sea is a void region of N2O data. The objectives of this study are to estimate emission rate of N2O from the ocean to the atmosphere, and to improve understanding of nitrification and denitrification processes in the Amundsen Sea.

Work at sea

Seawater samples for N2O measurement were drawn from the Niskin bottles of CTD/rosette system into specially designed glass jar bottles. A 50 ml of pure N2 (99.9999%) gas was subsequently injected into the glass jar bottles using a syringe to make a headspace. The N2O samples were then poisoned with 200 μl of HgCl2 to halt biological activity and stored in plastic containers at room temperature (25°C) prior to chemical analyses. The measurement of N2O is scheduled to be conducted in the laboratory of Korea Polar Research Institute. In the laboratory, the headspace air is taken using the syringe and injected into sample loops equipped in gas chromatography in order to measure N2O concentration in water column. N2O is separated in packed column and detected in electron capture detector (ECD), and quantified by calibrating the gas chromatographic system using a series of calibration gases. A total of 71 samples collected over the Amundsen Sea during the expedition will be analyzed (Table 2.3).

References

Ramaswamy, V., Boucher, O., Haigh, J., Hauglustaine, D., Haywood, J., Myhre, G., Nakajima, T., Shi, G. Y., and Solomon, S., (2001) Radiative forcing of climate change. In "Climate Change 2001: Cambridge University Press, Cambridge, Chapter 6, pp. 527–585.

2.6 Water sampling for the measurement of noble gases

Doshik Hahm
Korea Polar Research Institute, Korea

Objectives

The noble gases, especially helium isotopes (^{3}He and ^{4}He) in conjunction with tritium (^{3}H), have been widely used to trace water mass movement due to their conservative behavior in the environment and to give time constraints (i.e., ^{3}H-^{3}He age) on physical and biological processes in the ocean (e.g., Jenkins, 2008). Another interesting application is to detect ice-related processes using their different partitioning behavior in water, sea-ice and glacier (e.g., Hohmann et al. 2002; Huhn et al., 2008). The hydrography of the Amundsen Sea is in substantial change due to rapid loss of glacier ice sheet and sea ice, occurring around the west Antarctica. Given the high resolving power of noble gases for ice-related processes, they will provide invaluable information on the influence of glacier and sea ice loss of this area on the changes of its hydrography and, in turn, biological processes.

Work at sea

Water samples for noble gases were collected at 23 selected stations (stations with white circles in Fig. 2.4) among the 35 CTD stations covered in the cruise. The sampling locations complete 4 cross sections: (1) along, so called, 'the Amundsen Trough' section from Station 1 to 24, (2) across the trough section from Station 12 to 16, (3) along the Getz Ice Shelf from station 28 to 32, and (4) along the Dotson Ice Shelf from Station 22 to 26. The preliminary results of CTD casts suggest that the western side of the Dotson Ice Shelf exhibit more pronounced Circumpolar Deep Water (CDW) upwelling and its mixing with overlying Winer Water (WW) as seen in ANA02C expedition. However, the boundary between WW and CDW was deeper than in the previous expedition, suggesting weaker intrusion of CDW and thus resultant less glacial melting.

References

Hohmann, R., Schlosser, P., Jacobs, S., Ludin, A., Weppernig, R., 2002. Excess helium and neon in the southeast Pacific: Tracers for glacial meltwater. Journal of Geophysical Research-Oceans, 107, doi:10.1029/2000JC000378.

Huhn, O., Hellmer, H. H. , Rhein, M., Rodehacke, C., Roether, W. , Schodlok, M. P., Schroeder, M. 2008. Evidence of deep- and bottom-water formation in the western Weddell Sea. Deep-Sea Research Part I, 55, 1098–1116.

Jenkins, W. J. , 2008. The biogeochemical consequences of changing ventilation in the Japan/East Sea. Marine Chemistry, 108, 137–147.

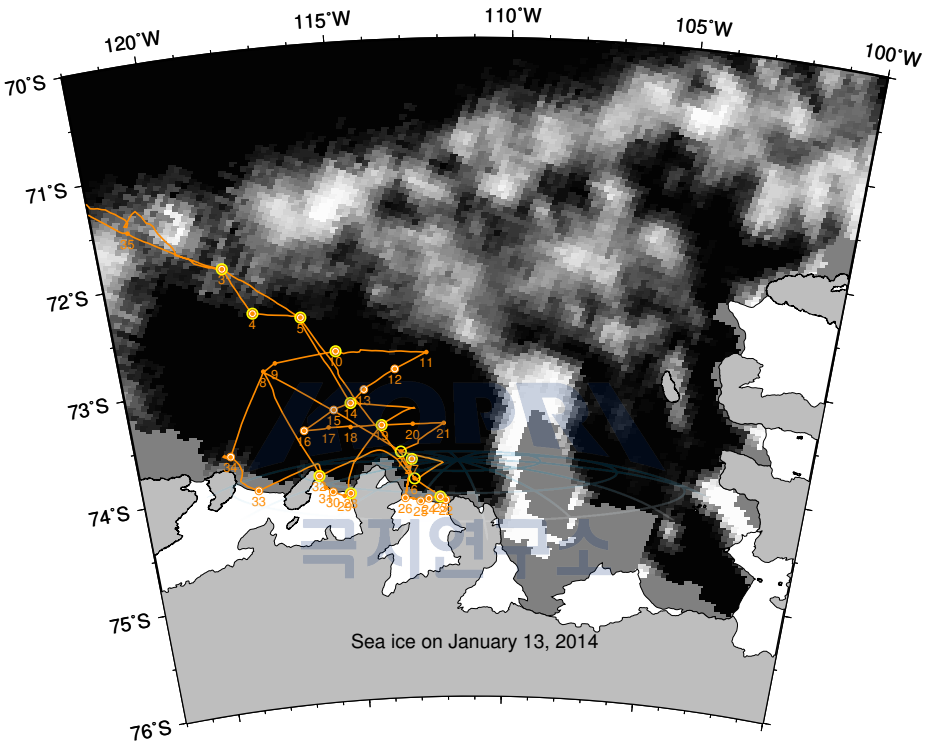

Figure 2.4: Map showing the cruise track and CTD stations (orange dots and numbers). Stations where water samples for noble gases and dissolved oxygen collected are indicated in white and yellow circles, respectively. Shown together are the cruise track along which underway measurements were performed. The measured parameters are temperature, salinity, fluorescence, pCO_2 and $\Delta O_2/Ar$ (See section 2.7).

2.7 Continuous O_2/Ar measurement as a proxy of net community production

Doshik Hahm
Korea Polar Research Institute, Korea

Objectives

Net community production (NCP), defined as the difference between autotrophic photosynthesis and (autotrophic and heterotrophic) respiration, produces O_2 proportional to the amount of net carbon. By measuring chemically and biologically inert Ar together with O_2, it is possible to remove O_2 variation by physical processes (e.g., air temperature and pressure change and mixing of water masses) and deduce O_2 variation by biological processes (Craig and Hayward, 1987).

To determine the net community (oxygen) production underway, we adopted a continuous O_2/Ar measurement system developed by Cassar et al. (2009). The so called 'equilibrator inlet mass spectrometer (EIMS)' is centered around a quadrupole mass spectrometer that measures dissolved gas molecules equilibrated with air in and supplied by an equilibrator. Water temperature, salinity, oxygen and fluorescence were also obtained to help the interpretation of temporal and spatial variation of O_2/Ar.

Preliminary results

The preliminary results were summarized in Fig. 2.5 and Fig. 2.6. ΔO_2/Ar (the excess of biological O_2) in the open ocean crossed during the transit between Christchurch to the Amundsen Sea were slight higher than zero (before December 30, 2013). The values became as low as -10% in the sea ice covered regions north of the continental shelf around Stations 1 and 2. It was noticed that the northern boundary of the Amundsen Sea Polynya was extended to further north from that of ANA02C expedition in February of 2012. The ΔO_2/Ar values within the polynya (from January 2 to 13) were mostly higher than 20%. It is noteworthy that significant ΔO_2/Ar increase was observed at selected revisit stations. For example, the mean values at station 19 increased from ~20% on January 7 to 35% January 13, 2014. Overall, the variation of ΔO_2/Ar in the Amundsen Sea polynya resembled that of SST as seen in the previous two expeditions (i.e., ANA01C and ANA02C).

References

Cassar, N., Barnett, B. A., Bender, M. L. , Kaiser, J. , Hamme, R. C., Tilbrook, B. 2009. Continuous high-frequency dissolved O_2/Ar measurements by equilibrator inlet mass spectrometry. Analytical Chemistry, 81, 1855–1864.

Craig, H., Hayward, T., 1987. Oxygen supersaturation in the ocean: Biological versus physical contributions. Science 235, 199–202.

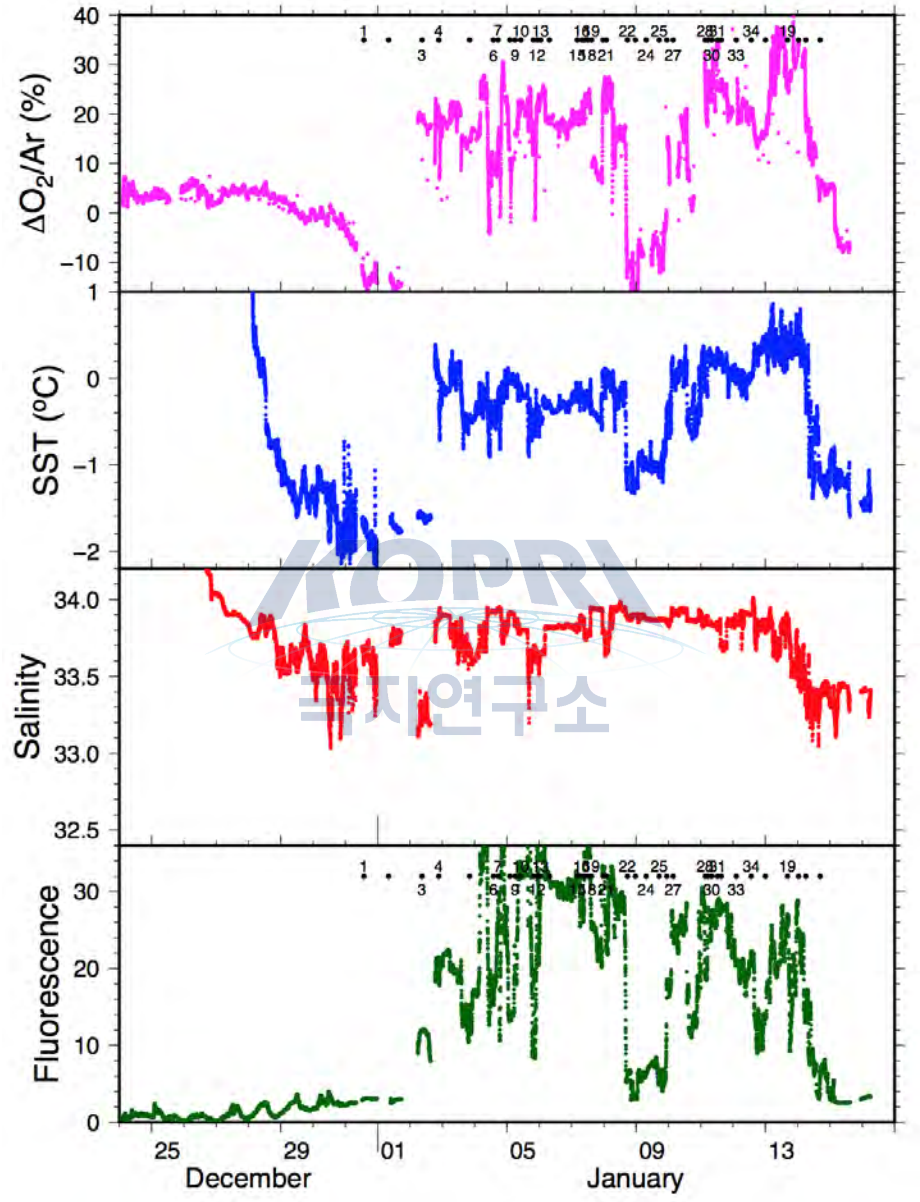

Figure 2.5: The preliminary results of $\Delta O_2/Ar$, temperature, salinity, and fluorescence.

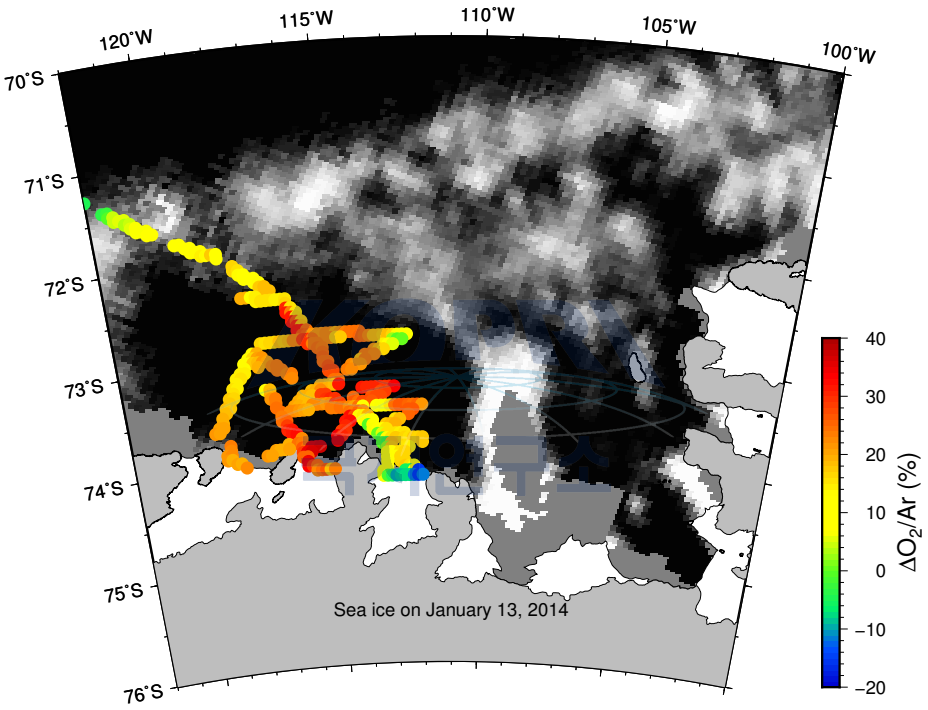

Figure 2.6: Spatial variation of $\Delta O_2/Ar$ superimposed on the ice concentration map on January 13, 2014.

2.8 Trace metals and Cd stable isotopes in the Amundsen sea

J. K. Park, D. J. Jang, M. S. Choi
1Department of Ocean Environmental Sciences, Chungnam National University, Korea

요약문

해양환경에서 몇몇 미량금속은 일차생산에 중요한 역할을 하며 식물 플랑크톤의 군집 조성에도 큰 영향을 준다고 알려져 있다. 해양에서 미량금속 농도 분포는 공급원의 종류 및 성격, 내부 순환 양상, 용존상-입자상 반응, 제거 기작에 의해 조절되며 금속 동위원소는 공급원과 생지화학적 과정에 대한 정보를 제공해주어 최근에 많은 연구들이 진행되고 있다. 본 연구는 남극 연안해역에서 생물 생산성이 가장 높은 아문젠 해역의 미량금속 분포 특성을 공급원 및 내부 순환의 관점에서 살펴보고 미량금속과 생물 생산성 사이의 관련성을 규명하고자 한다. 또한 Cd 동위원소의 식물플랑크톤에 의한 동위원소 분별 작용을 파악하여 생물에 의한 Cd 동위원소 분별 조건들을 살펴보고자 한다. 일반적으로 남극주변부 대양의 미량금속 농도는 매우 낮은 수준으로 보고되어있어 배에서 채수장비를 이용하여 채수 시 다양한 오염원에 의한 오염이 발생할 위험이 있다. 그러므로 이러한 오염을 예방하기 위하여 케블라 와이어가 장착된 윈치, 티타늄 재질의 로젯에 테플론으로 코팅된 추를 부착하였으며 GO-FLO 채수 병을 사용하였다. 위와 같은 방법으로 아문젠해에서 총 10개의 정점에서 수심에 따라서 깊이를 달리하여 채수하였다. 채수한 채수 병은 곧바로 청정 실험 실로 옮겨 실험실 내에서 전부 처리하였으며, 샘플은 받는 순서에 따라서 필터를 하지 않은 0.5L, 필터 한 1L, 2L의 샘플을 받아 정제염산을 넣어 산성화하였다. 샘플분석은 입자상과 용존상을 모두 분석할 예정이다.

Objectives

Trace metals play a key role in primary production in the marine environment and called micronutrients. In addition, they are also influential in mediating phytoplankton community composition (e.g. Pickell et al., 2009; Boyd et al., 2010). Input sources, internal cycles, dissolved-particulate reaction and removal processes were responsible for the distribution of trace metals in seawaters. Recently, metal stable isotopes could be fractionated by biogeochemical processes involved and inform about the source signal. This study aims the investigation for the distribution of trace metals in the Amundsen Sea where was known the most productive area in coastal regions of the Antarctica. Generally, dissolved trace metals in seawater was in the very low level. The extremely low natural concentration of many trace metals in seawater and the ubiquity of these materials in the sampling platforms (ships and sampling equipment such as bottles and frames) results in samples being highly susceptible to contamination during the sampling and subsampling process. Therefore, we adopt several methods to prevent contamination. Firstly, to avoid the problem of potential cable contamination for Cu, Cd, Zn and Ni by using non-metallic Kevlar wire with plastic sheave. Secondly, we used Teflon coated GO-FLO bottles for sampling, which contain no internal spring s and could be deployed in the closed position, thus avoiding surface water slicks that are believed by many to be potential sources

of contamination. Thirdly, we used Ti-framed rosette mounted with 12 GO-FLO bottles (5L). In addition, we also set up the sampling procedure including handling sampling bottles and filtration within/outside the clean cell.

Work at sea

Following above methods, seawater samples were collected at different depths of 10 stations. Sample handling was performed within a clean cell. GO-FLO bottles have been modified slightly from the original manufacturer's design. The modifications consist of drilling out the receptacles to accept the air vent fixtures and sampling valves. After racking the bottles and removing the hair cab from the subsampling cocks, the vent cabs are then removed, and initial unfiltered samples (0.5 L) are drawn from the cocks. The bottles must be drained slightly at this stage to lower the sample level below the air vent cabs. Bottles are then connected to clean hose (equipped with air filter) fittings and pressurized with compressed air, seawaters was filtered through an in-line filter (0.45 μm membrane filter, 3L). All the samples were acidified using concentric hydrochloric acid within the clean cell. We plan to analyze both dissolved and particulate metals.

2.9 Estimation of POC export flux using $^{234}Th/^{238}U$ disequilibrium in the Amundsen Sea, Antarctic

Kim, Miseon; Choi, Mansik
Department of Ocean Environmental Science, Chungnam National University

요약문

남극 아문젠 해에서 탄소 순환을 이해하는데 중요한 지표인 export production (EP)을 알아보기 위해 $^{234}Th/^{238}U$ 비평형법을 이용하여 총 ^{234}Th을 측정하였다. 이와함께 유광대 입자의 화학 조성에 따른 EP의 지역적 변화를 검토해보고자 해역별 10개의 정점에서 수층에 따라 3L씩 채수하여 여과된 해수를 현장에서 Mn 공침 후 β-spectrometer로 ^{234}Th를 측정하였다. 이는 6개월 후 다시 측정할 예정이다. 0.5 – 3L의 해수를 GF/F와 nuclepore에 여과한 입자상 물질은 실험실에서 분석할 예정이다.

Objectives

The export fluxes of particulate organic carbon (POC) play an important role in the transfer of carbon between the atmosphere and the ocean. Accurate estimates of POC export fluxes are critical for constraining models of the global carbon cycle. Over the past few decades, the radioisotope pair ^{238}U and ^{234}Th has been increasingly used to estimate POC export fluxes from the euphotic zone. This method is based on the uptake of ^{234}Th onto biogenic particles in the euphotic zone and the subsequent sinking of particles into deep water. The POC export flux is determined by multiplying the depth-integrated ^{234}Th flux by the POC/^{234}Th ratio on sinking particles. This study aims to estimate the POC

export fluxes in the Amundsen Sea using $^{234}Th/^{238}U$ disequilibrium method, and to discuss the variability of export ratio (export flux/primary production)in several regions.

Work at sea

A given amount of seawater samples were collected at water depths of 10 stations.

1. 3L of seawater at 8 water depths per each station for total ^{234}Th analysis
2. 20L of seawater at 100m depth (lower thermocline) for particulate ^{234}Th and POC analysis
3. 10L of seawater at SCM depth for POC, BioSi and Al analysis

Total and dissolved ^{234}Th activities were analyzed for bulk and filtered seawaters, respectively, using a gas-flow proportional β-spectrometer manufactured by Risø National Laboratories (Roskilde, Denmark) following methods described in Buesseler et al. (2001).Three liters of seawater was acidified using 3ml of concentric nitric acid immediately after collection, and was then spiked with 1g of 230Th (IRMM-061, 24pg/g) solution. After equilibration for 8–12 hours, the pH of seawater was adjusted to 8.0±0.15 using ammonia solution. Manganese precipitates were created by adding KMnO4 (7.5 g KMnO4/L) 100 μL and MnCl2(33.3 g MnCl2 · 5H2O/L) 100 μL. The precipitates were aged by heating the seawater at 80°C in a water bath for 2–3 hours and filtered using QMA filter paper with 25-mm diameter and 1.2-μm pore size. After drying the precipitates, the QMA filter papers were directly counted by spectrometer five times every 24 days. The background counts were about 0.2 cpm using only filter paper, and each sample was counted for 12 hrs. Initial ^{234}Th activities were acquired after best fitting of the radioactive decay equation for ^{234}Th.

2.10 POC cycling on the Amundsen Shelf : Insights from radiocarbon analysis

Minkyoung Kim, Jeomshik Hwang
POSTECH

요약문

서남극 아문젠 해는 빙상과 빙붕의 급격한 감소를 보이며 지구 온난화의 영향을 크게 받고 있는 해역 중 한 곳이다. 기후 변화로 인한 해빙의 감퇴는 해양 일차생산자인 식물 플랑크톤에 의한 일차생산을 비롯한 탄소순환 양상에 영향을 미칠 것으로 예상된다. 본 연구에서는 나이와 기원에 대한 정보를 제공할 수 있는 방사성탄소동위원소를 이용하여 아문젠해 유기탄소 순환을 이해하려 하였다.

Introduction

The Antarctic region is being influenced by climate change most severely. Physical changes such as seasonal sea ice melting and CO_2 absorption will influence

the carbon cycling in this region. The change in carbon cycling in turn will affect the future climate change through feedback mechanisms. Understanding the cause of the change in carbon cycling of this region will provide information to enhance the model performance for future climate projection.

Work at sea

Various particulate organic carbon (POC) samples were collected including sinking POC, suspended POC in surface water, phyto/zooplankton and sediment on the Amundsen shelf, Antarctica, during the 2013/14 cruise on the IBRV Araon.

Sediment samples were collected using a box–core (Marine Tech. Korea) at 4 locations along the Dotson trough. Stations K1 (72 ºS, 117 ºW; 520 m), K2 (73 ºS, 115 ºW; 830 m), K3 (74 ºS, 112 ºW; 1055 m) and K6 (74 ºS, 113 ºW; 780 m) represent the sea ice zone (SIZ) near polynya, inside the polynya and near the ice shelf. Sediment trap were deployed each stations. Upon detachment of the canister, plastic cores of 8 cm diameter and 60 cm length were gently pushed in for sub–cores. Each sediment core was sliced into 1–2 cm thick subsamples on board and stored in pre–baked glass jars and kept frozen until analysis.

Suspended material in surface water was collected by filtration of sea water from the ship's uncontaminated sea water intake on pre baked 47 mm GFF filters with nominal pore size of 0.7 μm (Whatman) without any pre filtration. Depending on the amount of particles 1.5 – 5 L of surface water was filtered under low vacuum (500 mmHg). Each filter was folded and stored frozen in a pre-combusted aluminum foil pouch until further analysis.

Chapter 3

Biological Oceanography

3.1 Carbon and nitrogen productions of phytoplankton in the Amundsen Sea, Antarctic

Bo Kyung Kim
Pusan National University, Korea

요약문

식물플랑크톤 탄소와 질소 섭취율을 알아보기 위해 아문젠해 12개 정점 (revisit 정점 2개포함)에서13C-15N-dual isotope tracer를이용한방법으로 6개의 light depths (표층 PAR의 100, 50, 30, 12, 5, 1%)에서 얻어진 해수를 4-5시간 배양하여 시료를 얻었다. 식물플랑크톤 생리상태를 알아보기 위해 7개의 정점에서 거대분자 생산력 실험이 이루어졌으며 배안 실험실로 옮겨와 바로 GF/F 필터에 여과한 후 냉동 보관 (-80 ℃) 하였다. 현장조사가 끝난 후, 시료는 알래스카대학교 안정동위원소 실험실에 있는 Finnigan Delta+XL mass spectrometer를 이용하여 탄소와 질소 동위원소를 동시에 측정할 예정이다.

Introduction

The Antarctic has low chlorophyll a (chl-a) despite high concentration of nutrients in ambient water (Minas et al., 1986), where is low primary production compared to other regions (upwelling, coastal and estuary) on an annual basis. On the other hand, this region is crucial role in air - heat exchange, global deep seawater (such as Antarctic Bottom Water) formation, and efficient biological pump in world's ocean (Siegenthaler and Sarmiento, 1993). The Amundsen Sea is located in the West Antarctic, which is known as one of the most productive polynya with Ross Sea and Ronne Ice Shelf, Prydz Bay and sum of these regions were accounting for over 75 % of total primary production in the Antarctic (Arrigo and van Dijken, 2003). Recently, the West Antarctic was issued region, covered by West Antarctic Ice sheet (WAIS) which has been declining in extent and thinning unlike East Antarctic (Rignot et al., 2008). The primary production has been estimated by satellite observations in the Amundsen Sea (Arrigo et al., 2008; Arrigo et al., 2012), but in situ field data are scarce due to a difficult accessibility caused by sea ice cover (Lee et al., 2012). Therefore, in this study

Figure 3.1: In situ incubation on deck for 4-5 hours.

we measured in situ carbon and nitrogen uptake rates to investigate seasonal variations in primary and new productions of phytoplankton in the Amundsen Sea.

Methods and Materials

To estimate carbon and nitrogen uptake of phytoplankton at different locations, productivity experiments were executed by incubating phytoplankton in the incubators on the deck for 4-5 hours (Fig. 3.1) after stable isotopes (13C, 15NO3, and 15NH4) as tracers were inoculated into each bottle. Total12productivity experiments (Fig. 3.2) were completed during this cruise. At every CTD station, the productivity waters were collected by CTD rosette water samplers at 6 different light depths (100, 50, 30, 12, and 1%). In addition, Along with the small (1 L) productivity bottle experiments, 7 large volume (8.8 L) productivity experiments for three depths (100, 30, and 1% light depths) were executed to study the physiological status and nutritional conditions of phytoplankton at the productivity stations (Fig. 3.2). These filtered (GF/F, ø = 47 m) samples will be chemically analyzed for the macromolecular level end products (such as lipids, proteins, polycarbonates and LMWM) of photosynthesis. After the incubation, all productivity sample waters were filtered on GF/F (ø = 25 mm or 47 mm) filters for laboratory isotope analysis at University of Alaska Fairbanks after this cruise.

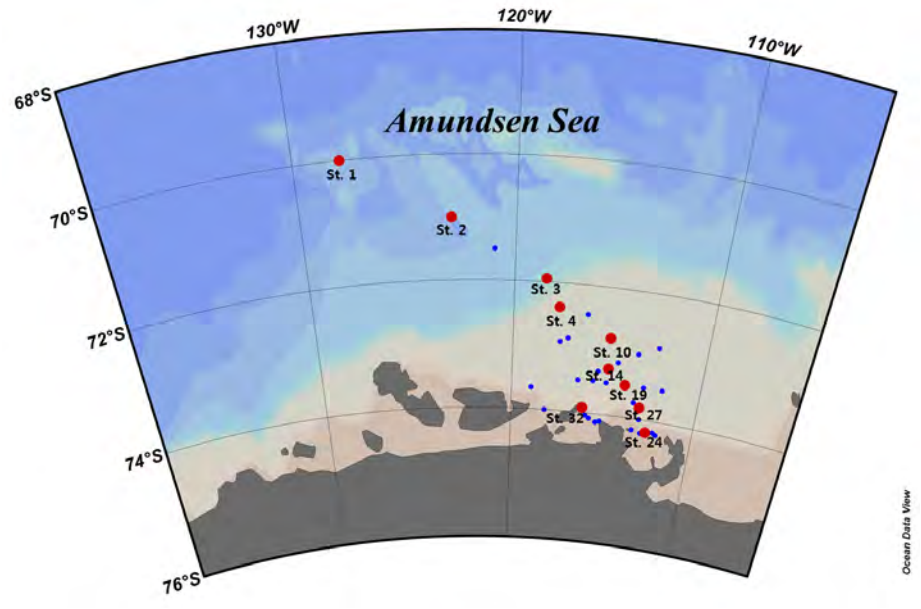

Figure 3.2: Stations for primary and macromolecular productivity during the Amundsen Sea cruise.

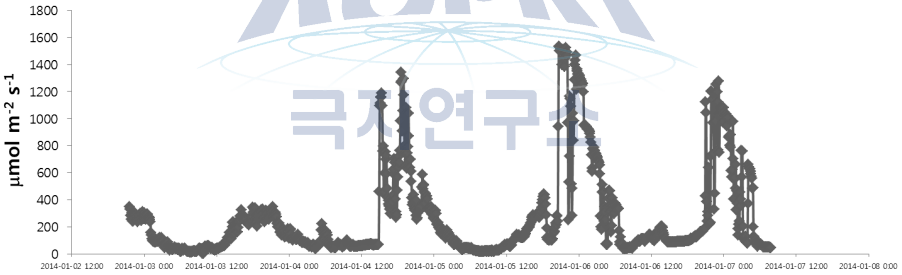

Figure 3.3: Air surface light intensity during the cruise in 2014

Preliminary Results

Light intensity during the cruise

Air surface light intensity measured during the cruise ranged from over 1500μmol m-2 s-1 for day time to about 0.8 μmol m-2 s-1 for night (Fig. 3.3). There is a distinct pattern of light intensity for day and night cycle although night time is not dark at all most of time during the Antarctic summer. Therefore, the incubation time for phytoplankton productivity experiments should be executed during the day time when the light intensity high enough for their growth.

Size-fractionation of phytoplankton

The size-fractionated chl-a concentrations were obtained from 3 light depths (100, 30, and 1 %). Phytoplankton community in the Amundsen Sea except

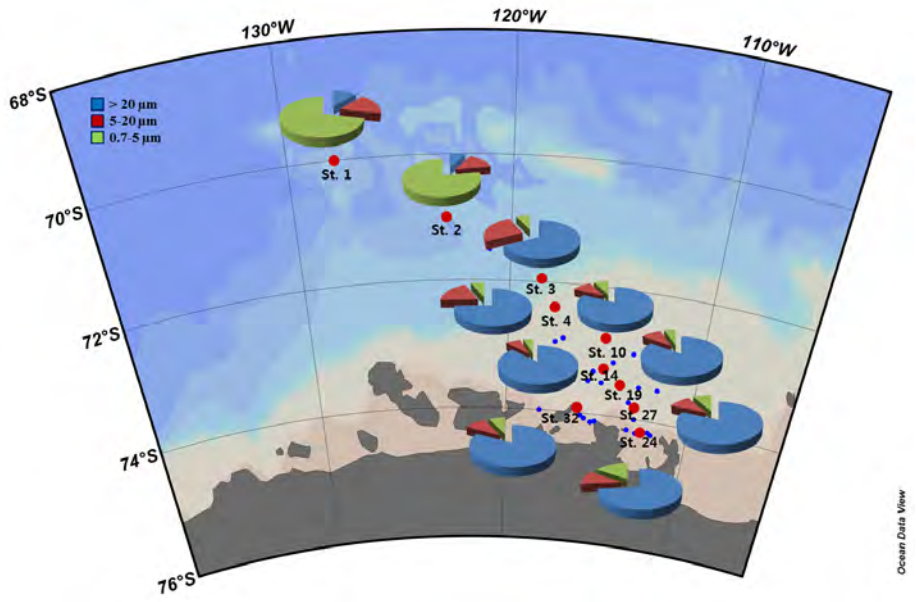

Figure 3.4: Compositions of different size chlorophyll-a concentrations at the productivity stations.

2 stations (St. 1 and 2) was dominated by large-sized phytoplankton (> 20 μm) accounting for 79.4 ± 6.9 % of the total chl-a concentration, followed by middle (5-20 μm; 12.8 ± 6.3 %) and small cells (0.7-5 μm; 7.8± 3.3 %) (Fig. 3.4). In offshore regions (St. 1 and 2), small-sized phytoplankton (0.7-5μm) were predominant (74.7 8± 4.3%) for the phytoplankton community (Fig. 3.4).

References

Arrigo, K.R., Lowry, K.E., and van Dijken, G.L. (2012) Annual changes in sea ice and phytoplankton in polynyas of the Amundsen Sea, Antarctica. Deep Sea Res., Part II, 5: 71-76.

Arrigo, K.R., van Dijken, G.L.(2003) Phytoplankton dynamics within37 Antarctic coastal polynya systems. J. Geophys. Res. 108.doi:10.1029/2002JC001739.

Arrigo, K. R., van Dijken, G. L., and Bushinsky, S. (2008) Primary production in the Southern Ocean, 1997–2006. J. Geophys., Res., 113: DOI: 10.1029/2007JC004551.

Arrigo, K. R., Worthen, D. L. and Robinson, D. H. (2003) A coupled ocean - ecosystem model of the Ross Sea: 2. Iron regulation of phytoplankton taxonomic variability and primary production. J. Geophys. Res., 108 (C7): 3231, doi:10.1029/2001JC000856.

Lee, S.H., Kim, B.K., Yun, M.S., Joo, H.T., Yang, E.J., Kim, Y.N., Shin, H.C., and Lee, S.H. (2012) Spatial distribution of phytoplankton productivity in the Amundsen Sea, Antarctica. Polar Biol., 35: 1721-1733.

Minas, H. J., Minas, M. and Packard, T. T. (1986) Productivity in upwelling areas deduced from hydrographic and chemical fields. Limnol. Oceanogr., 31:

1182-1206.

Rignot, E., Bamber, J. L., Van den Broeke, M. R., Davis, C., Li, Y. H., van de Berg, W. J. and van Meijgaard, E. (2008) Recent Antarctic ice mass loss from radar interferometry and regional climate modelling. Nat.Geosci., 1 (2): 106-110. Siegenthaler, U. and Sarmiento, J. L. (1993) Atmospheric carbon dioxide and the ocean. Nature, 365: 119-125.

3.2 Responses of phytoplankton physiology to iron addition in the Amundsen Sea

Park, Jisoo
Korea Polar Research Institute, Korea

요약문

식물플랑크톤 광합성과 관련된 생리활성도는 Fluorescence Induction and Relaxation (FIRe 2)를 이용하여 측정되었다. 총 25개 정점 (5정점 재방문)의6개 수층에서 채수한 해수를 분석하였으며, 연구항차 중 선저 펌프로부터 공급되는 표층해수를 이용한 연속관측도 이루어졌다. 이를 통해 얻어진 광합성 양자효율 변수는 아문젠해역 식물플랑크톤의 영양분 부족 (특히 철분 부족)을 알 수 있는 대리변수로 사용될 수 있다. 또한 연구해역 식물플랑크톤의 철분 부족에 따른 성장제한 효과를 관찰하기 위해 고안된 배양실험을 통해 영양염, 유기탄소 등의 변화와 함께 식물플랑크톤 엽록소 농도와 생리활성도의 변화를 측정하기 위한 실험이 총 4곳 (외해, 아문젠 사면입구, 폴리냐 중심, 빙붕 앞)에서 이루어졌다. 실험을 위한 해수는 Go-FLO 채수기를 사용하여 채수시의오염을 방지하였으며 7일 이상의 기간 동안 갑판에서 배양하며 주기적으로 변화를 측정하였다.

Objectives

To investigate the impact of physico-chemical conditions on photosynthesis, we measured photosynthetic characteristics of phytoplankton at 25 stations (5 stations were revisited) using a Fluorescence Induction and Relaxation (FIRe 2) system (Fig. 3.5). Active (and fast) fluorometry is a non-destructive and rapid method, and it has been used to monitor variations in the photochemistry (Kolber and Falkowski 1993; Falkowski and Kolber 1995). These measurements provide an express diagnostics of the effects of environmental factors on photosynthetic processes by nutrient limitation (especially iron limitation).To demonstrate that iron limited responses of natural phytoplankton assemblages, we carried out iron assimilation experiments at four stations (open sea, outer shelf, polynya center, front of ice shelf) during more than seven days respectively.

Work at sea

The total stations were 25 which include ice margin, Amundsen polynya, and open sea (Fig. 3.6). After collection from Niskin bottles at six depths, samples were kept under in situ temperature in light bottles. Light bottle samples were measured after 30 minutes low light adaptation. Photosystem II (PSII) parameters such as the minimal fluorescence yield (F0; when all reaction centers are open), the maximal fluorescence yield (Fm; all reaction centers are closed),

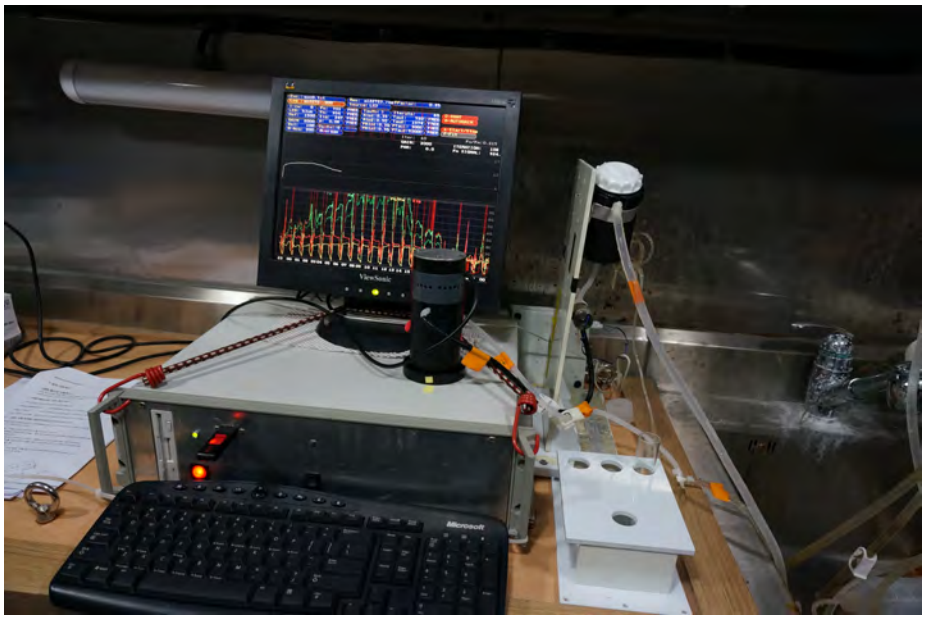

Figure 3.5: A Fluorescence Induction and Relaxation (FIRe 2) system which was installed on the ARAON.

the quantum efficiency of PSII (Fv/Fm), the functional (or effective) absorption cross-section of PSII (σPSII) were measured as described in Kolber et al. (1998). Quantum efficiency of photochemistry in PSII (Fv/Fm) was calculated as a ratio of variable fluorescence (Fv=Fm-F0) to the maximum one (Fm). The fluorescence measurements were corrected for the blank signal recorded from filtered seawater (by 0.2 um syringe filter set).Go-FLO rosette system was operated at the subsurface (ca. 15 m) for the iron assimilation experiment (Fig. 3.7). Seawater samples were kept in 22 liter carboy (triplicate of control and +Fe, respectively), and incubated on the deck (ambient water temperature were controlled) during more than seven days, and changes of photosynthetic parameters were monitored at every day. Moreover, we also observed photosynthetic parameters using pumped seawater through a flow-through cuvette in a fluorometer on deck laboratory of a ship during the cruise and ARAON transit from Incheon to the Amundsen Sea.

Preliminary results

During the on-board incubation, the photosynthetic efficiencies (Fv/Fm) were changed at all stations as time passes on (Fig. 3.8). We could observe that the Fv/Fm values of Fe added samples were significantly different from those of control samples. Also, in case of Fe added samples, the Fv/Fm values were somewhat increased by five or six days and decreased after that time. In case of control samples, the values were also increased during several days at polynya center and open sea stations. However, the values were decreased from the beginning at outer shelf and front of ice shelf stations where the initial values of Fv/Fm were relatively high. The implications are discussed after looking at

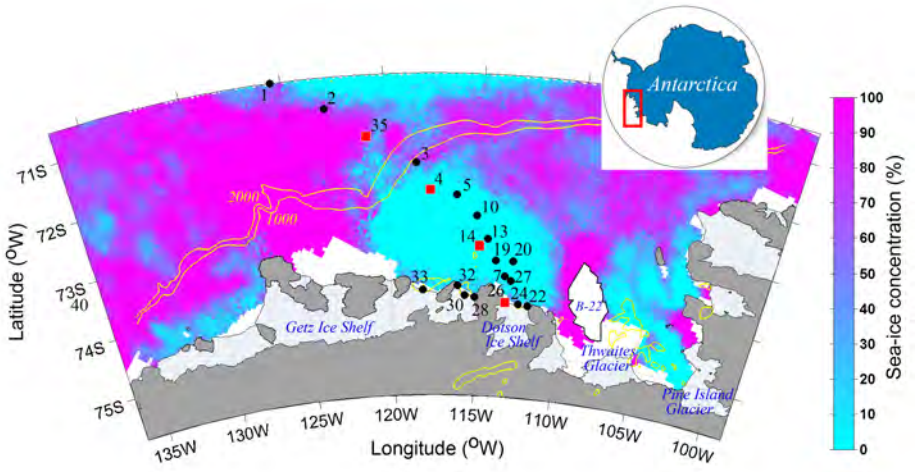

Figure 3.6: Station map during the 2014 Amundsen cruise. Colors represent sea-ice concentration at 10th January. Yellow lines represent bottom topography. Red rectangles indicate the stations where GO-FLO sampler was operated for iron addition experiment.

Figure 3.7: Sampling of metal free seawater using Go-FLO rosette system for iron assimilation experiment.

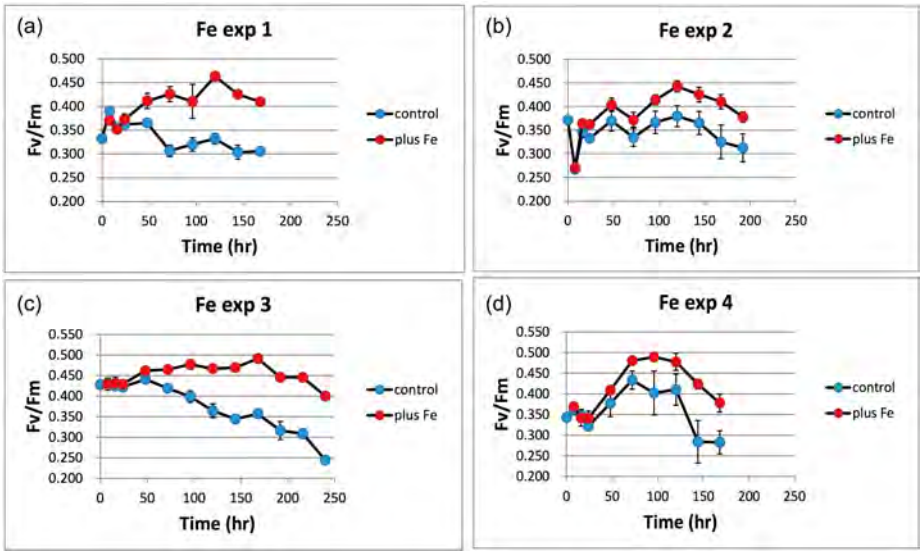

Figure 3.8: Temporal evolution of photosynthetic efficiencies (Fv/Fm) at four iron assimilation stations of the Amundsen Sea during the 2014 cruise. Stations are located at (a) outer shelf (st. 4), (b) polynya center (st. 14), (c) front of ice shelf (st. 26), and (d) open sea (st. 35), respectively.

other environmental parameters such as nutrient concentrations, iron concentrations, and DOC with chlorophyll-a concentrations.

References

Falkowski, P. G. and Z. Kolber (1995). "Variations in chlorophyll fluorescence yields in phytoplankton in the world oceans." Aust. J. Plant Physiol.22(2): 341-355.

Kolber, Z. and P. G. Falkowski (1993). "Use of active fluorescence to estimate phytoplankton photosynthesis in situ." Limnol. Oceanogr.38(8): 1646-1665.

Kolber, Z. S., O. Prasil, et al. (1998). "Measurements of variable chlorophyll fluorescence using fast repetition rate techniques: defining methodology and experimental protocols." Biochimica et Biophysica Acta-Bioenergetics1367(1-3): 88-106.

3.3 Grazing impacts and community structure of heterotrophic protists

Yang Eun Jin, Oh Jin A
Korea Polar Research Institute

요약문

아문젠 폴리니아에서 2014년 1월에 원생동물의 생물량, 군집구조, 식물플랑크톤 및 박테리아에 대한 섭식률 실험을 총 18개 정점에서 수행하였다. 원생동물의 생물량

분포 및 군집구조 분석은 현장에서 고정하여 실험실로 가져간 후 분석 되어질 예정이다. 또한 해수 희석법을 이용하여 측정한 식물플랑크톤과 박테리아에 대한 섭식률 측정은 2010/11년 자료와 비교하여 분석되어질 예정이다.

Background study

Heterotrophic protists ingest a broad size spectrum of prey, from bacteria to microphytoplankton, and are themselves important prey items for mesozooplankton. Many researches suggest that heterotrophic protists contribute to the trophic linkage between phytoplankton and mesozooplankton and are important in the pelagic food webs of many oceanic waters. The importance of heterotrophic protists in pelagic ecosystems has become increasingly evident in the past two decades, and trophic interaction between heterotrophic protists and phytoplankton has been reported in various marine. Studies of protozooplankton in the Southern Ocean have emphasized the importance of protozooplankton in microbial communities and their role as major consumers of phytoplankton (Burkill et al., 1995; Froneman and Perissinotto, 1996; Landry et al., 2001; Pearce et al., 2011; Safi et al., 2007; Selph et al., 2001). Overall, previous research has suggested that knowledge of the structure of the microbial community and protozoan grazing impacts, is central to developing an understanding of carbon flux in the Southern Ocean. However, comprehensive studies on protozooplankton assemblages have been generally limited to the Weddell Sea, Bellingshausen Sea, and the Atlantic and Indian sectors of the Southern Ocean, particularly the marginal ice-edge zone (Froneman et al., 2004; Klass, 1997; Safi et al., 2007). There is no information on the relative importance of heterotrophic protists in the pelagic ecosystem of the Amundsen Sea. The Amundsen Sea, which is historically known as a region of heavy ice, is undergoing sea ice recession within the last decades (Jacobs and Comiso, 1993), and extensive phytoplankton blooms near the coast have been observed (Smith and Comiso,2008). In this study area, we investigated the meso-scale variations and structure of heterotrophic protist communities and grazing rates on phytoplankton in the various environmental conditions such as sea ice zone and polynya. During this cruise, we investigated protozoa abundance, biomass and grazing rate in total18 stations. This data will be compared to ANA01 data set.

Work at Sea

Abundance and community composition of heterotrophic protists

This study was conducted total 18 stations (Fig. 3.9). To determine the abundance of heterotrophic protists, a CTD-Niskin rosette sampler was used to take water samples from the following 6 depths. For ciliates and sarcodina, 1,000 ml water from the vertical profiles was preserved with 1% acid Lugol's iodine solution these samples were then stored in darkness. For heterotrophic nanoflagellates and heterotrophic dinoflagellates smaller than 20 μm, 500 ml of water was preserved with glutaraldehyde (0.5% final concentration) and stored at 4° C.

Grazing experiments

Grazing rates of heterotrophic protists were determined by the dilution method (Landry and Hassett 1982). Water for grazing experiments was collected from 3 depth (surface, SCM, 1% light depth) of each station, and gently

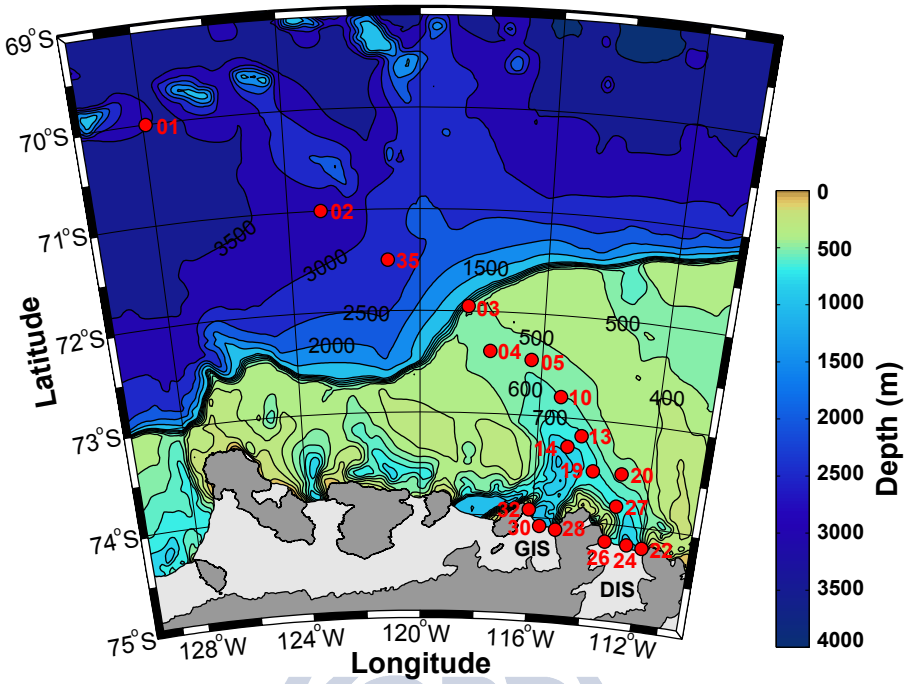

Figure 3.9: The sampling stations of protozoa community and grazing rate

filtered through a 200-μm mesh. At each station, 30L seawater were collected in a Niskin bottle and transferred to a polycarbonate carboy. Part of this water was filtered through the 0.22-μm filtration system. Dilution series were set up in ten 1.3-l PC bottles. Ten bottles were used to establish a nutrient-enriched dilution series consisting of replicate bottles with 11, 28, 50, 75, and 100% natural seawater. The bottles were incubated on deck for 24 – 48 h at ambient sea surface temperatures and screened to the ambient light level with neutral density screening. Subsamples were collected from replicate bottles at 0 and 24-48h to determine chlorophyll-a concentrations and bacterial abundance.

References

Jacobs, S. S., Comiso, J. C. 1993. A recent sea-ice retreat west of the Antarctic Peninsula. Geophysical Research Letters 20: 1171-1174.

Smith, W. O. Jr., Comiso, J. C. 2008. Influence of sea ice on primary production in the Southern Ocean: a satellite perspective. Journal of Geophysical Research 113 doi:10.1029/2007JC004251.

Pearce, I., Davidson, A.T., Thomson, P.G., Wright, S., van den Enden, R., 2011. Marine microbial ecology in the sub-Antarctic Zone: Rate of bacterial and phytoplankton growth and grazing by heterotrophic protists. Deep-Sea Res. Part II. 58, 2248-2259.

Safi, K.A., Griffiths, F.B., Hall, J.A., 2007. Microzooplankton composition, biomass and grazing rates along the WOCE SR3 line between Tasmania and Antarctica. Deep-Sea Res. Part I. 54, 1025-1041.

Selph, K.E., Landry, M.R., Allen, C.B., Calbet, A., Christiansen, S., Bidigare, R.R., 2001. Microbial community composition and growth dynamics in the Antarctic Polar Front and seasonal ice zone during late spring 1997. Deep-Sea Res. Part II. 48, 4059-4080.

Landry, M.R., Brown, S.L., Selph, K.E., Abbott, M.R., Letelier, R.M., Christensen, S., Bidigare, R.R., Casciotti, K., 2001. Initiation of the spring phytoplankton increase in the Antarctic Polar Front Zone at 170°W. J. Geophys. Res. 106(C7), 13,903-13,915.

Froneman, P.W., 2004. Protozooplankton community structure and grazing impact in the eastern Atlantic sector of the Southern Ocean in austral summer 1998. Deep-Sea Res. Part II. 51, 2633-2643.

Landry, M.R., Hassett, R.P., 1982. Estimating the grazing impact of marine microzooplankton. Mar. Biol. 67, 283-288. Froneman, P.W., Perissinotto, R., 1996. Structure and grazing of the microzooplankton communities of the subtropical convergence and a warm core eddy in the Atlantic sector of the Southern Ocean. Mar. Ecol. Prog. Ser. 135, 237-245.

Burkill, P.H., Edwards, E.S., Sleigh, M.A., 1995. Microzooplankton and their role in controlling phytoplankton growth in the marginal ice zone of the Bellingshausen Sea. Deep-Sea Res. Part II. 42, 1277-1299.

3.4 Iron limiting Experiment

Yang, E.J[1], Park, J.S.[1], Hyun, J.H.[2], Jung, J.Y.[1], Ha, S.Y.[1], Lee, D.B.[1], Kim, S.H.[2], Kim, B.K.[3], Oh, J.A.[1]
[1]Korea Polar Research Institute
[2]Hanyang University
[3]Pusan National University

요약문

2014년 1월에 아문젠 폴리니아와 그 주변해역에서 플랑크톤 군집 및 조성에 영향을 미치는 요인중에 하나로 제시되고 있는 철(Fe) 제한 실험을 수행하였다. 총 4회의 실험을 수행하였고, 실험은 폴리니아 중앙수역 (Fe 2), Dotson Ice shelf 앞 (Fe 3) 과 폴리니아 바깥수역인 continental shelf area (Fe 1)와 open sea (Fe 4)에서 수행하였다. 철제한 실험은 3개의 대조구 (control)와 3개의 실험구 (철첨가, 최종 농도 5-10 nM)로 구성되었으며, 8일-10일 동안 표층 해수 펌프 시스템을 사용하여 선상에서 수행되었다. 실험기간 동안 매일 다음과 같은 항목들이 측정되었다: 엽록소-a, 박테리아, 바이러스, 식물플랑크톤, 원생동물, Fv/Fm, HPLC, 영양염, DOC, POC.

Introduction

Iron availability are important limiting factors for the organism in many areas of the world ocean, and it has been predicted to change in future climate scenarios (Rose et al., 2009). During the two decades, iron limitation of Southern Ocean phytoplankton communities has been indicated in numerous shipboard bottle incubation studies (de Baar et al., 1990, 1995; Hutchins et al., 2001; Leblanc et al., 2005) and by mesoscale Fe fertilization experiments (Boyd et al., 2007;

Gervais et al.,2002; Coale et al., 2004). However, Iron (Fe) has been shown to be a limiting nutrient for phytoplankton growth in Southern Ocean, even in the productive continental shelves surrounding the Antarctic continent. In the Ross Sea polynya, the largest and most well studied polynya of the Antarctic, the availability of Fe controls the magnitude of annual primary productivity whereas light availability determines phytoplankton species distribution (Arrigo et al. 2003). Currently, the polynyas of Amundsen Sea has been described as one of the most productive area (Arrigo et al., 2012). However, it is not known that intense and long-lasting phytoplankton bloom are influenced by Fe concentration. However, the objective of this study was to examine changes in plankton community structure and carbon and nutrient biogeochemistry when high concentrations of iron are added in Amundsen Sea polynya. Here we assessed the relative effect of Fe on plankton assemblages in the Amundsen Sea Polynya using controlled Fe addition bioassay experiments in four contrasting regions of the Amundsen Sea over the summer growing seasons

Work at Sea

Experiments were conducted during the Amundsen Sea expedition (ANA04B) in January, 2014, onboard the Araon. Water was collected at four site (Table 3.1) using Teflon-coated Go-Flo bottle. Water was prescreened through acid-washed 200 μm Nitex mesh to eliminate large zooplankton. Collected water dispensed into six 22-L acid washed trace metal clean polycarbonate carboy. Incubation bottles were randomly filled to ensure homogeneity between experimental bottles. Half of the bottles were spiked with 5 10nM FeCl3 (final concentration) at the beginning of the experiment. Experimental manipulations consisted of tree Fe treatment and control treatment(no addition). Temperature in the incubators was controlled by pumping surface seawater through the units that maintained ambient sea surface temperature throughout the experiments. One of the three replicates from each condition spiked with stable isotopes (13C, 15NO3, and 15NH4) to measure phytoplankton production. Incubators were screened 50% of ambient surface irradiance using neutral density film on continuous surface temperature shipboard system. Bottles were incubated for 7-10 days and sampled daily. Daily sampling included total chlorophyll, Fv/Fm, bacteria, virus, HPLC, microzoopolankton, dissolved nutrient, POC, and DOC. Samples for total dissolved iron were taken on the initial and final days of the experiments.

References

Arrigo, K.R., van Dijken, G.L., 2003. Phytoplankton dynamics within 37 Antarctic coastal polynya systems. J. Geophys. Res. 108 (C8), 3271. http://dx.doi.org/:10.1029/2002JC001739.

Arrigo, K.R., Lowry, K., van Dijken, G., 2012. Dynamics of sea ice and phytoplankton in polynyas of the Amundsen Sea, Antarctica. Deep-Sea Res. II 71–76, 5–15.

Boyd, P.W., Jickells, T., Law, C.S., Blain, S., Boyle, E.A., Buesseler, K.O., Coale, K.H., Cullen, J.J., de Baar, H.J.W., Follows, M., Harvey, M., Lancelot, C., Levasseur, M., Owens, N.P.J., Pollard, R., Rivkin, R.B., Sarmiento, J.,

Table 3.1: General information for Fe bioassay experiments.

Exp. no. (station)	Fe 1 (St. 4)	Fe 2 (St. 14)	Fe 3 (St. 26)	Fe 4 (St. 35)
Sampling date	03 Jan., 20:40	07 Jan., 8:30	11 Jan., 10:10	15 Jan., 14:30
Latitude (S)	72° 23.006	73° 16.887	74° 10.456	71° 30.005
Longitude (W)	117° 42.639	114° 56.978	113° 19.724	121° 00.011
Sampling periods	8 days	8 days	10 days	7 days
Temperature (℃)	0.08	-0.31	-0.44	-1.45
Salinity	33.88	33.81	33.83	33.40
Sampling depth (m)	15	15	15	20
Chl-a (ug L^{-1})	7.03	8.28	4.77	1.39
PO_4 (umol kg^{-1})	0.92	1.23	1.55	1.85
NO_3 (umol kg^{-1})	10.46	11.03	18.56	23.87
SiO_2 (umol kg^{-1})	68.46	83.26	83.54	64.60

Schoemann, V., Smetacek, V., Takeda, S., Tsuda, A., Turner, S., Watson, A.J., 2007. Mesoscale iron enrichment experiments 1993–2005: synthesis and future directions. Science. 315 (5812), 612–617.

Coale, K.H., and others. 2004. Southern Ocean Iron Enrichment Experiment: Carbon cycling in high- and low-Si waters. Science 304: 408-414.

de Baar, H.J.W., Buma, A.G.J., Nolting, R.F., Cadee, G.C., Jacques, G., Treguer, P.J., 1990. On iron limitation of the Southern Ocean: experimental observations in the Weddell and Scotia Seas. Mar. Ecol.-Prog. Ser. 65, 105–122.

de Baar, H.J.W., de Jong, J.T.M., Bakker, D.C.E., Loscher, B.M., Veth, C., Bathmann, U., Smetacek, V., 1995. Importance of iron for plankton blooms and carbon dioxide drawdown in the Southern Ocean. Nature 373, 412–415.

Hutchins, D.A., Sedwick, P.N., DiTullio, G.R.B., Boyd,P.W., Que´guiner, B., Griffiths, F.B., Crossley, C., 2001. Control of phytoplankton growth by iron and silicic acid availability in the subantarctic Southern Ocean: experimental results from the SAZ project. J.Geophys.Res.106, 31559–31572.

Gervais, F., Riebesell, U., Gorbunov, M.Y., 2002. Changes in primary productivity and chlorophyll a in response to iron fertilization in the Southern Polar Frontal Zone. Limnol. Oceanogr. 47 (5), 1324–1335.

Leblanc, K., Hare, C.E., Boyd, P.W., Bruland, K.W., Sohst, B.,Pickmere, S., Lohan, M.C., Buck, K., Ellwood, M., Hutchins, D.A., 2005. Fe and Zn effects on the Si cycle and diatom community structure in two contrasting high and low-silicate HNLC areas. Deep-Sea Research I 52, 1842–1864.

Rose, J. M., Y. Feng, G. R. DiTullio, R. B. Dunbar, C. E. Hare, P. A. Lee, M. Lohan, M. Long, W. O. Smith Jr., B. Sohst, S. Tozzi, Y. Zhang, and D. A. Hutchins, 2009. Synergistic effects of iron and temperature on Antarctic phytoplankton and microzooplankton assemblages. Biogeosciences, 6, 3131–3147.

3.5 Distribution of mesozooplankton and metabolism of major copepods and euphausiids

Lee, Doo Byoul
Korea Polar Research Institute, Korea

요약문

남극 아문젠 해역에서 중형동물플랑크톤 분포와 우점 동물플랑크톤이 식물플랑크톤에 미치는 섭식압, 그리고 우점 요각류의 물질대사(호흡률)를 파악하기 위한 현장 조사를 실시하였다. 중형동물플랑크톤 시료는 봉고네트를 이용하여 총 12개 정점에서 채집하였다. 채집된 시료는 연구실에서 분석될 예정이며, 우점 요각류 및 크릴의 섭식량은 gut pigment contents를 분석할 예정이며, 이들의 호흡률은 micro respiration system을 이용하여 측정하였다.

Introduction

Copepods and euphausiids constitute >70 % of the total metazooplankton biomass in Antarctic waters (Mayzaud et al. 2002; Atkinson et al. 2012),

where they play a major role in energy flow and biogeochemical cycles. Some of the ingested organic carbon of zooplankton is used for metabolic activities, so quantifying this carbon is of prime importance to better understand energy transfer and elemental cycling via zooplankton in Antarctic ecosystems. Feeding behavior plays an important role in the adaptive strategies of marine organisms. Feeding is also the main route for the transfer of energy and material from lower to higher trophic organisms within communities and, as such, its quantification is a key factor in understanding trophic interactions. Grazing impact by zooplankton, especially copepods and Euphausiids, is a key factor in controlling composition and dynamics of phytoplankton communities in the Southern Ocean. It has been suggested that zooplankton grazing may at times control phytoplankton composition and the development of such phytoplankton blooms. The primary objectives are (1) to quantify the mesozooplankton community, (2) to understand interactions among the environmental factors, protozoa and mesozooplankton community, (3) to evaluated the grazing impact of major mesozooplankton on the phytoplankton (4) to examine the oxygen consumption rate of the major species with different life cycle strategies using an oxygen microsensor and to compare the results with those obtained in other Antarctic ecosystems.

Material and methods

Field sampling for mesozooplankton

Zooplankton samples were collected with a Bongo net (330 and 500 μm mesh) at 12 selected stations (Table 1). The net was towed twice vertically within the upper 200 m of water column. Tow duration was about 15-20 minutes. Samples from the first tows were immediately fixed and preserved with buffered formaldehyde (pH 8, final concentration ca. 5%) for quantitative analyses. From the second-towed samples, healthy individuals were transferred to 10 l polycarbonate carboys filled with natural seawater. The animals were transferred into 20 ml vials containing filtered seawater. These vials were frozen at -80°C deep freezer for the gut content analyses.

Preparations for measurement of respiration rate

Undamaged healthy adult females of each copepod species and E. crystallorophias were immediately sorted and transferred into 2.6 l polycarbonate bottles where they were acclimated for a few hours in 200-μm prescreened natural seawater at in situ temperatures. Each individual was placed in a 4 ml BOD-style glass micro respiration chamber filled with 0.45 μm filtered seawater in a dark room. The chamber was equipped with capillary pores to allow access for the oxygen microsensor. The pore size was sufficiently small to minimize gas and liquid exchange. I allocated just one individual animal per each experimental chamber to examine the individual variation in respiration. Control chambers containing only 0.45 μm filtered seawater without any animals were set up alongside the experimental chambers. All chambers were dark incubated for up to 6 h in a water bath under the in situ seawater temperature.

Measurement set-ups

Respiration rate was monitored with a Micro respiration system (Unisense A/S, Denmark), which allows continuous recording of dissolved oxygen (DO) concentration with a time interval between consecutive measurements of 10 s. Measurements of DO concentration were made using Clark-type oxygen micro-

electrodes (Revsbech 1989) with a 500-μm diameter tip connected to a picoammeter. Microelectrodes were calibrated using a two-point procedure with 0 % (bubbling with nitrogen) and 100 % (bubbling with air) saturation DO concentrations as endpoints. The respiration chambers rested in a submerged rack in a temperature-controlled water bath. Both control and experimental chambers were equipped with glass-coated mini magnetic stirrers rotating at 500 rpm to prevent oxygen gradient development. Animals were protected from interference with the stirrers by acid-proof stainless steel mesh dividers (200 μm) resting on glass cylinders. Individual stirrer heads were located in the rack directly underneath the chambers and did not emit heat. Moreover, magnet rotation did not alter the animals' swimming or position in the chamber. Animals were allowed to acclimate for 10 min following transfer into the chambers, after which the oxygen consumption rate was taken as the linear slope of the DO concentration plotted against time for the next several hours. The short incubation times minimized the problem of oxygen depletion at the end of the incubation.

References

Atkinson A, Ward P, Hunt BPV, Pakhomov EA, Hosie GW (2012) An overview of Southern Ocean zooplankton data: abundance, biomass, feeding and functional relationships. CCAMLR Sci 19:171–218.

Mayzaud P, Razouls S, Errhif A, Tirelli V, Labat JP (2002) Feeding, respiration and egg production rates of copepods during austral spring in the Indian sector of Antarctic Ocean: role of the zooplankton community in carbon transformation. Deep Sea Res I 49:1027–1048.

Revsbech NP (1989) An oxygen electrode with a guard cathode Limnol Oceanogr 34:474–478

3.6 Bacteria

Hyun, Jung-Ho; Kim, Sung-Han
Department of Marine Sciences and Convergent Technology Hanyang University, Korea

요약문

남극 아문젠해의 아문젠 polynya(AP)의 outer-shelf, polynya 및 ice-shelf에 위치한 연구정점들에서, 수층의 물리-화학-생물 요인의 변화에 따른 박테리아의 생체량 및 미생물 호흡율 변화양상을 규명하기 위한 연구를 수행하였다. 호흡율은 polynya (51–138 mmol $m^{-3}d^{-1}$)가 outer shelf (27–72 mmol $m^{-3}d^{-1}$), ice-shelf (14–42 mmol $m^{-3}d^{-1}$) 및 외양역(16–18 mmol $m^{-3}d^{-1}$)에 비해 높은 값을 나타냈다. 폴리냐 중앙부의 높은 호흡율(60 mmol $m^{-3}d^{-1}$)은 같은 정점의 표층에서 관측 된 이산화 탄소의 높은 분압(235 μ atm)에 영향을 미친 것으로 인식된다. 이는 미생물의 호흡이 아문젠 폴리냐의 탄소순환을 조절하는 중요한 생물요인임을 나타내는 것이다. 향후 식물플랑크톤 bloom의 시기에 따른 미생물 요인의 시 계열 분석을 통해, 미생물 호흡이 아문젠 폴리냐의 탄소순환에 미치는 영향 및 아문젠 폴리냐가 남극해의 해양-대기간 탄소순환을 조절하는 역할에 대한 정보가 획득 될 수 있을 것으로 전망된다. 한편, 미생물 생체량 분포 및 미생물 생장조절 요인을 파악하기 위한 다양한 실험들(UV 효과, 생장제한 영양요인 등)을 선택된 연구 정점들에서

추가적으로 실시하였으며, 추후 연구실에서의 분석을 위해 확보된 시료들을 냉장 또는 냉동상태로 보관하였다.

Background

Respiration represents the transfer of carbon from organic pool to inorganic pool, and reflects the rate of organic matter supply that is available to the biota within the system (Jahnke and Craven, 1995). Long-term shifts in respiration have a potential to provide the best warning system for global change (del Giorgio and Williams, 2005). Therefore, it is particularly important to measure the respiration in polar ocean to better understand any shifts in biogeochemical carbon cycles associated with large-scale climate changes.

Work at sea

During this cruise, we measured the plankton community respiration rates and bacterial abundance at 4 different sites, polynya, outer shelf, ice-shelf and offshore. Water samples were collected using a Sea-bird Electronics CTD system equipped with specific sensors such as photosynthetically active radiation (PAR) sensor, fluorometer, transmissometer and dissolved oxygen meter. Water samples for bacterial abundance were fixed with glutaraldehyde (final concentration, 1%) and kept in the freezer for cell enumeration in the lab. Respiration rates were measured onboard from the decrease of dissolved oxygen concentration during incubation using a spectrophotometeric-Winkler method (Labasque et al. 2004). Briefly, water samples were taken using 20-l Niskin bottles at 3 – 5 different water depth in the surface layer, and were then transferred into six 300-ml BOD bottles (Wheaton Co.) that were washed and rinsed with acid (10% HCl) and distilled water, respectively. The BOD bottles were filled using a silicon tubing inserted almost to the bottom, and overflowed by at least one bottle volume. The BOD bottles were then wrapped with aluminum foil, and incubated for 20 – 25 hours in the dark in incubator through which in situ seawater continuously flowed. At the end of incubation, BOD bottles were immediately fixed by adding 2 ml of manganese chloride solution (3 M) and 2 ml of alkaline iodide reagents (NaOH, 8 M; NaI, 4 M). After being vigorously shaken for about 1 min, the BOD bottles were stored in the dark. When most of the flocculation had settled, the bottles were reopened and 2 ml of sulfuric acid solution (10 M) was added. The mixture was then gently stirred with a magnetic stirrer until all the precipitate had dissolved. Absorbance was measured onboard within 3 min using a Shimadzu UV-1700 spectrophotometer. The spectrophotometric Winkler method has a precision of 0.1% for the onboard measurement. Respiration rates were calculated from the linear regression of time-course measurement of dissolved oxygen concentration with time.

Preliminary results

Vertical profiles of microbial community respiration measured at offshore, outer shelf (i.e., polynya margin), polynya center and ice shelf sites are presented in Fig. 3.10. Respiration rates at polynya (0.797 – 60.005 mmol $m^{-3}d^{-1}$) were higher than those measured at outer shelf (0.715 – 16.025 mmol $m^{-3}d^{-1}$), ice-shelf (1.087 – 10.500 mmol $m^{-3}d^{-1}$) and offshore sites (4.656 – 8.455 mmol

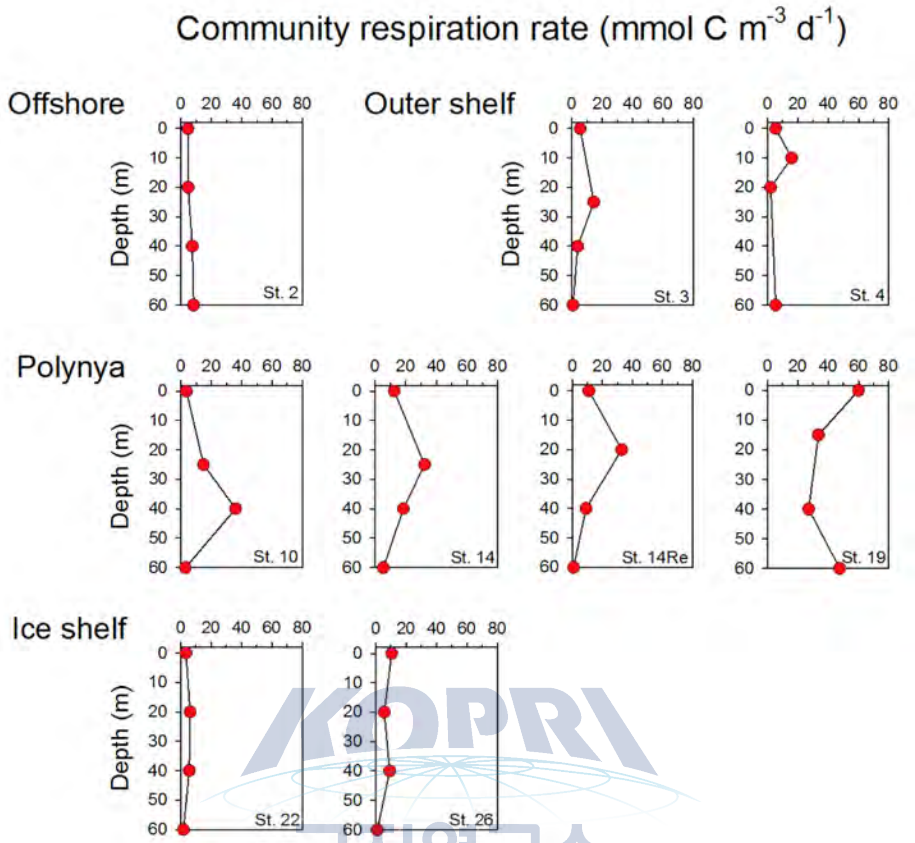

Figure 3.10: Vertical profiles of microbial community respiration rates measured at open sea, sea-ice zone (outer shelf), polynya and ice-shelf sites. Note that respiration rates were highest at polynya.

$m^{-3}d^{-1}$). Highest community respiration observed at the center of the polynya (60 mmol $m^{-3}d^{-1}$ at St. 19) at late stage of the bloom, seems to be responsible for the elevated fCO_2 (235 μatm). The results indicated that time series investigation on the community respiration according to the bloom stage may provide certain information on the biogeochemical C cycles associated with microbiological process and on the role of the Amundsen polynya as either C sink or source for atmospheric CO_2. Other parameters associated with the community respiration such as bacterial abundance, DOC and cDOM will be presented after completing further analyses in the lab.

References

del Giorgio, P. A. and Williams, P. J. le B., 2005. The global significance of respiration in aquatic ecosystems: from single cells to the biosphere. In: P.A. del Giorgio and P. J. le B. Williams (eds) respiration in aquatic ecosystems. Oxford University Press, New York, pp. 267-303.

Jahnke, R. A. and Craven, D. B., 1995. Quantifying the role of heterotrophic

bacteria in the carbon cycle: a need for respiration rate measurements. Limnology and Oceanography. 40: 436-441.

Labasque, T., Chaumery, C., Aminot, A., and Kergoat, G., 2004. Spectrophotometric Winkler determination of dissolved oxygen:re-examination of critical factors and reliability, Marine Chemistry, 88, 53-60.

3.7 Viral ecology in the Amundsen Sea

Chung Yeon Hwang, Yirang Cho
Korea Polar Research Institute, Incheon 406-840, South Korea

요약문

바이러스는 열대에서 극지역에 이르는 모든 해양 생태계에서 가장 많은 개체수로 출현하는 구성원이다. 생지화학적 순환에서 바이러스는 입자성 유기물인 숙주를 용균시켜 용존성 유기물을 증가시키며, 숙주에 포함되어 있는 영양염을 해수로 용출시켜 재순환시키는 역할을 담당한다. 이러한 바이러스 분지(viral shunt)는 식물 플랑크톤 또는 미생물에 의해 표층에서 고정된 탄소를 심층으로 침강시키는생물학적 펌프(biological pump)의 효율을 변화시킬 수 있다. 또한 해양 바이러스는 생태적으로 중요한 유전자(예를 들면, 광합성, 인산염신진대사)를 이동시키는 등바이러스-숙주 상호간의 생태 진화에서도 중요한 역할을 담당하는 것으로 알려져 있다.본 탐사에서는 아문젠해 폴리냐 및 인근 해역에 출현하는 바이러스의 개체수와 생산력을 측정하여 연구 해역의 미생물 먹이망(microbial loop) 특성을 보다 자세하게 이해하고자 하였다. 또한 획득된 DNA/RNA 바이러스 메타게놈자료는 높은 일차 생산력을 보이는남극 폴리냐 바이러스의 군집 구조를 최초로 밝힐 것으로 여겨진다.

Abstract

Viruses are the most abundant entities in marine environments extending from tropical to polar regions. In the biogeochemical cycle, viruses play vital roles in the production of dissolved organic matters (DOM) and increase regeneration of nutrients by destruction of their hosts formed in particulate.This process, viral shunt, mayalterthe efficiency of the biological pump in transporting carbon from the surface ocean to depth.In addition, marine viruses play important roles in eco-evolution of virus-host dynamics by transferring ecologically critical genes such as photosynthesis-related and phosphate metabolism.During the cruise, viral abundance and productions were investigated in the Amundsen polynya and its vicinity for better understanding the microbial loop of the study area.DNA/RNA virus metagenomes, for the first time,will unveil the viral community in a highly productive area of the Antarctic polynya.

Introduction

Viruses are ubiquitous in marine ecosystems and significantly influence the production of DOM and the recycling of nutrients by viral lysis of host organisms (Fuhrman, 1999). Despite their abundance and ubiquity, the study of Antarctic viral ecology is still in its infancy with only a limited number of studies addressing either virus mediated mortality or virus production (Guixa-Boixereu et al.,

2002; Evans et al., 2009) and no study on marine virus community to date.The limited studies showed that virally mediated mortality accounted for a quarter to all of the bacterial productions in waters adjacent to the Antarctic Peninsula (Guixa-Boixereu et al., 2002) and in the Polar Frontal zone of the Australian sector of the Southern Ocean (Evans et al., 2009).Furthermore, contributions of lytic and lysogeny virus productions, major pathways of viral replications, have been not assessed in summer Antarctic Oceans nevertheless UV is an effective agent of lysogeny induction (Jiang & Paul, 1996). During the cruise, 3 independent approaches to measure viral production were employed in order to accuratelyestimate viral impacts on microbial mortality along with estimating the significance of lysogeny in the Amundsen Sea.

Materials and methods

Seawater sampling for microbiological study was made at 19 stations (including 4 revisiting stations)during the icebreaker R/V Araon expedition (ANA04B) in the Amundsen Sea (Fig. **??**). Water samples were obtained from 6-15 depths, using 10 L Niskin bottles mounted on a conductivity-temperature-depth profiler (CTD; SBE 911plus, Sea-Bird Electronics) rosette. For measurement of viral (VA) and bacterial abundance (BA), seawater samples (0.7-4.9 ml) were fixed with 0.02 μm filtered formalin (final conc. of 2%), and were filtered through 0.02 μm pore size Anodisc filters (Whatman). Filters were then laid on a drop of 100 μl of diluted SYBR Gold (final dilution, 2.5 $\times$ 103-fold; Noble & Fuhrman, 1998) for 15 min in the dark. For measurement of viral production (VP), 3 different assays were used including viral decay (VD), VP based on transmission electron microscopy (VPTEM) and virus reduction (VR) experiments. (1) VD was determined by the cyanide-inhibition method of Heldal & Bratbak (1991). (2) Samples for VPTEM were preserved with electron microscope grade glutaraldehyde (final conc. 2%) and immediately frozen in -80°C in the dark until analyses.Frequency of visibly infected cells and burst sizes will be measured as described previously (Hwang & Cho, 2008). (3) VR experiments were performed as described by Evans et al. (2009) using a tangential flow filtration system (Fig. **??**a). Lysogeny induction experiments were made for virus reduced samples and intact samples with amendment of mitomycin C (final conc. 1 μg ml-1; Weinbauer et al., 2003). Each sample for virus metagenome (virome), from 30-95 L of seawater, was pre-filtered by a 1.6 μm 150 mm GF/A filter followed by a 0.22 μm, 142 mm diameter nitrocellulose membrane filter (Merck Milipore Ltd) using a large volume seawater filtration system (Fig. **??**b). All filtrates were concentrated by the FeCl3-precipitation method (John et al., 2011). DNA and RNA virome analysis will be made according to the protocols of Duhaime et al. (2012) and Steward & Culley (2010), respectively.

Preliminary results

Preliminary results of viral ecology were not available on aboard since further analyses need to be made in a land-based laboratory. However, it is expected that viral distribution and production in the study area may reveal spatial variability along with a trophic gradient based on chlorophyll a concentrations.DNA/RNA virus metagenomes are also expected to provide new insights into roles of viruses in a highly productive area of the Antarctic polynya.

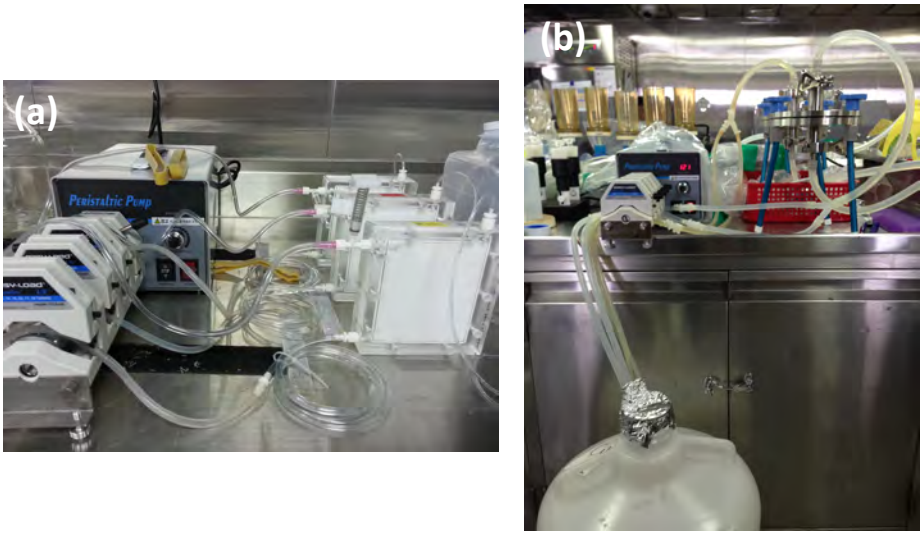

Figure 3.11: Photos of (a) a tangential flow filtration system and (b) a large volume seawater filtration system used in the present study.

References

Duhaime, M.B., Deng, L., Poulos, B.T. and Sullivan, M.B., (2012) Towards quantitative metagenomics of wild viruses and other ultra-low concentration DNA samples: a rigorous assessment and optimization of the linker amplification method. Environmental Microbiology, 14, 2526-2537.

Evans, C., Pearce, I. and Brussaard, C.P.D., (2009) Viral-mediated lysis of microbes and carbon release in the sub-Antarctic and Polar Frontal zones of the Australian Southern Ocean. Environmental Microbiology, 11, 2924-2934.

Fuhrman, J.A., (1999) Marine viruses and their biogeochemical and ecological effects. Nature, 399, 541-548.

Guixa-Boixereu, N., Vaqué, D., Gasol, J.M., Sánchez-Cámara, J. and Pedrós-Alió, C., (2002) Viral distribution and activity in Antarctic waters. Deep Sea Res Part II, 49, 827-845.

Heldal, M. and Bratbak, G., (1991) Production and decay of viruses in aquatic environments. Mar Ecol Prog Ser, 72, 205-212.

Hwang, C.Y. and Cho, B.C., (2008) Effects of storage on the estimates of virus-mediated bacterial mortality based on observation of preserved seawater samples with TEM. Aquat Microb Ecol, 52, 263-271.

Jiang, S.C. and Paul, J.H., (1996) Occurrence of lysogenic bacteria in marine microbial communities as determined by prophage induction. Mar Ecol Prog Ser, 142, 27-38.

John, S.G., Mendez, C.B., Deng, L., Poulos, B., Kauffman, A.K.M., et al. (2011) A simple and efficient method for concentration of ocean viruses by chemical flocculation. Environmental Microbiology Reports, 3, 195-202.

Noble, R.T., and Fuhrman, J.A., (1998) Use of SYBR Green I for rapid epifluorescence counts of marine viruses and bacteria. Aquat Microb Ecol, 14, 113-118.

Steward, G.F. and Culley, A.I., (2010) Extraction and purification of nucleic acids from viruses.Manual of Aquatic Viral Ecology, 16, 154-165.

Weinbauer, M.G., Brettar, I. and Höfle, M.G., (2003) Lysogeny and virus-induced mortality of bacterioplankton in surface, deep, and anoxic marine waters. Limnol Oceanogr, 48, 1457-1465.

3.8 Samplings for metagenomic analysis of microbial community

Rhee, Sung-Keun; Kim, Jong Geol
Chungbuk National University

요약문

서남극해의 아문젠해역 폴리냐는 전세계 어느 지역보다 1차 생산성이 높은 흥미로운 생태계환경이다. 2011-2012년 탐사를 통하여 식물플랑크톤과 연관된 미생물의 조성과 다양성에 대한 연구가 이루어졌다. 2014년 연구탐사를 통하여 이들 미생물의 기능(플랑크톤 유래의 폴리머 분해, DMS등 가스물질 전환, 광이용성, 질소순환, 황순환, 등)에 대한 심도 있는 유전자 수준의 연구를 위하여 메타지놈(Metagenome)분석을 위한 시료 채취를 실시하였다. 2012년 샘플링 시기는 식물플랑크톤 성장의 후반부에 해당하는 반면, 2014년 탐사시기는 식물플랑크톤의 최대 성장기에 해당한다. 따라서, 식물플랑크톤 증식시기에 따른 미생물 메타지놈 비교분석연구에도 동시에 활용하고자 한다. 이를 위하여 폴리냐 센터를 중심으로 표층 클로로필 최대 깊이에서 약 40 리터의 물로부터 미생물 바이오매스를 회수하였다. 회수된 미생물은 핵산추출을 위하여 -80C에 보관하였다. 폴리냐에서 식물플랑크톤의 성장시기와 세균의 조성에 영향을 미칠 것으로 추정되는 바이러스의 분리/특성연구를 위한 시료를 확보하였다: 1) Flavobacteria 및 Gammaproteobacteria 분리를 위하여 각 정점 및 깊이에서 해수 2리터를 냉장보관하였다. 2) 접종에 이용할 바이러스 시료를 확보를 위하여 2리터의 해수로부터 30 kDa 필터를 이용하여 바이러스를 농축하여 -80C에 냉동보관하였다.

Introduction

Most pelagic communities in polar seas are seasonally covered with sea-ice, and ice-free sections, called 'polynyas', regularly develop due to non-uniform melting of the sea-ice pack. Particularly, emphatic influences of solar radiation, nutrients, and temperature in polynyas merge to create strong phytoplankton blooms. In fact, polynyas of the Amundsen Sea are regarded as one of the most biologically productive regions (reaching up to 160 g Cm-2) in the world's oceans, and are an ecological hotspot in the Antarctic ocean (Arrigo and van Dijken, 2003). The high productivity coupled with the formation of Antarctic bottom water contributes formation of organic rich deep water, and thus, biological carbon sequestration. They also release heat and moisture to the atmosphere, and are an exchange site for greenhouse and ozone-depleting gases (N2O, CH4, DMS etc.,) between the atmosphere and the ocean in the Antarctic. Bacteria are abundant, and are involved in many biogeochemical cycles and food webs and undergo great seasonal variations in polar oceans. Activity of these cold-adapted Bacteria is

associated with remineralization of fixed carbon, and thus, contributes to the efficiency of carbon sequestration in high latitudes. Association of heterotrophs, including members of Cytophaga-Flavobacteria-Bacteroides, Gammaproteobacteria, and Alphaproteobacteria, with phytoplankton blooms were reported (Kim et al., 2003) in a polynya of Amundsen oceans. In order to understand the functional roles of prokaryotes in polar oceans, the detailed revelation of metagenome information is pre-requisite. In antarctic polynyas, the metagenomic analysis of procaryotes successionally associated with phytoplankton blooms has been rare (Teeling et al 2013). Top-down control by viral predation is involved in bacterial population dynamics and activities (Avrani et al 2012). Here, our aims of this cruise were 1) to collect biomass of procaryotes for metagenomic analysis of microbial functional succession in a polynya of the Amundsen Sea using next generation sequencing technologies and 2) to collect samples for isolation of dominant bacterial hosts and their viral predators. The results obtained from these studies will be crucial for understanding the biogeochemical cycles involved in the polynya bloom and concurring greenhouse gas dynamics, which will give insight into climate change in the Antarctic area.

Preliminary results

Water samples from stations at a polynya (polynya center and margins), sea-ice, and ice-free open oceans were collected during the expedition, between 1 and 16 January, 2014.

- For collection of large prokaryotic cell masses, peristaltic pump-based high throughput filter system (Millipore) with 147 mm diameter filter was used. Above 40 liters of seawaters were used for filtration of biomass in subsurface chlorophyll maximum (SCM) zones at key stations. After removal of detritus using 3 um filters, planktonic bacteria were collected with 0.2 um filters. In two hours, the process of sample collection was finished and the filters were stored at -70C in deep freezer until metagenomic DNA/RNA extraction.

- For isolation of dominant copiotrophic heterotrophic bacteria which will be used as virus isolation hosts, vertical water samples (2 liter each) were collected at each station. The samples were stored at 4C refrigerator.

- For isolation of viruses infecting dominant heterotrophic bacteria, viral particles were concentrated from vertical water samples. The filtrate of 0.2 um filter obtained during bacterial cell harvest was used as bacteria-free virus samples. Two protocols were used for viral particle concentration from the bacteria-free waters. 1) FeCl3 were added into the bacteria-free seawater to co-precipitate viral particles. The precipitate was harvested using 0.8 um filter (Millipore System). The filters were stored at -80C in deep freezer. 2) Tangential flow ultra-filtration system was used for directly concentrating the viral particles. The pore size of the ultra-filtration system was 30 kDa. The virus concentrates were frozen at -80C in deep freezer.

The summary table of sampling information is attached below:

Table 3.2: Summary of sampling data for metagenomes analysis and virus isolation

Stations (Date)	Metagenome (vol)	Virus (vol)	Bacteria (vol)
1 (Jan-01)	SCM (20 l) (5, 0.2)*	SCM,2000,Bot (2 l) (0.2, Fe)*	
2 (Jan-01)		SCM. 1,500 (2 l) (0.2, Fe)	SCM. 1,500 (2 l)
3 (Jan-02)		SCM. 450 (2 l) (0.2, Fe)	SCM. 450 (2 l)
4 (Jan-03)			SCM. 450 (2 l)
8 (Jan-05)	SCM (40 l) (3, 0.2)	SCM (2 l) (0.2, Fe)	SCM (2 l)
10 (Jan-05)	SCM (40 l) (3, 0.2)	500 (2 l) (0.2, Fe)	SCM. 500 (2 l)
14 (Jan-06)	SCM (40 l) (3, 0.2)	SCM. 330 (2 l) (0.2, Ultra)	SCM. 300 (2 l)
19 (Jan-08)	SCM (40 l) (3, 0.2)	SCM. 300 (2 l) (0.2, Ultra)	SCM (2 l)
24 (Jan-09)	SCM (50 l) (3, 0.2)	SCM. 350 (2 l) (0.2, Ultra)	SCM (2 l)
27 (Jan-10)	SCM (40 l) (3, 0.2)	SCM. 300 (2 l) (0.2, Ultra)	SCM (2 l)
32 (Jan-12)	SCM (40 l) (3, 0.2)	SCM. 300 (2 l) (0.2, Ultra)	SCM (2 l)
35 (Jan-15)	2,700 (50 l) (3, 0.2)		
2-rev (Jan-15)	3,200 (70 l) (3, 0.2)	700. 3,200 (2 l) (0.2, Ultra)	3,200 (2 l)

*Filters used for preparation of samples. The pore sizes of two successive filters were indicated within parenthesis. Fe and Ultra mean iron precipitation (0.8 um pore size filter) and ultrafilteration (30 KDa pore size) for harvest, respectively.

References

1. Arrigo, K.R., and van Dijken, G.L. (2003) Phytoplankton dynamics within 37 Antarctic coastal polynya systems. J Geophys Res 108: 3271.

2. J.-G. Kim, S.-J. Park, I.-T. Cha, S.-J. Kim, K.-H. Kim, E.-J. Yang, Y.-N. Kim, S.-H. Lee, S.-K. Rhee (2013) Unveiling abundance and distribution of planktonic Bacteria and Archaea in a Polynya in Amundsen Sea, Antarctica Environ Microbiol. Online accepted.

3. Teeling H. et al. (2012) Substrate-controlled succession of marine bacterioplankton populations induced by a phytoplankton bloom Science 336, 608

4. Avrani S, Wurtzel O, Sharon I, Sorek R & Lindell D (2013) Genomic island variability facilitates Prochlorococcus–virus coexistence. Nature 474: 604-608

3.9 Trophic relationships between potential organic matter sources and microzooplankton

E.J. Choy
Korea Polar Research Institute, Incheon, 406-840, South Korea

요약문

서남극 아문젠 해역의 다양한 해역에서 중형동물플랑크톤의 먹이습성관계를 안정동위원소추적자를 이용하여 파악하기 위해서 중형동물플랑크톤과 잠재기원유기물질을 채집하였다. 그리고 동물플랑크톤의 잠재기원유기물질의 아문젠 해역에서의 분포특성과 공간분포의 차이를 이해하기 위해서 유기입자물질을 분석하기위한 시료처리를 하였다. 이러한 분석결과가 향후 급변하는 서남극 아문젠 해역에서 물질순환에 관여하는 먹이습성과 유기입자물질의 거동을 파악하는데 중요한 정보를 제공할 수 있을 것이라 판단된다.

Abstract

Microzooplankton and the potential organic matter sources were collected to understand the trophic feeding relationships using the stable isotope tracers along the oceanographical gradients in Amundsen areas. And also to understand the spatial variations and the composition of the potential organic matter sources supporting the suspended organic matters, the water samples also were collected and treated. This data can give an information to understand the feeding relationships in relation to the material cycles and energy flows of microzooplankton and the fate of organic matter sources according to the rapid ecosystem changes in Antarctic Amundsen areas.

Introduction

Polynya ecosystems are the most productive in polar region. The Amundsen sea coastal polynya is the one of the most productive regions. The thinning of the ice sheets around the Amundsen sea has been reported. It is important to understand the fate of the organic matters relating the biogeochemical processes and primary food sources to microzooplankton according to the rapid ecosystem changes by the intrusion of warm Circumpolar Deep water

Characterizing pathways of energy flow is central to understanding the marine ecosystems. The Stale isotope methods are increasingly used as tracers to study material transport in food webs. The analysis of the stable isotopes of carbon and nitrogen can provide indications on the origin of organic matter sources and further flows through the food web (Fry and Sherr, 1984; Michener and Schell, 1994). Slight enrichment of heavier isotopes in the tissues of organisms during the course of metabolism occurs, and these metabolic fractionations are predictable (0.8‰ for carbon, Fry and Sherr, 1984; 2–5‰ for nitrogen, Vander Zanden and Rasmussen, 2001; McCutchan et al., 2003). Stable isotopes have therefore proven to be a powerful tool in the interpretation of food actually assimilated by consumers over time.

Microzooplankton, which are the primary link between primary producers and the consumers in the oceans, are omnivores capable of utilizing the allochthonous and autochthonous carbon sources (Kleppel, 1993). In order to understand the organic matter sources supporting the microzooplankton and the composition of the organic matter sources along the oceanographical gradients (open ocean – polynya - ice shelf) in Amundsen sea, the samples were collected during the 2014 expedition (ANA04B). The purpose of the sample treatments are :

- To understand the trophic relationships between the potential organic matter sources and microzooplankton along the oceanographical gradients (open ocean-polynya-ice shelf) in Amundsen sea, Antarctica using stable isotope tracers.
- To identify the spatial variation of the particulate organic matter sources along the oceanographical gradients in Amundsen sea, Antarctica using stable isotope tracers.

Materials and methods

Microzooplankton samples were taken during austral summer along the open ocean and Amundsen polynya and ice shelf. Specimens were collected a using a 300mm mesh Bongo net. Phytoplankton samples were obtained by vertical net using 20 mm mesh phytoplankton net. To remove carbonates were quickly acidified (1M HCl) and rinsed with Milli-Q water, freeze-dried and then kept at 20°C until analysis. About 20 l of water were sampled at a depth of about 5 m below the water surface and sieved through a 300-μm mesh net to remove zooplankton and large particles. For chlorophyll a (chl a), Particulate organic carbon and nitrogen (POC/PON), and stable carbon and nitrogen analysis of seston, duplicate water samples were immediately filtered on pre -combusted Whatman GF/F glass fiber filters (47 mm), kept frozen in dry ice (20 °C), and transported to the laboratory.

References

Fry, B., Sherr, E.B., 1984. δ^{13}C measurements as indicators of carbon flow in marine and freshwater ecosystems. Contributions in Marine Science 27, 1347.

Klepple, G.S., 1993. On the diets of calanoids copepods. Marine Ecology Progress Series 99,183195.

McCutchan, J.H., Lewis, W.M., Kendall, C., McGrath, C.C., 2003. Variation in trophic shift for stable isotope ratios of carbon, nitrogen and sulfur. Oikos 102, 378390.

Vander Zanden, M.J., Rasmussen, J.B., 2001. Variation in δ^{13}C and δ^{15}N trophic fractionation, implications for aquatic food web studies. Limnology and Oceanography 46, 20612066.

3.10 Acoustic observation of krill distribution along the ice shelves

H.S. La
Korea Polar Research Institute, Incheon 406-840, South Korea

요약문

아문젠 해역의 대표적인 빙붕인Dotson과 Getz 빙붕에서 크릴 분포의 변동성을 파악하기 위한 음향조사를 실시하였다. 음향시스템은아라온에설치된과학어군탐지기 (scientific echo sounder) EK60을사용하였으며 3개의주파수 (38, 120, 200 kHz)를이용하여표층에서수심500 m까지데이터를수신하였다.음향 신호에 영향을 미치는 생물을 확인하기 위해서 관측 지역내 7 정점에서 사각 네트 (Rectangular net)를 이용하여 사선 채집 (Oblique sample)을 실시하였다.관측 결과 아이스 크릴 (Ice krill, Euphausia, crystallorophias)이 우점하였으며 현장에서 약 2000개체의 길이 (body length/ total length) 분포를 측정하였다.아이스 크릴의 길이는 최소 4 mm에서 최대 31 mm의 범위에서 분포하였으며 평균 길이는 12.5mm (표준편차: 5.9 mm)로 측정되었다. 본 레포트에서는 120 kHz 에코그램으로부터 Dotson과 Getz 빙붕에서 관측된 음향 산란층의 분포 특성을 확인하였다. Dotson 빙붕에서는 주요 음향 산란층이 100-300 m수심에서 확인된 반면 Getz 빙붕과 그 외 지역에서는 100-300 m 수심 뿐만 아니라 표층-100m 수심에서도 높은 음향 산란층을 확인할 수 있었다. 향후, 두개 주파수 (38와 120 kHz)의 음향강도 차를 이용하여 아이스 크릴 밀도의 변동성을 파악할 예정이며 밀도 변동성에 영향을 미칠 수 있는 두 빙붕의 해양환경 특성을 파악하고자 한다.

Abstract

Acoustic survey was conducted to understand the variability of krill distribution along two representative ice shelves in the Amundsen Sea: Dotson ice shelf (DIS) and Getz ice shelf (GIS).Acoustic data were collected from surface to 500-m depths using a scientific echo sounder (EK60, Simrad) configured with down-looking 38, 120, and 200 kHz split-beam transducers mounted in the hull of IBRV Araon. The rectangular net was hauled to obtain the length-frequency distribution of dominant species, which can affect the distribution of sound scattering layer. Euphausia crystallorophias (ice krill) was predominant species and mean body length was 12.5 mm (SD: 5.9 mm) ranged from 4 to 37 mm. In this report, 120-kHz echogram shows the horizontal and vertical variability of acoustic signals between DIS and GIS. Around DIS, the strong sound scattering layer was mainly detected above 100-m depth, while this was distributed not only above 100-m depth but also below 100-m around GIS. Further study will be investigated to reveal variability of ice krill density associated with different environmental conditions between DIS and GIS.

Introduction

The DIS and GIS, two representative ice shelves in the Amundsen Sea coastal polynya, have dramatically thinned during the past two decades: the elevation have been changed 36 ±2 cm year-1and –17±6 cm year-1from 1992 to 2001 (Shepherd et al., 2004).This rapid ice-shelf thinning is linked to basal melting by the intrusion of warm Circumpolar Deep Water (CDW) (Walker et al., 2007; Wahlin et al., 2010). During the two Amundsen Sea expeditions (ANA01C and ANA02C), we found that ice shelf is one of main habitats for ice krill and high density of ice krill was distributed within coastal polynya. Interestingly, two closed ice shelf showed different environmental condition, as well as ice krill density was highly different that the higher density was represented around GIS than that around DIS (La et al., 2013 submitted). In order to understand krill distribution along two different ice shelves related to physical and biological processes, shipborne measurements were conducted during the 2014 expedition (ANA04B). The overall purposes of acoustic observation are:

- To identify the horizontal and vertical distribution of krill from DIS to GIS,
- To reveal the main forcing that affects the variability of krill distribution,

Materials and methods

Acoustic survey was conducted along ice shelf: DIS, GIS A, and GIS B (Fig. 3.12). Acoustic data were collected using a multi-frequency echo sounder (EK60, Simrad) configured with down-looking 38, 120, and 200 kHz split-beam transducers mounted in the hull of the IBRV Araon. Because of stability of the acoustic data, confined data with ship speed below 10 knots were used. In order to avoid any signal interference with other acoustic systems, a synchronization unit was used during the entire running time.

Acoustic data sampled were compressed using virtual echogram (Myriax, Echoview software version 4.10). The raw acoustic data were converted to raw volume backscattering strengths (SV) binned into mean SV cells with an interval of 0.1 nautical · mile (nmi) horizontal distance and a width of 1-m depth. The data were threshold to 85 dB at both frequencies. The contribution of other zooplankton such as copepod and amphipod were negligible because of their low densities and low mean target strength. For example, target strength is about 103 dB for a 2-3 mm long copepod at 120 kHz (Stanton and Chu, 2000).

Oblique, 400 m to surface, tows were undertaken using a Rectangular net (1 m-2 mouth area, 330 μm mesh) to verify the species composition of scattering layer. To determine the length-frequency distribution, seven tows were conducted at a speed of 2-3 knots for about 0.5-h period. The body length was defined as length from the anterior margin of the eye to the tip of the telson without terminal spines. The body lengths of about 2000 specimens were measured and the length-frequency distribution would be used to estimate krill density.

Preliminary results

The sound scattering layer was likely to be contributed by more than about 95% ice krill of the composition of all the rectangular net samples at seven stations sampled (Fig. 3.13). The mean length of ice krill was 12.5 mm (SD=5.9 mm) and varied from 4 to 31 mm.

A 120 kHz echogram clearly shows the horizontal and vertical variability of sound scattering layers along the ice shelves(Fig. 3.14).The vertical variability of sound scattering layer by sun's periodicity was not observed as the survey was conducted during the midnight sun.T1 shows the vertical distribution of sound scattering layer along the trough around DIS. The sound scattering layer from 80 to 73 dB was mainly observed at about 43-m depth with 30 m thickness. Near DIS, the sound scattering layer was deeper between 100 and 200 m.T2 shows the vertical distribution of sound scattering layer along the ice shelves from DIS to GIS B. In the DIS, the strong sound scattering layer of>80 dB was represented between 100 and 300-m depth, while it is noticeable that there was no strong sound scattering layer of >85 dB from surface to 100-m depth. With regard to GIS, two different sound scattering layers were present with depth along both GIS A and GIS B. Sound scattering layer from 80 to 73 dB was constantly observed about 50-m depth with about 30 m thickness. Another sound scattering layer between 100 and 200 m showed a little weaker intensity from 82 to 76dB.The depth of maximum sound scattering layer was relatively variable between 90 and 200 m with about 60 m thickness. Maximum intensity of sound scattering layer was 70 dB, which was observed at 70 m along GIS A. This suggests that the water mass from surface to 100 m might be different condition between DIS and GIS. Further study will be investigated to reveal variability of ice krill density associated with different environmental conditions between DIS and GIS.

References

La, H.S., Lee, H., Fielding, S., Ha, H.K., Atkinson, A., Park, J.S., Siegel, V., Lee, S. Shin, H.C., 2013. Environmental controls on ice krill (Euphausia cyrstallorophias) density in the Amundsen Sea coastal polynya, Antarctica. Submitted.

Shepherd, A., Wingham, D., Rignot, E., 2004. Warm ocean is eroding West Antarctic ice sheet. Geophysical Research Letters 31 (L23402).

Wahlin, A.K., Yuan, X., Bjork, G. and Nohr, C., (2010) Inflow of warm circumpolar deep water in the central Amundsen Shelf.Journal of Physical Oceanography, 40, 1427- 1434.

Walker, D.P., Brandon, M.A., Jenkins, A., Allen, J.T., Dowdeswell, J.A. and Evans, J., (2007) Oceanic heat transport onto the Amundsen Sea shelf through a submarine glacial trough. Geophysical Research Letters, 37(L02602), doi:10.1029/2006GL028154.

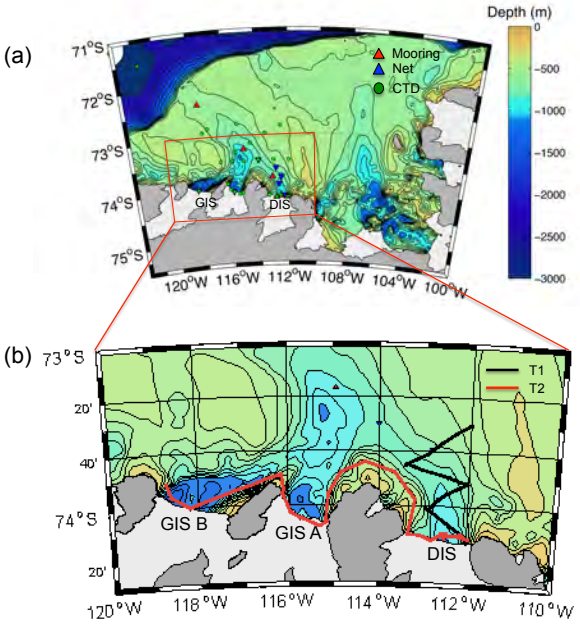

Figure 3.12: (a) Bathymetry of Amundsen Sea. (b)Map of study area with two acoustic transect lines (T1 and T2). DIS: Dotson Ice Shelf; GIS A and GIS B: Getz Ice Shelf.

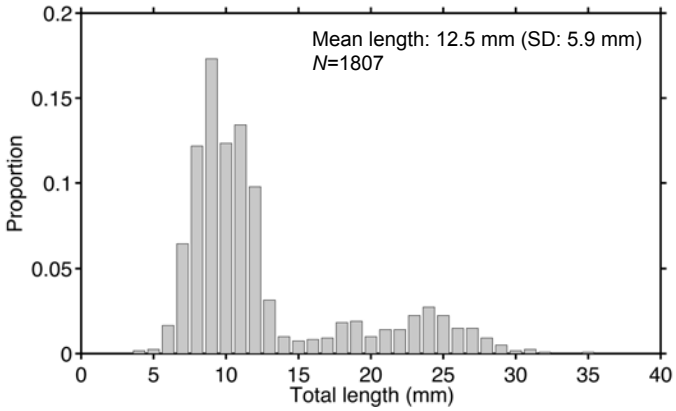

Figure 3.13: Length-frequency distribution of ice krill.

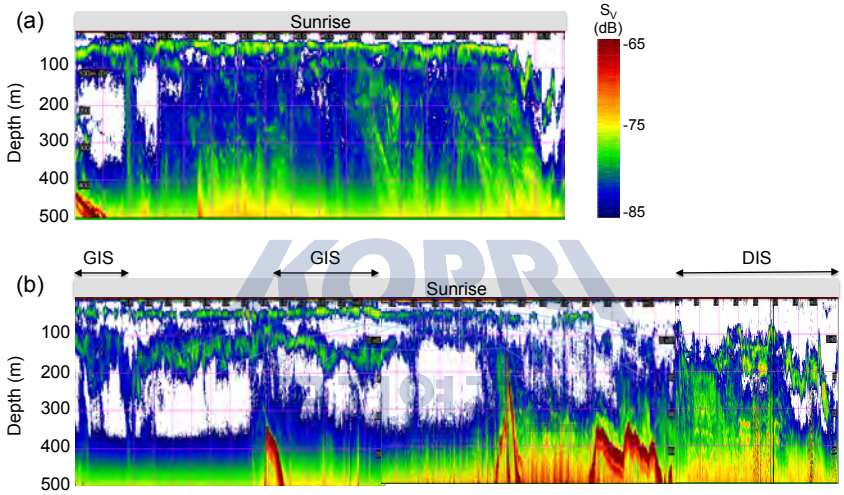

Figure 3.14: (a) Vertical distribution of sound scattering layer (T1). (b) Vertical distribution of sound scattering layer along the ice shelves (T2). DIS: Dotson Ice Shelf; GIS A and GIS B: Getz Ice Shelf. SV indicates the volume backscattering strength.

3.11 Analysis of Photosynthetic Pigments of Phytoplankton and Colored Dissolved Organic Matter in seawater

Lee YoonChang
Department of Oceanography, Pukyong National University, Korea

요약문

2013년 아문젠 하계 연구 기간동안 각기 다른 수괴환경에 따른 식물플랑크톤의 생물량과 군집조성(Pigment Analysis), 그리고 Colored Dissolved Organic Matter(CDOM)의 농도를 조사하여 식물플랑크톤의 개체 성장에 미치는 영향 및 수평적 또는 수직적 분포에 대하여 조사하였다. 조사 정점은 Chl.a 시료는 총 22개 정점에서 정점 당 표준수심에서 해수를 채수하였고, CDOM 시료는 연안에서 외양까지 직선이 되도록 8개의 정점을 선택하여 모든 수심에서 채수를 하였다. 채수한 해수 시료는 현장에서 여과 및 전처리 과정을 거쳐 냉동보관하였으며, 시료를 실험실로 가져와 Chl.a의 농도 및 군집조성, 그리고 CDOM농도를 분석할 계획이다.

Introduction And Objective

Rapid sea ice retreat and the melting of the glacier is expected to affect the primary production and community of phytoplankton in the Southern Ocean. So we investigate the composition of phytoplankton community through the pigment analysis by HPLC (High Performance Liquid Chromatography) and look into the environmental feature of the open sea and coastal polynya to understand the principal factors which can influence the phytoplankton community. And Colored Dissolved Organic Matter(CDOM) is the optically measurable component of DOM in water. CDOM occurs naturally in aquatic environments primarily from the decaying detritus by microorganisms and exudation of phytoplanktons and can have a significant effect on biological activity in aquatic systems. Because CDOM diminishes light as it penetrates water, so this has a population. CDOM also absorbs harmful UVA/B radiation, protecting organisms from DNA damage. Thus we investigate the interactions between polar environmental changes and CDOM in sea water in order to use as a biomarker for predicting the polar environmental changes. The effect of increasing UV-B and distribution of CDOM in different environments such as offshore, polynya and ice shelf of the study area in Antarctic Ocean will be investigated to find the effect on carbon cycle by the change in concentration of CDOM in polar environments.

Method

HPLC(Pigment Analysis)

2L water sample was filtered in situ and put it in the freezer to analyze Chl.a. Photosynthesis pigment of phytoplankton was extracted with 5 ml of 100% Acetone and Canthaxanthin 50 μl as an Internal Standard was added do compensate for sample loss. Cells will be broken up with supersonic wave for 5 minutes and put it in the cold dark place for 24 hours. Then, filter paper was ground and centrifuged for 10 minutes at 2000rpm. 1 ml supernatant water with 300μl

HPLC water was injected to HPLC for analysis. Concentration is calculated with following equation.

C = Area * Rf * (AIS/SIS)*Vi/Vs.

C : Concentration[ng/l] Area : area of the peak[area] Rf : standard response factor[ng l-1 area-1] AIS : peak area of the internal standard (IS) when 1 ml IS was mixed with 300ul of H20 SIS : peak area of IS added to sample Vi : volume of IS added to sample Vs : volume of filtered water sample

Colored Dissolved Organic Matter(CDOM)

Seawater samples for analysis of CDOM were collected using CTD system and were filtered under a gentle vacuum(<5 in/Hg) through Nuclepore membrane filters(0.2㎛) which rinsed with 0.1N HCl and collected directly into precleaned and precombusted sample glass bottles(125ml Clear narrow neck bottle). After filtration, sample glass bottles were covered with aluminium foil and stored in a freezer. Sample analysis will be done by Cary-100(spectrophotometer). The measurement of absorption uses a circular 10cm cuvettes for the wavelength from 200nm to 800nm and the scan speed is 100nm min-1. For the baseline correction , Millie-Q Water used for blank.

aCDOM = a(λ)*2.303/0.1 (m-1)

a(λ) : Absorbance value of dissolved organic matter on wave length. 2.303 : Constant value. 0.1 : path length on 10cm cell.